ออกซิเดชันในน้ำภาวะเหนือวิกฤตเชิงเร่งปฏิกิริยาสำหรับการบำบัดของเสียอินทรีย์จากห้องปฏิบัติการ

นางสาว ธีรดา ร่วมชาติ

วิทยานิพนธ์นี้เป็นส่วนหนึ่งของการศึกษาตามหลักสูตรปริญญาวิทยาศาสตรดุษฎีบัณฑิต
สาขาวิชาเคมีเทคนิค ภาควิชาเคมีเทคนิค
คณะวิทยาศาสตร์ จุฬาลงกรณ์มหาวิทยาลัย
ปีการศึกษา 2550

CATALYTIC SUPERCRITICAL WATER OXIDATION FOR ORGANIC LABORATORY WASTE TREATMENT

Miss Teerada Ruamchat

A Dissertation Submitted in Partial Fulfillment of the Requirements
for the Degree of Doctor of Science Program in Chemical Technology
Department of Chemical Technology
Faculty of Science
Chulalongkorn University
Academic year 2007

Thesis Title	CATALYTIC SUPERCRITICAL WATER OXIDATION FOR ORGANIC LABORATORY WASTE TREATMENT
By	Miss Teerada Ruamchat
Field of Study	Chemical Technology
Thesis Advisor	Associate Professor Somkiat Ngamprasertsith, Ph.D.
Thesis Co-advisor	Professor Yoshito Oshima, Ph.D.

Accepted by the Faculty of Science, Chulalongkorn University in Partial Fulfillment of the Requirements for the Doctoral Degree

S. Hannongbua ....Dean of the Faculty of Science

(Professor Supot Hannongbua, Ph.D.)

THESIS COMMITTEE

....Chairman

(Professor Pattarapan Prasassarakich, Ph.D.)

Somkiat Ngamprasertsith ....Thesis Advisor

(Associate Professor Somkiat Ngamprasertsith, Ph.D.)

....Thesis Co-advisor

(Professor Yoshito Oshima, Ph.D.)

....Member

(Associate Professor Kejvalee Pruksathorn, Ph.D.)

....Member

(Assistant Professor Nuttaya Pongstabodee, Ph.D.)

....Member

(Thawach Chatchupong, Ph.D.)

ธีรดา ร่วมชาติ : ออกซิเดชันในน้ำภาวะเหนือวิกฤตเชิงเร่งปฏิกิริยาสำหรับการบำบัดของเสียอินทรีย์จากห้องปฏิบัติการ. (CATALYTIC SUPERCRITICAL WATER OXIDATION FOR ORGANIC LABORATORY WASTE TREATMENT)
อ. ที่ปรึกษา : รศ.ดร. สมเกียรติ งามประเสริฐสิทธิ์, อ. ที่ปรึกษาร่วม: Prof. Yoshito Oshima, 160 หน้า.

เทคโนโลยีออกซิเดชันในน้ำภาวะเหนือวิกฤต มีการศึกษาและนำไปประยุกต์สำหรับการบำบัดน้ำเสียหลากหลายชนิด โดยการเปลี่ยนสารอินทรีย์ให้เป็นคาร์บอนไดออกไซด์และน้ำผ่าน ปฏิกิริยาออกซิเดชันที่ภาวะเหนือจุดวิกฤตของน้ำ (อุณหภูมิวิกฤต 374 องศาเซลเซียส และความดันวิกฤต 218 บรรยากาศ) และใช้เวลาในการสลายสารอินทรีย์อย่างสมบูรณ์สั้นมาก อย่างไรก็ตามการบำบัดของเสียจำพวกสารประกอบอินทรีย์ที่มีคลอไรด์เป็นองค์ประกอบด้วยวิธีนี้จะทำให้ผนังเครื่องปฏิกรณ์เกิดการกัดกร่อน เพื่อเป็นการแก้ปัญหานี้ งานวิจัยนี้ จึงได้มีการออกแบบเครื่องปฏิกรณ์แบบเชื่อมต่อระหว่างปฏิกิริยาไฮโดรไลซิสและปฏิกิริยาออกซิเดชันในน้ำภาวะเหนือวิกฤตขึ้น โดยใช้ไดคลอโรมีเทนซึ่งใช้อย่างแพร่หลายในการสังเคราะห์สารอินทรีย์และการสกัดแยกในห้องปฏิบัติการทางเภสัชกรรมเป็นตัวอย่างของสารอินทรีย์ที่มีคลอไรด์เป็นองค์ประกอบ จากงานวิจัยที่เกี่ยวข้องได้มีผู้ศึกษาเป็นจำนวนมากเกี่ยวกับไฮโดรไลซิสของไดคลอโรมีเทนและรายงานว่าผลิตภัณฑ์หลักที่เกิดขึ้นคือ ฟอร์มาลดีไฮด์และกรดไฮโดรคลอริก ในขณะที่มีการศึกษาค่อนข้างน้อยเกี่ยวกับจลนพลศาสตร์ของฟอร์มาลดีไฮด์ออกซิเดชันในน้ำภาวะเหนือวิกฤต ดังนั้นในงานวิจัยนี้จึงเน้นศึกษาออกซิเดชันของฟอร์มาลดีไฮด์ โดยใช้และไม่ใช้ตัวเร่งปฏิกิริยาในน้ำภาวะเหนือวิกฤต มีการเสนอกระบวนการเชื่อมต่อระหว่างสองเครื่องปฏิกรณ์ โดยมีปฏิกิริยาไฮโดรไลซิสเป็นเครื่องปฏิกรณ์แรกตามด้วยเครื่องปฏิกรณ์ออกซิเดชันในน้ำภาวะเหนือวิกฤต เพื่อสลายโครงสร้างของไดคลอโรมีเทนอย่างสมบูรณ์ จากผลการทดลองพบว่า ที่อุณหภูมิ 400 องศาเซลเซียส และความดัน 25 เมกะพาสคัล ฟอร์มาลดีไฮด์สลายตัวได้อย่างสมบูรณ์รวดเร็ว ในเครื่องปฏิกรณ์เชิงเร่งปฏิกิริยาแบบกะทัดรัดที่มีแมงกานีสออกไซด์เป็นตัวเร่งปฏิกิริยา นอกจากนี้ยังได้มีการออกแบบและศึกษาการแยกกรดไฮโดรคลอริกที่ออกมาจากเครื่องปฏิกรณ์แรกด้วยวิธีต่างๆ อีกด้วย

ภาควิชา	เคมีเทคนิค	ลายมือชื่อนิสิต ธีรดา ร่วมชาติ
สาขาวิชา	เคมีเทคนิค	ลายมือชื่ออาจารย์ที่ปรึกษา
ปีการศึกษา	2550	ลายมือชื่ออาจารย์ที่ปรึกษาร่วม

4673811323 : MAJOR CHEMICAL TECHNOLOGY

KEY WORD: SUPERCRITICAL WATER OXIDATION / DICHLOROMETHANE / FORMALDEHYDE / HYDROCHLORIC ACID

TEERADA RUAMCHAT: CATALYTIC SUPERCRITICAL WATER OXIDATION FOR ORGANIC LABORATORY WASTE TREATMENT. THESIS ADVISOR: ASSOC. PROF. SOMKIAT NGAMPRASERTSITH, THESIS COADVISOR: PROF. YOSHITO OSHIMA, 160 pp.

Supercritical water oxidation (SCWO) technology has been widely studied and applied to an extensive variety of wastewater. It converts organic compounds to CO_2 and H_2O via oxidation reactions that exceed the critical point of water (T_c=374°C, P_c=218 atm) and needs short residence time for complete destruction of organic compound. However, the treatment of chlorinated organics with this technique may cause the corrosion problem of the reactor wall. In order to solve this problem, a new cascade process that consists of consecutive combination of hydrolysis and SCWO is proposed. Dichloromethane, which is widely used for the solvent of such chemical reactions as organic synthesis and extraction in pharmaceutical laboratory, is chosen as a representative model of chlorinated compounds. There have been many previous studies on the hydrolysis of dichloromethane, which results in co-production of formaldehyde and hydrochloric acid. Compared with the abundance of previous research on dichloromethane hydrolysis there has been less investigated on the kinetics of formaldehyde oxidation in SCW. Therefore, in this study focus on the oxidation of formaldehyde in supercritical water with and without catalyst. A new cascade process where two reactors are consecutively combined, aiming at hydrolysis in the first reactor followed by SCWO in the second reactor, for the complete destruction of dichloromethane is proposed. As a result, formaldehyde can be completely decomposed at 400°C and 25 MPa within a very short contact time in catalytic compact sized system with MnO_2 as catalyst. In addition, the different methods for HCl removal at the exit of first reactor are designed and experimentally investigated.

Department Chemical Technology
Field of study Chemical Technology
Academic year 2007

Student's signature Teerada Ruamchat
Advisor's signature Somkiat Ngamprasertsith
Co-advisor's signature

ACKNOWLEDGEMENTS

I would like to express my deepest gratitude my supervisors, Assoc. Prof. Somkiat Ngamprasertsith and Prof. Yoshito Oshima who reviewed this thesis during its preparation and offered many helpful suggestions, supervision and much encouragement throughout my research. I also would like to acknowledge Prof. Pattarapan Prasassarakich, Assoc. Prof. Kejvalee Pruksathorn, Asst. Prof. Nuttaya Pongstabodee and Dr. Thawach Chatchupong for their participation on the dissertation chairman and members of thesis committee, respectively.

I wish to express my thankfulness to all people in the associated institutions and companies for their kind assistance and collaboration: Dr. Rumiko Hayashi for her encouragement and helpful suggestion during this research at The University of Tokyo, Japan.

Many thanks are due to Oshima laboratory's members of the Department of Environmental System, The University of Tokyo for helping in maintaining the equipment and technicians of the Department of Chemical Technology, Chulalongkorn University.

Sincerest appreciation is also extended to Royal Golden Jubilee Scholarship (Thailand Research Fund) and the Research Grant for the Promotion of Science (Ministry of Education, Culture, Sports, Science and Technology of Japan) for financial support of this research.

Finally, I wish to acknowledge the support, encouragement, and love of my family throughout my Ph.D. program.

CONTENTS

PAGE

PAGE

PAGE

LIST OF TABLES

TABLE PAGE

LIST OF FIGURES

FIGURE PAGE

FIGURE PAGE

FIGURE PAGE

CHAPTER I

INTRODUCTION

1.1 Background

The laboratory wastes generated from scientific research sometimes contain various types of hazardous chemicals, and present a serious problem for universities. Supercritical water oxidation (SCWO) technology has been widely studied and applied to an extensive variety of hazardous wastes. Most organic compounds have been reported to be converted into CO_2 and H_2O by SCWO within a very short residence time at conditions above the critical point of water (374^oC, 218 atm) [1-5]. A compact sized reactor for the on-site treatment of laboratory wastewater have been recently developed, which expect to meet the two important and fundamental concepts of such waste treatment, "treatment at the origin" and "self-responsibility for waste". Among laboratory wastes, the wastewater from pharmaceutical laboratories is one of the most difficult wastewaters to treat with SCWO because it usually contains several types of halogenated compounds such as chloroform, barium chloride and dichloromethane. In this study, dichloromethane is chosen as a representative model of chlorinated compounds. In order to avoid the problem of corrosion by chloride, a new cascade process where two reactors are consecutively combined, aiming at hydrolysis in the first reactor followed by SCWO in the second reactor, for the complete destruction of halogenated organic compounds is proposed. The concept of the cascade process is shown in Figure 1.1

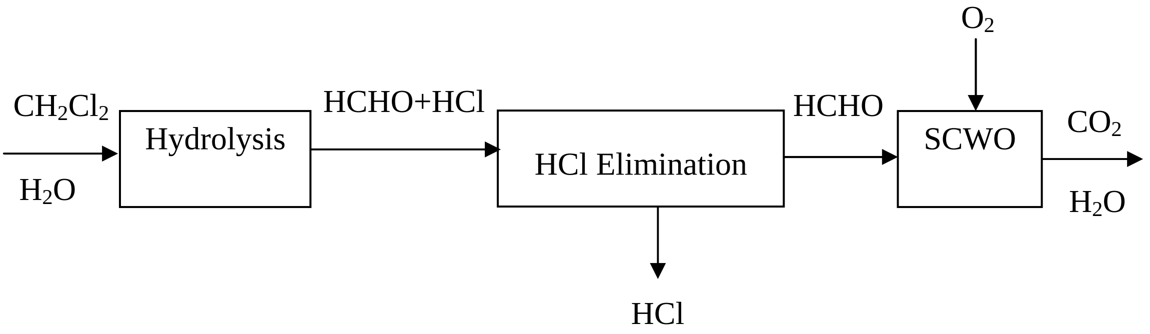

Figure 1.1 Schematic outline of proposed cascade process with consecutive combination of hydrolysis and SCWO for pharmaceutical laboratories wastewater treatment

There have been many previous studies on the hydrolysis of dichloromethane. Marrone et al. [6, 7] investigated the hydrolysis of CH_2Cl_2 in sub-critical water, and reported that the main products were formaldehyde (HCHO) and HCl. Salvatierra et al. [8] studied the hydrolysis kinetics of CH_2Cl_2 in liquid water from 100^oC to 250^oC. They proposed an empirical first-order rate expression using a standard Arrhenius equation for the rate constant. Oshima et al. [9] designed a corrosion-resistant flow reactor with a rapid-heating system and obtained kinetic information on CH_2Cl_2 hydrolysis in sub- and supercritical water. Compared with the abundance of previous research on dichloromethane hydrolysis, there has been less investigation on the kinetics of formaldehyde oxidation in supercritical water. Therefore, non-catalytic and catalytic SCWO of formaldehyde are experimentally examined, and carried out kinetic analyses to find out the optimal condition for the complete destruction of formaldehyde. Additionally, the results of methods to eliminate HCl before entering the oxidation stage are reported.

1.2 Objectives of study

1. Study kinetics of formaldehyde oxidation in supercritical water
2. Design and construct catalytic compact sized reactor for treatment of pharmaceutical laboratory wastewater by SCWO technique
3. Design and construct hydrochloric acid elimination method before SCWO reactor

1.3 Scope of dissertation

1. The plug flow reactor for kinetic study of formaldehyde oxidation in supercritical water is designed and constructed. The formaldehyde solution is prepared from 37 wt % commercial aqueous solutions which also contained about 8 % methanol as a preservative. The time profiles of formaldehyde conversion in different initial concentrations at 400, 450 and 500^oC are investigated. The empirical first order rate expression and mechanism of formaldehyde oxidation in SCW are also presented.
2. The catalytic compact sized reactor for the on-site treatment of pharmaceutical laboratory wastewater is designed and constructed. The optimal condition for complete destruction of organic compounds such as temperature, organic compounds concentration and excess oxygen are studied.
3. The hydrochloric acid elimination process in two different methods are designed and constructed; one is high pressure method which $Pb(CH_3COO)_2$ is used as precipitating reagent, and the other is low pressure method which HCl is adsorbed by ion exchange resin.
4. The reactor design of the whole system which consists of consecutive combination of hydrolysis and SCWO for complete destruction of dichloromethane is presented.

CHAPTER II

THEORY AND LITERATURE REVIEWS

2.1 Supercritical fluid (SCF)

Whether a fluid is in gaseous phase or liquid phase depends on the kinetic energy of it molecules and the energy of intermolecular forces. When the intermolecular forces dominate to a greater extent the molecular kinetic energy, a fluid will be a liquid with a certain measure of order, but when kinetic energy is dominant, it will be a gas with a random structure. Kinetic energy grows as temperature rises, and the shorter the distance between molecules, the more dominant the intermolecular forces will become. Thus, in general, a liquid will become a gas when its temperature is raised, and a gas will liquefy when it is compressed. However, above a certain temperature, molecular kinetic energy is greater no matter what the distance between the molecules and the substance will become a non-condensable fluid. This temperature, which is called the critical temperature, is unique to each substance and a fluid at or above its critical temperature is a supercritical fluid (SCF).

The position of SCF region can be shown on the conventional PVT phase diagram. The projections onto P-T plane and onto the P-V plane are shown in Figure 2.1 (a) and (b) with the critical point (C.P.) at each center; the SCF is in the region above C.P. on the P-T and P-V diagrams. [1-5]

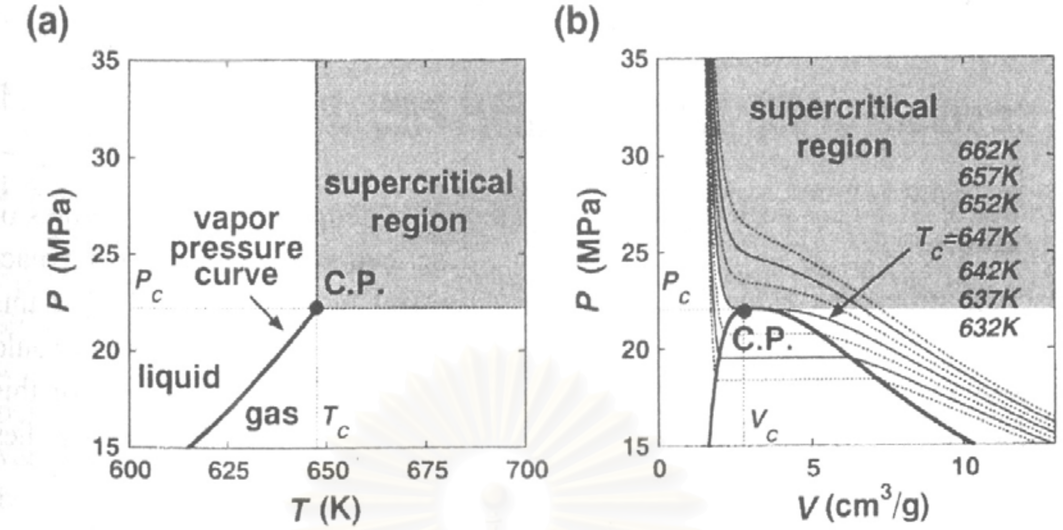

Figure 2.1 Projection of phase diagram of water (a) in the P-T plane and (b) in the P-V plane: C.P. = critical point [1].

Large fluctuations are seen in the density and energy at C.P. and in its close vicinity, where some physical properties exhibit a so-called critical anomaly. How to approach these anomalies has long been of interest in statistical mechanics. Such a large fluctuation rapidly disappears as the temperature T increases from T_c, which allows us to use a classical treatment. A characteristic feature of a SCF is the fact that in the SCF region the slope of the P-V isothermal shown in Figure 2.1 (b) is exceptionally small. This means that a small change in pressure leads to a large volume change. In other words, the isothermal compressibility of a SCF is very large. This is to be compared with the case of a fluid at higher pressure, where the compressibility is quite small. The critical constants of some typical molecules used as SCF solvents are shown in Table 2.1. The range considered to be the SCF region may depend on the problem to be solved, but generally it will be $1.01\ T_c < T < 1.2T_c$. [1-5].

Table 2.1 Critical constants of typical molecules used as SCF solvents [10]

Molecule	Critical Temperature (T_c) K	Critical Pressure (P_c) atm
Ethylene	282.4	49.7
Xenon	289.7	75.6
Carbon dioxide	304.2	72.8
Ethane	305.4	48.2
Methyl amine	430.0	73.6
1-Hexene	504.0	31.3
t-Butanol	506.2	39.2
n-Hexane	507.4	29.3
Acetone	508.1	46.4
i-Propanol	508.3	47.0
Methanol	512.6	79.9
Ethanol	516.2	63.0
Toluene	519.7	40.6
p-Xylene	616.2	34.7
Water	647.3	217.6
Tetralin	719.0	34.7

Supercritical fluids (SCFs) are attractive media for chemical reactions because of their unique properties. Many of the physical and transport properties of SCFs are intermediate between those of a liquid or a gas.

Table 2.2 Comparison of typical SCF, liquid and gas properties [10]

	Liquid	SCF	Gas
Density (g/cm^3)	1	0.1-0.5	10^{-3}
Viscosity (Pa.s)	10^{-3}	10^{-4}-10^{-5}	10^{-5}
Diffusivity (cm^2/s)	10^{-5}	10^{-3}	10^{-1}

The diffusivity in an SCF falling between in a liquid and a gas suggests that reactions are diffusion limited in the liquid phase could become faster in an SCF phase. Some properties of SCF comparison with liquid and gas phase are shown in Table. 2.2.

2.2 Supercritical water (SCW)

2.2.1 Supercritical water

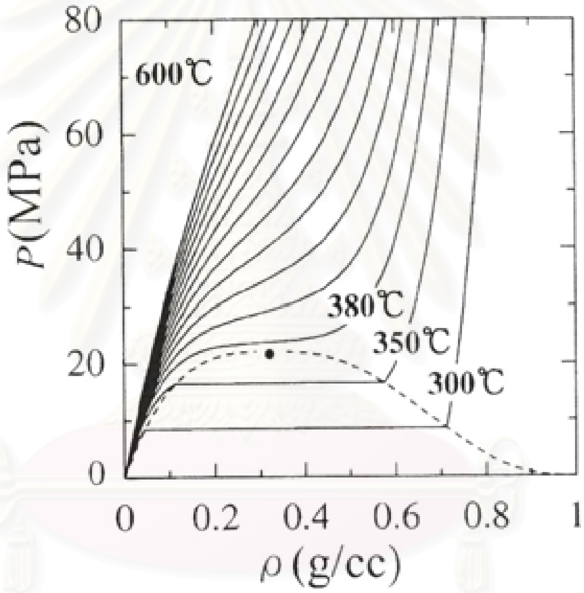

Figure 2.2 P, ρ and T relationship of water [1]

Water is an ecologically safe substance widespread throughout nature. Liquid water at standard condition (25^{o}C and 0.1 MPa) is an excellent solvent for many compounds and electrolytes because of its high dielectric constant, but it is poorly miscible with hydrocarbon and gases. Temperature and pressure have a great effect on the properties of water. As the temperature of water is increased, the dielectric constant decreases. The vapor pressure of water terminates at the critical point (T_c = 373.9^{o}C, P_c = 22 MPa, ρ_c = 322 kg/m^3), and the beyond this state, the density of supercritical water can be varied continuously to have liquidlike to gaslike values without abrupt changes associated with a phase transition over a wide range of conditions [11]. P, ρ and T relation depending on temperature and pressure are presented in Figure 2.2.

2.2.2 Properties of supercritical water in chemical reactions

2.2.2.1 Density

The structure changes of water also affect the dynamics of water molecules. The breaking of the hydrogen-bond network reduces the barrier for transitional and rotational motions. This effect contributes to the increase in the self-diffusivity of water with increasing temperature and decreasing density. Density of water dependence on temperature is shown in Figure 2.3. With the change in density from 1 to 0.1 g/cm^3, the diffusivity increases by roughly an order of magnitude. The diffusivity behavior at low densities is qualitatively consistent with the kinetic theory of gases [12].

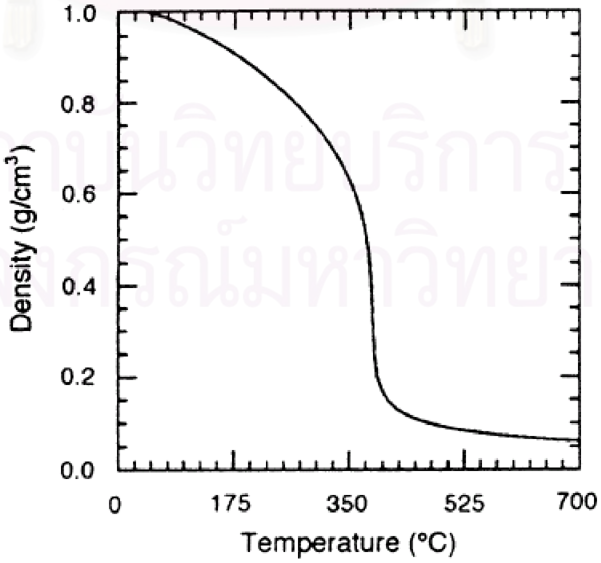

Figure 2.3 Water densities as a function of temperature [12]

2.2.2.2 Viscosity

The large diffusion coefficients and low viscosities of SCW, along with the complete miscibility of SCW with many substances, can accelerate chemical reactions and can improve reaction efficiency. For example, the rate of cellulose decomposition above 350^{o}C increases greatly because of the miscibility of cellulose with SCW [11]. Viscosity of water dependence on temperature is shown in Figure 2.4.

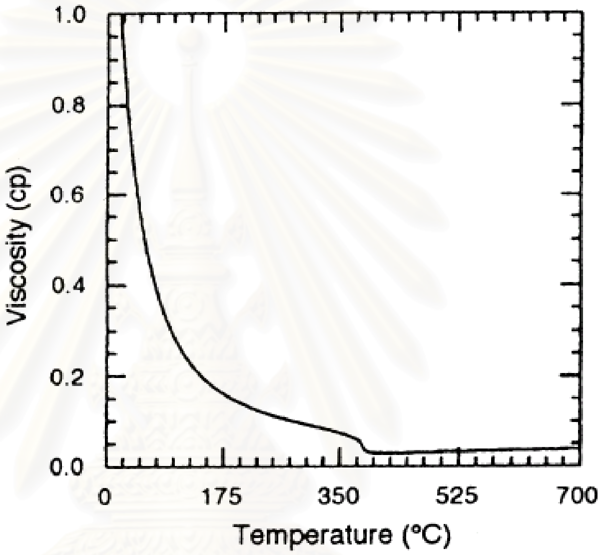

Figure 2.4 Water viscosity as a function of temperature [12]

2.2.2.3 Pressure

Water becomes a collision partner in many chemical reactions, which means that reactions in the critical region can have large density dependence due to the influence of solvent density on free radicals. Experimental and theoretical studies show that the rate of free radical reactions exhibit pressure dependence. The reaction rate constants for free radical reactions typical increase with pressure up to a certain plateau value. This behavior has been called the limiting high pressure rate coefficient due to frequent collisions of the reactant with the surrounding molecules. A further increase in pressure leads to no change in the reaction rate until the falloff pressure is reached, at which diffusion control occurs and the reaction rate decrease with pressure [11].

2.2.2.4 Dielectric Constant

One of the most important parameters for the solvent effects of water in the reactions is the dielectric constant. Water dielectric constant dependence on temperature is presented in Figure 2.5. For example, the dielectric constant is 21 at 300°C and 4.1 at 500°C, compared to 78 for ambient. With such a low dielectric constant, SCW behave more like polar organic solvents rather than ambient liquid water under certain conditions. Consequently, small organic compounds are highly soluble in SCW and complete miscible in SCW. Whereas ions generally exist as contact pairs, resulting in reduced solubility for inorganic salts [11, 12].

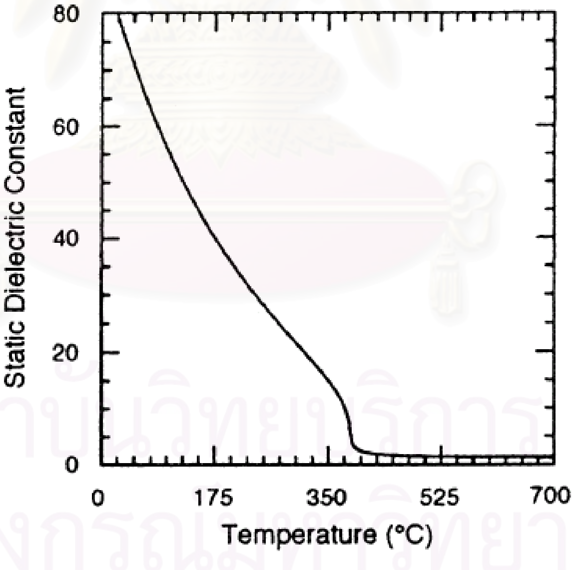

Figure 2.5 Water dielectric constant at 250 bar as a function of temperature [12]

2.2.2.5 Molecule

Water is a molecule with a permanent dipole, and therefore it is reactive in a variety of cases. In some key reaction step in total oxidation, SCW is assumed to take part in the activation complex. By forming a complex, the activation energy is lowered, which means that water acts as a catalyst in these reactions. Molecular reactions are important for understanding reaction mechanism around the critical point of water, where ionic and radical reactions also competitively occur. As a solvent, water can most likely affect chemical reactions for cases where the activated complex has a polarity that is different from that of the initial compounds [11].

2.2.2.6 Ion product

The ion product of water (K_w) has a strong influence on reaction. Figure 2.6 shows the ion product increases slightly with temperature up to around 10^{-11} in the range between 200 and 300^{o}C. The K_w in SCW at high pressure can be some orders of magnitude higher than that in ambient water. In this region, water may play the role of an acid or base catalyst because of the high concentration of H_3O^+ and OH^- ions. Acid- or base-catalyzed reactions in water at high pressure and high temperatures show a characteristic non-Arrhenius kinetic behavior near the critical point of water. Below the critical temperature of water, the reaction rates usually increase with temperature until the critical temperature is reached. At the critical point, reaction rate can decrease or increase drastically depending on the chemistry and properties [11].

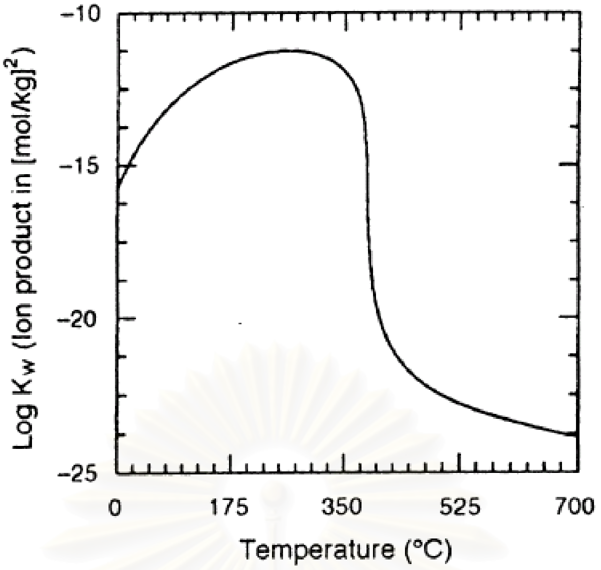

Figure 2.6 Ion product of water as a function of temperature [12]

2.2.3 Advantage and disadvantage of supercritical water

2.2.3.1 Advantage

- Eliminating inter-phase transport limitations that would exist in multi-phase reacting system (e.g., hydrogenation, partial oxidation).

- Providing easier product separation because solubility can be a strong function of pressure and temperature in the critical region.

- Allowing in situ extraction of coke precursors and hence a longer time on stream for hydrocarbon processing catalysts.

- Optimizing the strongly pressure-dependent properties of the supercritical reaction medium for the given reaction.

- Providing higher diffusivities than liquids and better heat transfer than gases.

2.2.3.2 Disadvantage

- Elevated pressure and temperature are required for supercritical water [12].
- Chlorinated compound is corrosive to reactor wall in SCW condition.

2.2.4 Heterogeneous catalysis in supercritical water

By making use of the characteristic features of supercritical water, the reaction performance of a lot of catalytic reactions can be remarkably improved. Through exploiting the unique solvent properties of supercritical water, it may be possible to enhance reaction rates while maintaining or improving selectivity. Also separating product from reactants or catalyst can be greatly facilitated by the ease with which the solvent power of SCW solvent can be adjusted.

If the catalytic reaction field is supercritical water oxidation, the following merits can be expected.

- Gases reactants such as hydrogen are able to mix well with SCW at high concentration. The reaction rate, dependent on gas concentration, will be enhanced. Its high diffusion coefficient can enhance the reaction rate in the diffusion-controlled reaction regime.
- Organic compounds become soluble in SCW to form a homogeneous reaction phase, leading to high reactivity and selectivity.

The high mass transfer efficiency and effective heat transfer capacity of SCW make process control easier and stabilize a lot of catalytic reactions.

2.3 Supercritical water oxidation (SCWO)

Supercritical water oxidation (SCWO) is a technique for the treatment of hazardous materials in water at temperatures and pressures above the critical point of water. High destruction efficiencies of this process have established for a wide variety of organic materials, and most of the organic compounds have been found to be oxidized within reasonable residence times. The complete oxidation of organic compounds in supercritical water has received much attention as a promising technology for waste treatment, not only because of the higher reaction rates compared to the conventional “wet oxidation” process, but also because of its unique physical and chemical properties as a solvent [1,14].

2.3.1 Characteristics of supercritical water oxidation

One advantage of SCWO for the treatment of waste is that the decomposition rates are extremely large for most organic compounds. The processing time for the complete conversion is an order of the seconds or minutes except for stable compounds such as ammonia and acids, which need higher temperature and longer processing times. This phenomenon is related to the unique physical properties of SCW. Due to the small values of dielectric constant and ion product for water at supercritical condition, ionic reactions are suppressed, and the solvent medium favors radical reactions.

Besides the high temperature, which promotes faster rates for each elementary reaction, the advantage of the SCWO technique is that reactions of organic compounds with excess oxygen in a single phase. Conventional wet oxidation, which is operated below the critical temperature and pressure of water, involves more than two phases, where the mass transport at the phase boundary could be rate-limiting. In SCW, on the contrary, organics and water are miscible, and the solubility of inorganic gases such as oxygen and air in water is also very high. Therefore, there are no interface transport limitations in SCWO. Higher concentrations of reactants in water are also expected, which may lead to the enhancement of overall efficiency of the degradation process.

2.3.2 Global reaction rates in supercritical water oxidation

The global rates of the oxidation reactions give useful and important information for process design, and help the better understanding of global reaction mechanisms. To obtain accurate global kinetics, a large amount of experimental data under different reaction condition should be accumulated and analyzed statistically. There have been many studies on the global reaction rates of SCWO from various compounds, most of which adopted the following equation based on the global rate law,

$$d[S]/dt = -k[S]^a[O_2]^b \tag{2.1}$$

Where [S] denoted the concentration of compound to be oxidized, the global rate constant *k* has Arrhenius-type temperature dependence as follows:

$$k = A\exp\left(-\frac{E_a}{RT}\right) \tag{2.2}$$

A, E_a, R and T mean the pre-exponential factor, activation energy, gas constant and temperature, respectively. The reported values of reaction orders and kinetic parameters for several compounds are summarized in Table. 2.3. The reaction order for most substrate is close to unity.

Table 2.3 Reported values of reaction orders and kinetic parameters in the SCWO of several compounds [1]

Compounds	Reaction orders		log A	Activation energy (kJ/mol)
	fuel	oxygen		
hydrogen	1.10±0.25	0.02±0.29	24.4±4.9	390±60
Carbon monoxide	0.96±0.30	0.34±0.24	8.5±3.3	134±32
methane	0.99±0.08	0.66±0.14	11.4±1.1	42.8±4.3
methanol	0.89±0.69	0.12±0.66	28.8±10.5	107±30
acetic acid	0.72±0.15	0.27±0.15	9.9±1.7	168±21
phenol	0.85±0.04	0.50±0.15	2.34±0.28	51.8±4.2

2.3.3 Catalytic oxidation in supercritical water

Most of the research done to date on catalytic oxidation in SCW has had complete oxidation of organic carbon to CO_2 as the goal. Converting organic wastes or hazardous organic compounds into innocuous products (CO_2 and water) is the goal of supercritical water oxidation, a waste treatment technology developed to compete with incineration and wet-air oxidation. Since complete conversion of organic carbon to CO_2 is the goal of SCWO, it is important to measure not just disappearance of the compound(s) in the feed stream, but also the disappearance of total organic carbon (TOC), or alternatively, appearance of CO_2. Catalytic oxidation has received attention because of the desire to increase reaction rates and to reduce SCWO processing temperatures. Faster rates and lower temperatures lead to smaller reactors and lower energy requirements, both of which improve the process economics [15]. Summarizes a variety of SCWO studies is shown in Table 2.4.

Table 2.4 Summary studies of catalytic oxidation in supercritical water [15]

Compound category	Catalysts
alcohol	CuO/ZnO
acetic acid	CuO/ZnO, TiO_2, MnO_2, $KMnO_4$
ammonia	Inconel beads, MnO_2
benzene	V_2O_5, MnO_2, Cr_2O_3
benzoic acid	CuO/ZnO
buthanol	CuO/ZnO
chlrophenol	Cu^{2+}, Mn^{2+}
dichlorobenzene	V_2O_5, MnO_2, Cr_2O_3
2,4-dichlorophenol	Pt(support), TiO_2
phenol	V_2O_5, MnO_2, Cr_2O_3, CuO/ZnO
2-propanol	CuO/ZnO
pyridine	Pt(support), TiO_2
quinoline	$ZnCl_2$

The first type involves aromatic compounds such as phenol, chlorinated phenols dichlorobenzene and pyridine; the second type deals with aliphatic compounds such as volatile acids, alcohols, methane, and methyl ethyl ketone; The third type includes inorganic compounds such as ammonia, H_2, and CO; and the fourth type lists various wastewater and sludges. The oxidation reaction may start by activation of either the dioxygen or hydrocarbon molecule. The oxidation reaction in SCW generally follows the free-radical mechanism that dominates gas-phase oxidation and Wet Air Oxidation (WAO). The free-radical reaction mechanism often involves an induction period, the generation of radical pool, and the fast free-radical reaction period. The induction time and free-radical concentration depend on the oxidizing agent, temperature, catalyst, and reactant.

2.4 Corrosion in supercritical water oxidation

Corrosion in aqueous systems up to supercritical temperatures was determined by several solution-dependent and material-dependent factors. Solution-depending factors were the density, the temperature, the pH value, and the electrochemical potential of the solution, and the aggressiveness of the attacking anions. Material-dependent parameters include alloy composition, surface condition, material purity, and heat treatment. The main corrosion in the SCWO process forms are the following [18, 19]:

- Pitting corrosion

Pitting corrosion is a localized form of corrosion occurring in the passive state of the metal, produced by aggressive anions such as chloride or bromide that can penetrate into the protecting oxide film and destroy it locally. Typical initiation points are inclusions or grain boundaries. The small pits formed in the first step lead to the oxidation and dissolution of metal components (such as nickel and/or chromium ions) that react as Lewis acids with the water producing a strong acidification of the solution inside the pits. Because of migration processes from the bulk solution, the concentration of aggressive anions increases. Thus, the solution becomes increasingly corrosive inside the pits and corrosion progresses. Pit growth generally occurs in high rates. High temperature additionally weakens the oxide film, favoring pitting corrosion.

- General corrosion

General corrosion is ascribed to a general instability of the oxide film and thus corrosion attacks the entire surface of the metal. It occurs when none of the alloy components is able to form a protective layer. The absolute material loss caused by general corrosion might be high, but because of the diffusion controlled character, the corrosion rates are linear and thus they can be predicted and considered in the calculations of wall thickness.

-Intergranular corrosion [intercrystalline corrosion (IC)]

Grain boundaries and their surroundings are chemically different compared to the bulk grains themselves. This fact makes possible the formation of new phases at the grain boundaries, such as metal carbides or nitrides. Further, an enrichment or segregation, respectively, of trace elements at the grain boundaries leads to detrimental conditions. Different corrosion mechanisms are observed, so IC can be observed under nearly all conditions, but in general, the penetration depth and amount of dissolved material are low. Therefore, IC is not as critical as the other forms of corrosion. However, whole grains may be dissolved at longer times and by the influence of mechanic stress, IC may lead to the dangerous stress corrosion cracking (SCC).

- Stress corrosion cracking (SCC)

SCC is an extremely dangerous form of corrosion, given that its nature and its occurrence are stochastic. Thus, failures can be catastrophic. SCC is commonly present in the transition ranges between the active and the passive, or the passive and the transpassive potential, respectively. Thus, SCC is observed in high-temperature water in the presence of either hydrogen (active region) or oxygen (transpassive region). Most detrimental anions are chloride, bromide, and sulfide [18].

Corrosion rates in water generally increase with temperature. Indeed, most corrosion processes have a minimum temperature, below which corrosion is limited or does not occur. For example, stainless steels are attacked by chloride-induced pitting corrosion above some 80–100°C, while the materials are resistant at lower temperatures. The temperatures and corrosion rates of the various forms of corrosion observed for nickel-base alloy 625 is shown in Table 2.5.

Table 2.5 Typical corrosion temperatures and corrosion rates observed for alloy 625 in oxidizing aqueous solutions of various acids [19]

	Temperature occurrence (^oC)	**Corrosion rate (μm/100 h.)**	**Occur in**
IC	> 100	10-20	All solutions
Pitting	> 150-200	500-1000	HCl/O_2 $NaCl/O_2$ HBr/O_2
General dissolution	> 250-300	500	HCl/O_2 $NaCl/O_2$ HBr/O_2 H_2SO_4/O_2 HNO_3/O_2
SCC	250-300	>> 1000	HCl/O_2 HBr/O_2

Delville et al. [20] used a specific experimental set-up, the cathodic polarization curves recorded under steady-state and quasi-stationary conditions, for 316L stainless steel, Alloy C-276 and T60 titanium materials, in oxidative chlorinated aqueous media. Measurements were carried out at temperatures and pressures reaching supercritical conditions (400^oC, 28 MPa). The influence of various parameters such as the pH, the nature of materials, the sub- or supercritical state of the medium, was investigated using the determination of the corrosion rate. They concluded that in supercritical water condition the use of 316L SS or alloy C-276 in presence of chloride or hydronium ions was not recommended, while titanium provides an interesting alternative.

2.5 Formaldehyde

2.5.1 Chemical identity

The Chemical identity of formaldehyde is located in Table 2.6.

Table 2.6 Chemical identity of formaldehyde [22]

Characteristic	Information
Chemical name	Formaldehyde
IUPAC name	Methanal
Synonym (s)	Formic aldehyde, Methanal, Methyl aldehyde, Methylene oxide, Oxymethylene, Methyladehyde, Oxomethane
Registered trade name (s)	
For 37 % aqueous solution	Formalin, Formal, Morbicid, Veracur
For polymeric form	Paraformaldehyde, Polyoxymethylene, Paraform, Formagene
Chemical formula	CH_2O or HCHO
Chemical structure	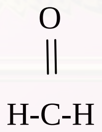 $\overset{\overset{O}{\Vert}}{H\text{-}C\text{-}H}$

2.5.2 Physical and chemical properties

The physical and chemical properties of formaldehyde are located in Table 2.7.

Table 2.7 Physical and chemical properties of formaldehyde [22]

Property	**Information**
Molecular weight	30.03
Color	Colourless
Physical state	Gas
Melting point (^oC)	-92
Boiling point (^oC)	-21
Critical temperature (^oC)	135
Critical pressure (atm)	65
Density at 20^oC	0.815 g/mL
Solubility:	
Freshwater at 20^oC	Very soluble; up to 55%
Organic solvent (s)	Ether, Alcohol, Acetone, Benzene
Polymerization	Polymerizes; polymerizes readily in water
Auto ignition temperature	300^oC
Flashpoint	60^oC

Although formaldehyde is a gas at room temperature, it is readily soluble in water. It is usually sold as a saturated aqueous solution with concentration of around 37 % formaldehyde, stabilized with 6-15 % methanol. In water, formaldehyde mostly converts to the hydrate $CH_2(OH)_2$. A few percent of methanol is usually added to these solutions to limit the extent of polymerization. Formalin reversibly polymerizes to produce its cyclic trimer, 1,3,5-trioxane or the linear polymer polyoxymethylene. The latter one can be heated to obtain methanol-free formaldehyde. Because of the formation of these derivatives, formaldehyde gas deviates strongly from the ideal gas law, especially at high pressure or low temperature [21-24].

2.6 Ion exchange resin

2.6.1 Ion exchange reactions

Ion exchange is a reversible chemical reaction where an ion (an atom or molecule that has lost or gained an electron and thus acquired an electrical charge) from solution is exchanged for a similarly charged ion attached to an immobile solid particle. These solid ion exchange particles are either naturally occurring inorganic zeolites or synthetically produced organic resins. The synthetic organic resins are the predominant type used today because their characteristics can be tailored to specific applications. An organic ion exchange resin is composed of high-molecular-weight polyelectrolytes that can exchange their mobile ions for ions of similar charge from the surrounding medium. Each resin has a distinct number of mobile ion sites that set the maximum quantity of exchanges per unit of resin. Most plating process water is used to cleanse the surface of the parts after each process bath. To maintain quality standards, the level of dissolved solids in the rinse water must be regulated. In a water deionization process, the resins exchange hydrogen ions (H^+) for the positively charged ions (such as nickel. copper, and sodium) and hydroxyl ions (OH^-) for negatively charged sulfates, chromates and chlorides. Because the quantity of H^+ and OH^- ions is balanced, the result of the ion exchange treatment is relatively pure, neutral water. Ion exchange reactions are stoichiometric and reversible, and in that way they are similar to other solution phase reactions. A resin with hydrogen ions available for exchange will exchange those ions for nickel ions from solution. The reaction can be written as follows:

$$2(R\text{-}SO_3H) + NiSO_4 = (R\text{-}SO_3)_2Ni + H_2SO_4 \qquad (2.3)$$

R indicates the organic portion of the resin and SO_3 is the immobile portion of the ion active group. Two resin sites are needed for nickel ions with a plus 2 valence (Ni^{+2}). Trivalent ferric ions would require three resin sites. As shown, the ion exchange reaction is reversible. The degree the reaction proceeds to the right will depend on the resins preference or selectivity, for nickel ions compared with its preference for hydrogen ions. Table 2.8 gives the selectivity of strong acid and strong base ion exchange resins for various ionic compounds. It should be pointed out that the selectivity coefficient is not constant but varies with changes in solution conditions. It does provide a means of determining what to expect when various ions are involved. In general terms, the higher the preference a resin exhibits for a particular ion, the greater the exchange efficiency in terms of resin capacity for removal of that ion from solution. Greater preference for a particular ion, however, will result in increased consumption of chemicals for regeneration. Resins currently available exhibit a range of selectivity and thus have broad application.

Table 2.8 Selectivity of ion Exchange Resins in order of decreasing preference [25]

Strong acid cation exchanger	Strong base anion exchanger
Barium	Iodide
Lead	Nitrate
Calcium	Bisulfite
Nickel	Chloride
Cadmium	Cyanide
Copper	Bicarbonate
Zinc	Hydroxide
Magnesium	Fluoride

2.6.2 Resin types

Ion exchange resins are classified as cation exchangers, who have positively charged mobile ions available for exchange, and anion exchangers, whose exchangeable ions are negatively charged. Both anion and cation resins are produced from the same basic organic polymers. They differ in the ionizable group attached to the hydrocarbon network. It is this functional group that determines the chemical behavior of the resin. Resins can be broadly classified as strong or weak acid cation exchangers or strong or weak base anion exchangers.

2.6.2.1 Cation resins

1) Strong acid cation resins

Strong acid resins are so named because their chemical behavior is similar to that of a strong acid. The resins are highly ionized in both the acid ($R\text{-}SO_3H$) and salt ($R\text{-}SO_3Na$) form. These resins would be used in the hydrogen form for water softening (calcium and magnesium removal) as follows:

$$2(R - SO_3H) + CaSO_4 \rightarrow (R - SO_3)_2Ca + H_2SO_4 \qquad (2.4)$$

The hydrogen and sodium forms of strong acid resins are highly dissociated and the exchangeable Na^+ and H^+ are readily available for exchange over the entire pH range. Consequently, the exchange capacity of strong acid resins is independent of solution pH. After exhaustion, the resin is converted back to the hydrogen form (regenerated) by contact with a strong acid solution, or the resin can be convened to the sodium form with a sodium chloride solution.

2) Weak Acid Cation rasins

Weak acid resin, the ionizable group is a carboxylic acid (COOH) as opposed to the sulfonic acid group (SO_3H) used in strong acid resins. These resins behave similarly to weak organic acids that are weakly dissociated. Weak acid resins exhibit a much higher affinity for hydrogen ions than do strong acid resins. This characteristic allows for regeneration to the hydrogen form with significantly less acid than is required for strong acid resins. Almost complete regeneration can be accomplished with stoichiometric amounts of acid. The degree of dissociation of a weak acid resin is strongly influenced by the solution pH. Consequently, resin capacity depends in part on solution pH.

2.6.2.2 Anion resins

1) Strong Base Anion Resins

Strong base resins are highly ionized and can be used over the entire pH range. These resins are used in the hydroxide (OH) form for water deionization. They will react with anions in solution and can convert an acid solution to pure water:

$$\mathrm{R - NH_3OH + HCl \rightarrow R - NH_3Cl + H_2O} \qquad (2.5)$$

Regeneration with concentrated sodium hydroxide (NaOH) converts the exhausted resin to the hydroxide form.

2) Weak Base Anion Resins

Weak base resins are like weak acid resins in that the degree of ionization is strongly influenced by pH. Consequently, weak base resins exhibit minimum exchange capacity above a pH of 7.0. These resins merely sorb strong acids: they cannot split salts.

In an ion exchange wastewater deionization unit the wastewater would pass first through a bed of strong acid resin. Replacement of the metal cations (Ni^{+2}, Cu^{+2}) with hydrogen ions would lower the solution pH. The anions (SO_4^{-2}, Cl^-) can then be removed with a weak base resin because the entering wastewater will normally be acidic and weak base resins sorb acids. Weak base resins are preferred over strong base resins because they require less regenerate chemical. A reaction between the resin in the free base form and HCl would proceed as follows:

$$\mathrm{R\text{ - }NH_2 + HCl \rightarrow R\text{ - }NH_3Cl} \qquad (2.6)$$

The weak base resin does not have a hydroxide ion form as does the strong base resin. Consequently, regeneration needs only to neutralize the absorbed acid: it need not provide hydroxide ions. Less expensive weakly basic reagents such as ammonia (NH_3) or sodium carbonate can be employed.

2.6.2.3 Heavy-metal-selective chelating resins

Chelating resins behave similarly to weak acid cation resins but exhibit a high degree of selectivity for heavy metal cations. Chelating resins are analogous to chelating compounds found in metal finishing wastewater; that is, they tend to form stable complexes with the heavy metals. In fact, the functional group used in these resins is an EDTA a compound. The resin structure in the sodium form is expressed as R-EDTA-Na. The high degree of selectivity for heavy metals permits separation of these ionic compounds from solutions containing high background levels of calcium, magnesium, and sodium ions. A chelating resin exhibits greater selectivity for heavy metals in its sodium form than in its hydrogen form. Regeneration properties are similar to those of a weak acid resin; the chelating resin can be converted to the hydrogen form with slightly greater than stoichiometric doses of acid because of the fortunate tendency of the heavy metal complex to become less stable under low pH conditions. Potential applications of the chelating resin include polishing to lower the heavy metal concentration in the effluent from a hydroxide treatment process or directly removing toxic heavy metal cations from wastewaters containing a high concentration of nontoxic, multivalent cations.

2.6.3 Ion exchange process equipment and operation

Most industrial applications of ion exchange use fixed-bed column systems, the basic component of which is the resin column. The column design must:

-Contain and support the ion exchange resin

-Uniformly distribute the service and regeneration flow through the resin bed

-Provide space to fluidize the resin during backwash

-Include the piping, valves, and instruments needed to regulate flow of feed, regenerant and backwash solutions.

2.6.4 Regeneration procedure

After the feed solution is processed to the extent that the resin becomes exhausted and cannot accomplish any further ion exchange, the resin must be regenerated. In normal column operation, for a cation system being converted first to the hydrogen then to the sodium form, regeneration employs the following basic steps:

1. The column is backwashed to remove suspended solids collected by the bed during the service cycle and to eliminate channels that may have formed during

this cycle. The backwash flow fluidizes the bed releases trapped particles and reorients the resin particles according to size. During backwash the larger, denser panicles will accumulate at the base and the particle size will decrease moving up the column. This distribution yields a good hydraulic flow pattern and resistance to fouling by suspended solids.

2. The resin bed is brought in contact with the regenerant solution. In the case of the cation resin acid elutes the collected ions and converts the bed to the hydrogen form. A slow water rinse then removes any residual acid.

3. The bed is brought in contact with a sodium hydroxide solution to convert the resin to the sodium form. Again, a slow water rinse is used to remove residual caustic. The slow rinse pushes the last of the regenerant through the column.

4. The resin bed is subjected to a fast rinse that removes the last traces of the regenerant solution and ensures good flow characteristics.

5. The column is returned to service.

For resins that experience significant swelling or shrinkage during regeneration, a second backwash should be performed after regeneration to eliminate channeling or resin compression. Regeneration of a fixed-bed column usually requires between 1 and 2 h. Frequency depends on the volume of resin in the exchange columns and the quantity of heavy metals and other ionized compounds in the wastewater.

2.6.5 Regenerant reuse

With strong acid or strong base resin systems, improved chemical efficiency can be achieved by reusing a part of the spent regenerants. In strongly ionized resin systems, the degree of column regeneration is the major factor in determining the chemical efficiency of the regeneration process. The need for acid doses considerably higher than stoichiometric means that there is a significant concentration of acid in the spent regenerant. Further as the acid dose is increased incrementally, the concentration of acid in the spent regenerant increases. By discarding only the first part of the spent regenerant and saving and reusing the rest, greater exchange capacity can be realized with equal levels of regenerant consumption. Regenerant reuse has disadvantages in that it is higher in initial cost for chemical storage and feed systems and regeneration procedure is more complicated. Where the chemical savings have provided justification, systems have been designed to reuse parts of the spent regenerant as many as five times before discarding them [25-27].

2.7 Laboratory wastewater

Laboratories are traditionally a source of hazardous and chemical waste that is difficult to generalize because of the wide variety of chemical testing and processing that is performed in individual labs throughout the country. However, all laboratories can make efforts to reduce both the amount of chemicals they use and the amount of wastes they generate through chemical or waste reduction and reuse techniques. Lifecycle of chemical organization laboratories such as university, hospital, government organization laboratories etc. begin with providing the substances needed from the chemical store to a coworker or student in laboratory. They are used for syntheses or analyses. Due to the application purposes contaminated starting materials, by-products, spent solvents, and spent chemicals are formed, which have to be decomposed or disposed of, if their recycling is not possible. In contrast to industrial wastes the chemical wastes from laboratories occur usually as small amounts of highly complex mixtures. Overall these represent a significant waste amount which has to be disposed of from the organization at its own expenses. To dispose of laboratory wastes, which may be different at different places, in an appropriate way depends on the type of the experiments conducted and chemicals used. But some type of hazardous wastes produced cannot be disposed of in the original form and have to be conditioned first [28, 29].

In this study, pharmaceutical laboratory wastewater, which contains several types of hazardous chemicals such as glacial acetic acid, halogenated compounds and non-halogenated compounds, is used as representative laboratory wastewater.

Table 2.9 The data of organic laboratory wastewater from Quality Assurance Division, Government Pharmaceutical Organization (GPO), Thailand.

Organic Compounds	**Average concentration (mol/L)**
Methanol	0.28
Ethanol	0.18
Acetone	0.15
Acetonitrile	0.15
Cyclohexane	0.07
Dichloromethane	0.15
Chloroform	0.13

Note: Average concentration is calculated from the data in Appendix A.

Table 2.9 shows the average concentration of pharmaceutical laboratory wastewater which is generated everyday in the total amount of waste about 40 L. In order to treat organic compounds by SCWO technique and meet the two important and fundamental concepts of such waste treatment, "treatment at the origin" and "self-responsibility for waste", the compact sized reactor by SCWO technique for the on-site treatment of laboratory wastewater is developed.

2.8 Literature reviews

2.8.1 Hydrolysis of dichloromethane

There have been many previous studies on the hydrolysis of dichloromethane, which results in co-production of formaldehyde and hydrochloric acid.

Marrone et al. [6] focused on the product identified from the hydrolysis and oxidation of CH_2Cl_2 and their subsequent reactions. A complete reaction network for CH_2Cl_2 and its product under hydrolysis condition is shown in Figure 2.7. The product detect were formaldehyde, hydrochloric acid, carbon monoxide, hydrogen, methanol, and carbon dioxide.

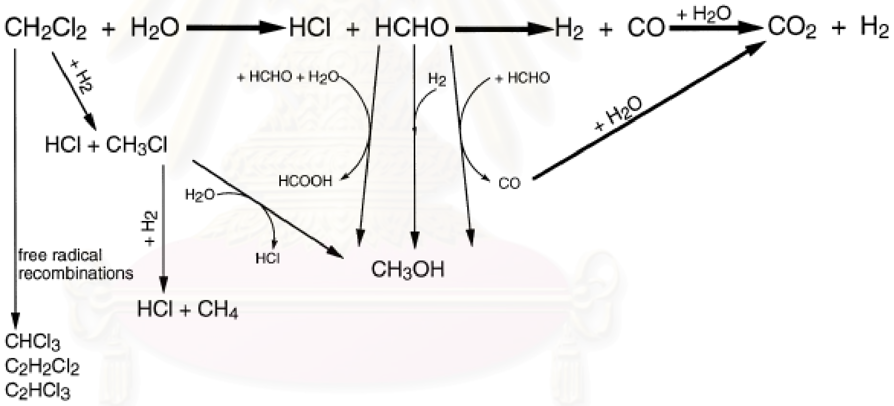

Figure 2.7 The proposed reaction network for CH_2Cl_2 under hydrolysis condition [6]

The product spectrum, yields, and distribution resulting from hydrolysis of CH_2Cl_2 in sub- and supercritical water had been measured and analyzed to identify and prioritize likely reaction pathways. The formation and destruction and their relative importance for all species were observed. The results showed that the main route for CH_2Cl_2 breakdown was via subcritical hydrolysis to formaldehyde and HCl, followed by decomposition of formaldehyde to CO and H_2, and subsequent CO conversion to CO_2 and H_2 by the water gas shift reaction.

Marrone et al. [7] interested to review the experimental data and provide the kinetics of dichloromethane under hydrothermal condition that not only a simple Arrhenius form for the rate constant but also Kirkwood theory and ab initio modeling. They reported that increased in the activation energy and a changing reaction profile with a decreasing dielectric constant provide a mechanism for a slowing of the reaction at higher temperatures. The hydrolysis of CH_2Cl_2 could generally be classified as a nucleophilic substitution reaction. As was usually the case with methyl and methylene halides, the reaction mechanism was most likely of the single-step, bimolecular type (S_N2) rather than the two-step, unimolecular type (S_N1). Under neutral conditions, water adds an OH group to the central carbon replacing one Cl, which combines with the extra H^+ to form HCl:

$$CH_2Cl_2 + H_2O \rightarrow CH_2ClOH + HCl \qquad (2.7)$$

The resulting unstable species CH_2ClOH then undergoes a much faster internal rearrangement, expelling another H^+ and Cl^- to form HCHO:

$$CH_2ClOH \rightarrow HCHO + HCl \qquad (2.8)$$

The net reaction was obtained by combining the two reactions:

$$CH_2Cl_2 + H_2O \rightarrow HCHO + 2HCl \qquad (2.9)$$

Salvatierra et al. [8] measured and modeled the kinetics of CH_2Cl_2 hydrolysis in sub- and supercritical water. Catalytic effects from a high nickel content alloy used for the reactor were studied by comparing kinetic data obtained in quartz ampules with and without metal present. Reaction rates from 100 to 500°C were measured to check the reproducibility and to extend the database for hydrolysis to the supercritical region in order to develop an empirical global rate expression. A fine powder of Hastelloy C-276 beads was used as metal in this experiment. The result shows that Hastelloy C-276 had no significant effect on the rate of CH_2Cl_2 decomposition.

Oshima et al. [9] pursued using a corrosion resistant flow reactor made from titanium tubing for CH_2Cl_2 hydrolysis and studied kinetic analysis of CH_2Cl_2 under hydrothermal condition. The relation between the CH_2Cl_2 conversion and residence time showed that hydrolysis of CH_2Cl_2 was first order. The rate constants of CH_2Cl_2 hydrolysis in this work were shown in Table 2.10.

Table 2.10 First order rate constants of dichloromethane disappearance [9]

Temperature (^oC)	**$[CH_2Cl_2]_0$ (mmol dm^{-3})**	**Rate constant (k/s^{-1})**	**Conditions**
250	0.6-5.1	$2.62 \pm 1.27 \times 10^{-2}$	H_2O
275	0.7-4.9	$2.51 \pm 1.48 \times 10^{-2}$	H_2O
300	1.1-5.6	$7.16 \pm 2.06 \times 10^{-2}$	H_2O
340	1.0-4.9	$1.49 \pm 0.23 \times 10^{-1}$	H_2O
360	0.9-4.4	$2.08 \pm 0.22 \times 10^{-1}$	H_2O
400	0.3-1.1	$2.53 \pm 0.43 \times 10^{-2}$	H_2O
450	0.2-0.8	$2.07 \pm 0.91 \times 10^{-2}$	H_2O
360	3.4	$2.14 \pm 0.29 \times 10^{-1}$	Oxidation, $[O_2]$ = 4.7 mmol dm^{-3}
360	3.4	$1.99 \pm 0.18 \times 10^{-1}$	Oxidation, $[O_2]$ = 23.7 mmol dm^{-3}
360	3.3	$1.94 \pm 0.06 \times 10^{-1}$	12 mmol dm^{-3} of NaCl added
360	3.3	$2.37 \pm 0.31 \times 10^{-1}$	58 mmol dm^{-3} of NaCl added
360	3.3	$2.70 \pm 0.42 \times 10^{-1}$	117 mmol dm^{-3} of NaCl added

The rate constant increased as the temperature was raised but dropped to a large extent above the critical temperature. The kinetic behavior could be explained base on a S_N2 mechanism under sub-critical condition. They reported that in the presence of natural salt, water molecules were considered to gather around the ionic species of the dissolve salt and the local density of the surrounding water was expected to increase of dielectric constant, which caused an increase of the hydrolysis reaction rate.

Watanabe et al. [11] reported that dichloromethane on SCW undergo rapid hydrolysis to HCHO and HCl. The first reaction step was assumed to be nucleophilic substitution of chloride by water. The intermediate formed, CH_2OHCl, was unstable and quickly forms CH_2O and HCl in the second reaction step. In Near Supercritical Water Oxidation (NCW) the reaction was found to be faster than SCW, despite the higher temperature of supercritical conditions. This can be explaining by considering the first reaction step, in which the bimolecular type (S_N2) reaction was strongly dependent on the properties of the solvent. At the system conditions, where was a higher relative dielectric constant. The activated complex of this reaction step was probably stabilized so that the activation energy was lower. Theoretical studies of the hydrolysis of CH_2Cl_2 using the modification of the Kirkwood solution model showed the influence of the reaction dielectric constant on the reaction rate. At supercritical conditions, the conversion was much lower due to a low relative dielectric constant and this trend was shown by both model and data. These solvent effects on the S_N2 reaction were captured quantitatively in a correction factor applied to the Arrhenius equation incorporated into the global rate expression proposed for CH_2Cl_2 hydrolysis.

Yamasaki et al. [30, 31] focused on hydrothermal of CH_2Cl_2 with and without alkali in temperature range of 150-300^oC by using batch reactor. ^1H, ^2H and ^{13} CNMR were used to analyze the quenched reactants, intermediate and products. They also used NaOH as alkali for dechlorination of CH_2Cl_2 in hydrothermal condition. In the presence of NaOH, the complete dechlorination was achieved in 270 min at 250^oC and 60 min at 300^oC. The gradual consumption of reactant CH_2Cl_2 was produced methanol and formate ion which could be confirmed by NMR analysis. The transformation of this hazardous compound to the safe and useful ones was completed in 270 min under the alkaline hydrothermal condition. The present NMR study clearly showed that CH_2Cl_2 could be completely transformed or recycled to safe and useful compounds without hazardous one. The mechanism of the hydrothermal reactions CH_2Cl_2 was discussed in term of the hydrolysis intermediate ($CH_2(OH)_2$). They proposed the reaction steps as follow: $CH_2Cl_2 + 2OH^- \rightarrow CH_2(OH)_2 + 2Cl^-$ and $2CH_2(OH)_2 + OH^- \rightarrow CH_3OH + HCOO^- + 2H_2O$. They have succeeded in the detecting the hydrolysis intermediate of the hydrothermal reaction of CH_2Cl_2 without alkali.

Yamasaki et al. [32] investigated fundamental reaction behavior in dechlorination of monochloroalkanes (methyl, ethyl, *n*-propyl, and *iso*-propyl chloride) at various hydrothermal conditions. The optimal condition for dechlorination treatment and solvent effects on the reaction had been discussed based on the results obtained under specific conditions of temperature, reaction time, stirring rate, solvent states, water content and concentration of the additives in the solvent on the dechlorination ratio. The reaction of monochloroalkanes obtained under critical temperature could be presented: $R\text{-}Cl + OH^- \rightarrow R\text{-}OH + \text{alkene} + R\text{-}O\text{-}R + Cl^-$
R means the alkyl group of the starting chloride.

Sinquin et al. [33] used $LaCoO_3$ and $LaMnO_3$ as good catalysts for the total oxidation of chlorinated volatile organic compounds (CVOCs) to CO_2 and HCl. Total destruction of CH_2Cl_2, $CHCl_3$ and CCl_4 was possible below 550^oC. Different by-products were obtained in function of the nature of the catalysts and the chlorinated compounds. CH_2Cl_2 was completely destroyed and CO_2 was the only carbon oxide formed for both catalysts. They proposed destruction step of dichloromethane on metal catalyst in Fig. 2.8. M represented to the transition metal.

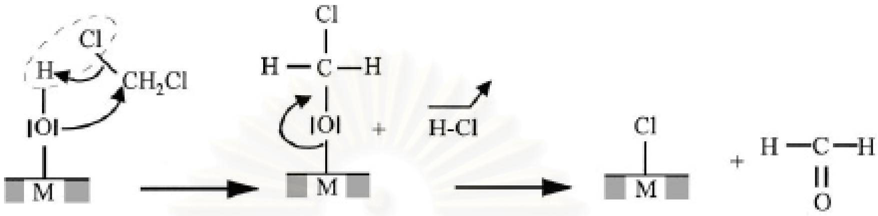

Figure 2.8 Destruction of dichloromethane on metal catalyst [33]

Pinard et al. [34, 35] investigated catalytic oxidation of dichloromethane in wet air over PtHFAU. They also studied hydrolysis mechanism of dichlromethane over this catalyst. Formaldehyde, the main reaction by-product could be formed through a direct hydrolysis of CH_2Cl_2 with water. To answer this proposal, experiments were carried out without water (only air) and in presence of nitrogen and water (without oxygen). In absence of water, catalyst deactivates rapidly and formaldehyde is not formed showing that this organic compound needs water for its formation. In these operating conditions, ($T = 340^oC$) only HCl, CH_3Cl, and CO were detected. They reported that only HCl and formaldehyde products from hydrolysis condition in the 2/1 molar ratio at temperatures lower than 380°C, appearance of other products: CO, CO_2 and methyl chloride (CH_3Cl) at higher temperatures. It could be concluded that over PtFAU zeolites, CH_2Cl_2 transformation occurs through a bifunctional pathway with hydrolysis of CH_2Cl_2 over the zeolite followed by oxidation of the formaldehyde intermediate over the Pt sites. The transformation pathway was shown in following step [35]:

$$CH_2Cl_2 \xrightarrow[\text{Support}]{H_2O} 2HCl + HCHO \xrightarrow[\text{Pt}]{O_2} CO_2 + H_2O + 2HCl \qquad (2.10)$$

2.8.2 Supercritical water oxidation of organic compounds

There have been some previous studies of formaldehyde reaction under hydrothermal condition. They presented the reaction mechanism of formaldehyde at high temperature but did not report about kinetic data or mechanism of formaldehyde oxidation in SCW condition.

Klein et al. [36] studied hydrolysis of formaldehyde at 800^{o}C and found that formaldehyde was decomposed by chain reaction. Carbon monoxide and hydrogen were formed in accordance with second-order rate laws. The kinetics of the pyrolysis of formaldehyde was such that it was independent of the surface to volume ratio of the reaction vessel. **Saito et al.** [37] used reflected shock tube and monitor time-dependent CH_2O and CO concentrations by IR emission. They proposed the mechanism formation and decomposition of formaldehyde that was an intermediate in oxidation of hydrocarbon. An Arrhenius expression for the second order reaction was also presented. **Tsujino et al.** [38] reported that methanol and formic acid were produced from cannizzaro type reaction of formaldehyde without catalyst at up to 250^{o}C and 4 MPa. **Takahashi et al.** [39, 40] investigated the ionic/radical association reaction in aqueous phase of $HCHO + OH \rightarrow HCHO - OH$ by Quantum Mechanism/Molecular Mechanism (QM/MM) simulation. The simulations had shown that there exists a potential energy barrier in an ionic association reaction both in the ambient water and SCW, though the reaction proceeds without potential barriers in the gas phase. They also presented the radical process of formaldehyde. **Watanabe et al.** [41] focused on formaldehyde reactions in supercritical water (400^{o}C and 25–40 MPa) with and without acid and base catalysts (homogeneous:H_2SO_4 and NaOH, and heterogeneous: CeO_2, MoO_3, TiO_2, and ZrO_2) by use of batch reactors. Cannizzaro reaction $2HCHO + H_2O \rightarrow CH_3OH + HCOOH$ and self-decomposition of formaldehyde $HCHO \rightarrow CO + H_2$ were found to be primary reactions for all the cases. **Osada et al.** [42] studied the water density dependence of formaldehyde reaction in supercritical water. It was found that the Cannizzaro reaction mechanism was the preferred reaction pathway for HCHO reaction in SCW. At higher water densities, CH_3OH yields increased confirming the predominance of the Cannizzaro reaction mechanism. At low water densities, CO yields increased and CH_3OH yields decreased, which indicated that monomolecular decomposition became the main reaction pathway.

The oxidation literature reviews of alcohols in supercritical water are shown as following below.

Boock et al. [43] investigated the pathways, kinetics and mechanisms under the potential environmental remediation process of oxidation in supercritical water and near-critical water. The free radical kinetic oxidation of C_1-C_3 alcohols and acetic acid exhibited features of both gas phase combustion and liquid phase oxidation chemistry. The mechanism was well represented by a set of eight reaction families: (1) H-abstraction by a molecule, (2) H-abstraction by radical, (3) oxygen addition to a radical, (4) isomerization, (5) scission of radical to form an olefin and a new radical, (6) decomposition of hydroxides to form two radicals, (7) non-terminating radical recombination, and (8) radical recombination.

Brock et al. [44] developed model comprised 148 reversible elementary reactions for the supercritical water oxidation of methane, methanol, carbon monoxide and hydrogen. Model predictions were compared with published experimental SCWO kinetics data for 450 - 650°C and 240 - 250 atm. The CHEMKIN package, which included thermodynamic data for many gas-phase species common to combustion systems, was used to calculate thermodynamically consistent reverse reaction rate constants. As a result, detailed chemical kinetics model based on a mechanism that comprised 22 species and 148 elementary, reversible, free-radical reactions was presented. HO, was an important free radical in SCWO kinetics. The rate constants for reactions involving HO, and the thermo chemical data for HO, must be known with better precision to reduce the uncertainty in predictive detailed chemical kinetics models for SCWO.

Brock et al. [45] studied the oxidation of methanol in supercritical water at 246 atm and temperatures between 500 and 589°C. Pseudofirst-order rate constants calculated from the data led to Arrhenius parameters. Formaldehyde was a primary product, while CO and CO_2 were secondary products. Formaldehyde was more reactive than methanol and its yield was always less than 24%. The temporal variation of the CO yield exhibited a maximum, whereas the CO_2 yield increased. The experimental data were consistent with a set of consecutive reactions $CH_3OH \rightarrow CH_2O \rightarrow CO \rightarrow CO_2$ with pseudo-first-order global kinetics. A reaction path analysis showed that the fastest reactions that consumed methanol involved OH attack and the resulting radicals produced formaldehyde, which was attacked by OH to form, eventually, CO. The CO was then oxidized to CO_2 via reaction with OH.

Rice et al. [46] studied the oxidation rate in the temperature range 440-500^{o}C of methanol and the subsequent production and destruction of the primary intermediate, formaldehyde that analyze by Raman spectroscopy. An elementary reaction mechanism, which produced accurately the quantitative features of methanol oxidation of formaldehyde production, was used to identify key rate controlling reactions during the induction period and the transition to the primary oxidation path.

Croiset et al. [47] determined the rate constant of hydrogen peroxide decomposition in supercritical water. Experiments were conducted at pressures ranging from 5.0 to 34.0 MPa and for temperatures up to 450°C. Kinetics modeling in several of the articles just mentioned points out the high sensitivity of organic oxidation to hydrogen peroxide decomposition: (M) is water.

$$\mathrm{H_2O_2} + (M) \rightarrow \mathrm{2OH} + (M) \qquad (2.11)$$

Hydrogen peroxide decomposition in water followed first-order kinetics in the aqueous, vapor, and supercritical phases. The homogeneous dissociation rate of hydrogen peroxide was found to be independent of the dissociation on surfaces of the reactor. The important factor determining the homogeneous rate of hydrogen peroxide thermal decomposition in water was the water density.

Anitescu et al. [48] investigated the methanol oxidation over a temperature range of 400^{o}C to 500^{o}C and residence time from 3.20 to 48.7 s. The isothermal and isobaric plug flow reactor was used in the experiment. The identified reactions were mainly CO and CO_2. The experimental data were consisting with a set of consecutive first order reactions $\mathrm{CH_3OH} \rightarrow \mathrm{CO} \rightarrow \mathrm{CO_2}$. The Global kinetics for SCWO of methanol may be conveniently examined by assuming that the global rate of this reaction network was proportional to the methanol concentration in the reactor at the given time and independent of the water and O_2 concentration.

$$\left(-\frac{d[Methanol]}{dt}\right) = k_1[Methanol]^a$$

For first order kinetics, a = 1 and a plot of ln $(1\text{-}X_1)$ versus residence time should represent a straight line at each temperature with slope providing a rate constant.

Oshima et al. [49] simulated the reaction progress in supercritical water oxidation of methanol in terms of a detailed chemical kinetics model (DCKM). The two ideal reactors, plug flow reactor (PFR) and continuous stirred tank reactor (CSTR) at pressure of 25 MPa., temperature 450^{o}C to 550^{o}C were studied. The calculation was performed using the CHEMKIN II package. The reaction had an induction time and character of first order reaction against the methanol concentration in PFR. The reaction did not depend on the oxygen concentration. In order to understand the contribution of individual elementary reaction progress, they carried out the sensitivity analysis. The result suggested that in both PFR and CSTR, the conversion of methanol was very sensitive to radical formation.

Rice et al. [50] studied the oxidation of ethanol at 24.5 MPa over a temperature range 410-470^{o}C. Concentration of ethanol, acetaldehyde, formaldehyde, methanol, carbon monoxide, carbon dioxide and hydrogen peroxide were measured as functions of time and temperature. They indicated that abstraction of hydroxyl hydrogen atom results primary in the production of formaldehyde and methyl radical as intermediate. Most of ethanol was converted in the formation of acetaldehyde from abstraction of the secondary hydrogen by OH, HO_2 and followed by removal of the hydroxyl hydrogen by oxygen to form HO_2. Acetaldehyde lost the aldehydic hydrogen to HO_2 forming H_2O_2 and CH_3CO, which decomposed to CO and CH_3.

Feng et al. [51] presented the measurements of the hydrogen abstraction from methanol by hydroxyl radical in water at temperatures from ambient to 390°C and at 250 bar. They indicated that many saturated and unsaturated organic compounds react with hydroxyl radicals by hydrogen abstraction to form water and a carbon radical.

$$\mathrm{RH} + \bullet\mathrm{OH} \rightarrow \mathrm{R} + \mathrm{H_2O} \qquad (2.12)$$

Methanol had been chosen as the model compound to conduct the hydrogen abstraction reaction from ambient to supercritical conditions. ●OH was generated by pulse radiolysis and the kinetics determined by monitoring the growth of the nitrohydroxycyclohexadienyl radical. There were two pathways for hydrogen abstraction from methanol by ●OH:

$$CH_3OH + \bullet OH \rightarrow CH_3O\bullet + H_2O \tag{2.13}$$

$$CH_3OH + \bullet OH \rightarrow CH_2\bullet OH + H_2O \tag{2.14}$$

Since hydrogen abstraction by hydroxyl radical had been identified as a key reaction in SCWO, this may explained the mixed success that had been observed when the free radical mechanism models were used for the SCWO process.

Henrikson et al. [52] studied the oxidation of methanol in supercritical water at 500°C to explore the influence of the water concentration (or density) on the kinetics. The rate increased as the water concentration increased from 1.8 - 5.7 mol/L. This effect of water density on the kinetics experiment was quantitatively reproduced by a previously mechanism-based, detailed chemical kinetics model (DCKM). They concluded that water accelerates the rate of methanol SCWO and low concentrations primarily through its role as a reactant in elementary steps that produce OH radicals. In these steps, water served as a hydrogen donor to a free radical. Net rate analysis revealed that the water concentration influenced the global SCWO rate by increasing the generation rate of highly reactive OH radicals. The important steps were ones wherein a free radical abstracted an H atom from water to form OH plus a molecular product.

Ploeger et al. [53] investigated base model from the combustion literatures which reported the product yields of stable intermediates over a range of temperature, pressure, concentration, and density conditions. The construction of SCWO mechanisms and kinetic rate models required the identification of reactive intermediate species, estimation of the new species' thermochemistry, identification of new reaction pathways, and estimation of rate constants. Hydroxyl ($OH\bullet$) and hydroperoxy ($HO_2^{\bullet}$) radicals held the central role in the oxidation of hydrogen, carbon monoxide, methane, and other intermediates. The mechanism of methane oxidation which formaldehyde was stable intermediates in supercritical water condition was also presented in their research. The overall conversion of methane was controlled by two major submechanisms. The C-1 submechanism governed the reactions involving all single-carbon compounds and the H_2/O_2 submechanism governed the reactions of hydrogen, water, oxygen, hydrogen peroxide, and HO_x radicals.

Hayashi et al. [54] investigated reaction kinetics of methanol and ethanol oxidation in supercritical water both experimentally and computational simulation at 520–530^{o}C and 24.7 MPa. They also studied the oxidation of the two alcohols in binary mixtures. Kinetic analyses based on the elementary reaction model showed that production of OH from the reaction of H_2O with HO_2 seemed to play an important role at the low methanol concentrations. For the binary system, it was found that methanol conversion was accelerated by ethanol addition whereas ethanol oxidation was slightly retarded by the presence of methanol. Calculation with an elementary reaction model could reproduce the phenomenological mutual effects of alcohols with respect to reaction rates, and it was found that the acceleration/retardation effect of conversions could be well characterized by the time profile of OH radical, rather than HO_2 radical.

There have been several previous studies of hazardous compounds oxidation by SCWO technique.

Oshima et al. [55] investigated phenol oxidation in supercritical water in a flow reactor at a temperature range from 370^{o}C to 430^{o}C, and about 100 data were taken under various conditions in order to determine the kinetic parameters. Experimental results showed that the global rate of phenol disappearance was proportional to the phenol concentration, and to the 0.48 power of O_2 concentration, which were in good accordance with the reported values. Their results also showed a negative dependence of the global reaction rate on the H_2O density in a certain range. The kinetic parameters obtained in the present work always gave higher rates than those of pervious research, though the reason for this difference has not yet been clarified.

Portela et al. [56] studied kinetic comparison between sub-critical and supercritical water oxidation of phenol in plug flow reactor at temperature 300-500^{o}C and fix pressure 25 MPa. As a result, reaction kinetics obtained in the sub-critical range proposed pseudo-first-order in (2.15) and (2.16).

$$\ln\frac{[Phenol]}{[Phenol]_o} = k'(t - t_I) \qquad (2.15)$$

$$k' = \exp\left(-\frac{E_a}{RT}\right) \qquad (2.16)$$

And reaction kinetics obtained in the supercritical range for this experiment could be expressed as

$$\begin{aligned}\ln(rate) &= \ln\left(-\frac{d[Phenol]}{dt}\right)\\ &= \ln A - \frac{E_a}{RT} + a\ln[Phenol] + b\ln[O_2] \qquad (2.17)\end{aligned}$$

In most cases, predictions from kinetics models obtained below and above the critical point of water are completely different. Furthermore, predictions from kinetic expressions obtained in the same range of operating conditions vary considerably. Moreover, most of rate expressions available in the literature have been compared in order to find the reasons for the discrepancies found. It was impossible to predict the real behavior of phenol oxidation under hydrothermal conditions. There were many aspects, like oxygen/phenol ratio, different geometry and material of the reactor, operating procedures, etc., that affect the reaction mechanism and, consequently, the result rate law expression.

Perez et al. [57] studied supercritical water oxidation system for high concentration of phenol in a pilot-scale. The reaction temperature and excess oxygen were used in the range of 400-500^{o}C and 0-34%, respectively at 25 MPa for 40 s. Phenol destructed from 94 to 99.98%. It was consistent with extrapolations of some global rate laws proposed in several literatures. The destruction of total organic carbon (TOC) was varied from 75 to 99.77%. The measurement of phenol conversion and TOC indicated that the higher level of both phenol and TOC destruction was produced at the higher temperature. The conversion data were functions of temperature, excess O_2 supplied, and residence time. The residence time of supercritical process was lower at the high reaction temperature. In most of the previous works on SCWO of phenol, the rate of phenol destruction was the first order dependence on phenol concentration.

Goto et al. [58] applied supercritical water oxidation technique to the destruction of municipal excess sewage sludge and alcohol distillery wastewater of molasses. The reaction was carried out in a batch reactor with hydrogen peroxide as an oxidant in the temperature range 400-500^{o}C. Total organic carbon was measured as a function of reaction time. The dynamic data was analyzed by a first-order reaction model. The municipal excess sewage sludge consisted of a slurry mixture of solid microorganisms and dissolved organic and inorganic materials, which reacts to produce solid-, liquid-, and gas-phase products after being cooled to ambient temperature. The solid-phase product was sediment with a pale red brown color. The liquid-phase product was odorless, transparent, and colorless after the complete reaction. The destruction rate was faster at a higher temperature, and the TOC reduced to almost zero in 60 s. at 500^{o}C. The dark color of distillery wastewater was completely removed so that it was colorless and transparent. The decomposition behavior was similar to the sewage sludge.

Jin et al. [59] used supercritical water oxidation to decompose carrots and beef suet in a batch reactor system with an H_2O_2 oxidant, at a temperature between 400 and 450°C and reaction times from 10 s. to 10 min. The results showed that the oxidative decomposition of carrots and beef suet proceeded rapidly and a high total organic carbon (TOC) decomposition of up to 97.5%. Carrots were destructed within 3 min at 420°C and within 5 min at 450°C for beef suet. The oxidation reaction for both carrots and beef suet may be separated into the fast reaction at the early stage and the slow reaction at the later stage. In the later stage following the reactions at the early stage, acetic acid, which was a fairly stable product of the early-stage (primary) reaction, was the reactant and the rate of overall oxidation reaction for complete decomposition was dominated by the later stage reaction. Oxidation of acetic acid could also be expressed as the first-order reaction.

Fang et al. [60] used micro reactor, batch reactors, and a flow reactor to study the oxidation of decachlorobiphenyl (10-CB) in supercritical water. In the microreactor experiments, it was found that complete dissolution of 10-CB occurred at excess O_2 (>93%). In experiments performed with the batch reactors, at excess O_2, 99.2% and 100% 10-CB could be destroyed in SCW without and with Na_2CO_3, respectively. Addition of the neutralization agent Na_2CO_3 promoted the destruction rate and reduced reactor corrosion significantly. A reaction mechanism for 10-CB destruction was proposed and this was examined further in flow experiments.

Wang et al. [61] explored oxidation of coal in supercritical water by using H_2O_2 as the oxidant source in a bench-scale semi-continuous system. The conversion of coal was increased as reaction time increased. Under the experimental conditions at 420°C, 25.0 MPa, and 5.0 ml/min of 5.0 wt % H_2O_2 solution, the conversion of coal was respectively 26.7%, 68.1%, and 82.1% for the reaction times of 5, 15, and 20 min. The oxidation of coal in SCW was a pseudo-first-order process.

Fauvel et al. [62] developed transpiring wall reactors to cope corrosion and salt precipitation in supercritical water oxidation which the inner porous shell was composed of pure R-alumina, to handle organic effluents generated by nuclear activities. A mixture of dodecane and tributyl phosphate was used as a model effluent. High destruction rates were actually achieved (>98%). The porous reactor was not proven to be very efficient for the continuous treatment of salty wastes. However, it was proven to be very efficient in regard to treating aggressive compounds. In fact, no corrosion damage was observed, either on the stainless steel vessel or on the pure R-alumina inner porous tube.

Bermejo et al. [63] designed transpiring wall on supercritical water oxidation reactors. Three designs were tested: a fully porous wall made of porous sintered AISI 316 and alloy 600 and two partially porous walls made of porous sintered alloy 600 and nonporous alloy 625. The temperature profile of the reactor was presented, showing that the existence of transpiring flow results in only a fraction of the reactor being used under supercritical conditions. Porous sintered stainless steel was not appropriate for the SCWO process because it fails to resist high temperatures. Porous sintered alloy 600 can endure the process only for a limited time because the materials were damaged by temperatures higher than 600°C.

Prikopsky et al. [64] used a transpiring-wall reactor for supercritical water oxidation containing a hydrothermal flame as an internal heat source. Two types of transpiring-wall elements with different porosity were investigated. Experiments with artificial wastewater containing methanol and sodium sulfate in concentrations up to 6 and 3 wt. %, respectively, were used for a maximum operation time of 3 h. About 65% of the salt introduced to the reactor was detected in the effluent. No plugging of the reactor and equipment was observed during the experiments and methanol conversion ratios higher than 99.99% were measured.

2.8.3 Catalysis in supercritical water oxidation

Recently, catalytic oxidation in supercritical water has received considerable research attention. The major thrust of this current research effort is attributable to the rapid development of supercritical water oxidation as an innovative wastewater treatment technology. The incentives of catalyst-enhanced processes may include increase reaction rates, reduce residence times and temperatures.

Yu et al. [65] used bulk MnO_2 as catalyst for phenol oxidation in supercritical water at 380-420^{o}C and 219-300 atm in a flow reactor. The bulk MnO_2 catalyst enhances both the phenol disappearance and CO_2 formation rates during supercritical water oxidation, but it does not affect the selectivity to CO_2 or to phenol dimers at the given phenol conversion. The role of the catalyst appears to be accelerating the rate of formation of phenoxy radicals, which then react in the fluid phase by the same mechanism operative for non-catalytic SCWO of phenol. The rate of the phenol disappearance and CO_2 formation are sensitive to phenol and O_2 concentrations but independent of the water density. **Yu et al.** [66] also investigated oxidation of phenol in supercritical water using CuO/Al_2O_3 as a catalyst in a packed-bed flow reactor. The CuO catalyst has the desired effects of accelerating the phenol disappearance and CO_2 formation rates relative to non-catalytic supercritical water oxidation. The rates of phenol disappearance and CO_2 formation were sensitive to the phenol and O_2 concentrations, but insensitive to the water density. The supported CuO catalyst exhibited a higher activity, on a mass of catalyst basis, for phenol disappearance and CO_2 formation than did bulk MnO_2 or bulk TiO_2. The CuO catalyst had the lowest activity, however, when expressed on the basis of fresh catalyst surface area. The CuO catalyst exhibited some initial deactivation, but otherwise maintained its activity throughout 100 h of continuous use. Both Cu and Al were detected in the reactor effluent, however, which indicates the dissolution or erosion of the catalyst at reaction conditions.

Yu et al. [67] studied the catalytic activity, stability, and transformations during oxidation in supercritical water. They used three different catalysts (bulk MnO_2, bulk TiO_2, and CuO/Al_2O_3) to oxidize phenol in supercritical water in a tubular flow reactor. CuO/Al_2O_3 was the most active of the three on a mass of catalyst basis whereas MnO_2 was the most active on an area basis. All three catalysts largely maintained their activities for phenol disappearance and for CO_2 formation throughout more than 100 h of continuous use. MnO_2 and TiO_2 were stable in the sense that no Mn or Ti was detected in the reactor effluent. The CuO/Al_2O_3 catalyst, on the other hand, was not stable. Both Cu and Al were detected in the reactor effluent.

Oshima et al. [68] investigated disappearance rate in catalytic oxidation of phenol over MnO_2 in supercritical water at a fixed temperature of 425°C and pressures between 22.7 and 27.2 MPa. The non-supported MnO_2 catalyst possessed a strong activity for promoting phenol oxidation. A Langmuir-type mechanism, in which phenol and oxygen adsorbed on the catalytic sites and water adsorbed on the same site to inhibit the phenol and oxygen adsorption, was proposed to explain the reaction orders for phenol, oxygen, and water.

Armbruster et al. [69] studied hydrolysis of ethyl acetate in sub-critical (360^oC, 20 MPa.) and supercritical water (400^oC, 24 MPa.) in a tubular flow reactor as a model reaction for the depolymerisation of polyesters. The reaction products ethanol and acetic acid were stable under these conditions. Additionally, oxidative decomposition experiments were carried out using ethyl acetate, ethanol and acetic acid as feed in the presence of air, non-catalysed as well as in the presence of a heterogeneous MnO_2–CuO/Al_2O_3 catalyst. The catalyst caused only slight increase of ethyl acetate conversion in oxidation compared to hydrolysis, but a noticeable increase in CO_2 formation due to destruction of ethanol and acetic acid.

Yu et al. [70] oxidized acetic acid in supercritical water over a bulk MnO_2 catalyst in a nominally isothermal, isobaric packed-bed reactor operating at steady state. Most experiments were conducted at 380°C and 250 atm. They identified a global rate law that was both qualitatively and quantitatively consistent with experimental results. They found that the use of MnO_2 as an oxidation catalyst could reduce the reactor volume required comparison with literature rate laws for non-catalytic to treatment of acetic acid in SCW condition more than 2 orders of magnitude.

Suppes et al. [71] oxidized phenol, methanol, ethanol, n-propanol and n-butanol at temperatures between 200 and 374^oC and pressures between 2 and 220 bar. Reactions were conducted in packed-bed flow reactors with ZrO_2 and $CaCO_3$ packings with a stoichiometric amount of H_2O_2. At temperatures > 200^oC over a range of pressures, $CaCO_3$ showed increasing catalytic activity with increasing temperatures for methanol, ethanol, n-propanol, and n-butanol oxidation. At temperatures, > 200^oC $CaCO_3$ enhances oxidation rates equal to or better than the best reported performance of catalysts based on noble and transition metals. $CaCO_3$ performance was achieved without toxicity concerns related to catalyst leaching, corrosion, or erosion, and for applications with low pH or halogenated hydrocarbons. The calcium could buffer the pH and convert halogens to benign salts.

Matsumura et al. [72] studied activated carbon that was a novel catalyst for supercritical water oxidation of phenol. High-concentrations of phenol were treated in supercritical water at 400^{o}C and 25 MPa with an equivalent amount of oxygen in a reactor packed with activated carbon. Although activated carbon itself was oxidized in the reaction field, its weight decrease was sufficiently slow for its catalytic effect on phenol oxidation to be observed. The catalytic effect of activated carbon consisted of an enhancement of the reaction rate, a decrease in the tarry product yield, and an increase in the gas yield. This report was the first to indicate the catalytic effect of carbonaceous materials on supercritical water oxidation, and it demonstrated that supercritical water oxidation using lower operation temperatures and inexpensive carbon catalysts may be possible.

Tomita et al. [73] examined the stability of catalytic activity and the effect of supercritical water on the phase and structural properties of MnO_2 through a catalytic supercritical water oxidation of phenol at 425^{o}C and 24.7 MPa. The conversion of phenol slightly declines during the first 6 h, which was due to the transformation of the crystal structure from MnO_2 to Mn_2O_3 in supercritical water. The lattice oxygen could be involved in the oxidation and play a role as an oxidizer. The oxygen supplied to the system functions to compensate for the lattice oxygen used. It was also important to supply oxygen for the maintenance of the catalytic activity, because the lack of supplied oxygen would promote the transformation of the structure of the catalysts.

CHAPTER III

EQUIPMENTS AND EXPERIMENTAL PROCEDURES

In this section, equipments, materials and experimental procedures of non-catalytic study of formaldehyde oxidation, catalytic compact sized reactor by SCWO technique and elimination hydrochloric acid before SCWO reactor are located as follows.

3.1 Non-catalytic study of formaldehyde oxidation in SCW

The SCWO of formaldehyde in order to obtain the kinetic information is investigated. The experiments are conducted using a plug flow reactor (PFR). The experimental apparatus is shown in Figure 3.1. Reactor is made of Hastelloy C-276 tubing, inside diameter 0.11 cm, outside diameter 0.16 cm and length 4 m, volume of reactor is 3.52 cm^3. The fluidized sand bath is used for heating up the reactor and preheating lines, and the temperature is monitored at the inlet and outlet of the reactor using thermocouples. For non-catalytic study of formaldehyde oxidation in SCW, the effects of temperature, initial formaldehyde concentrations and methanol concentration as a stabilizer on formaldehyde conversion are investigated.

3.1.1 Equipments

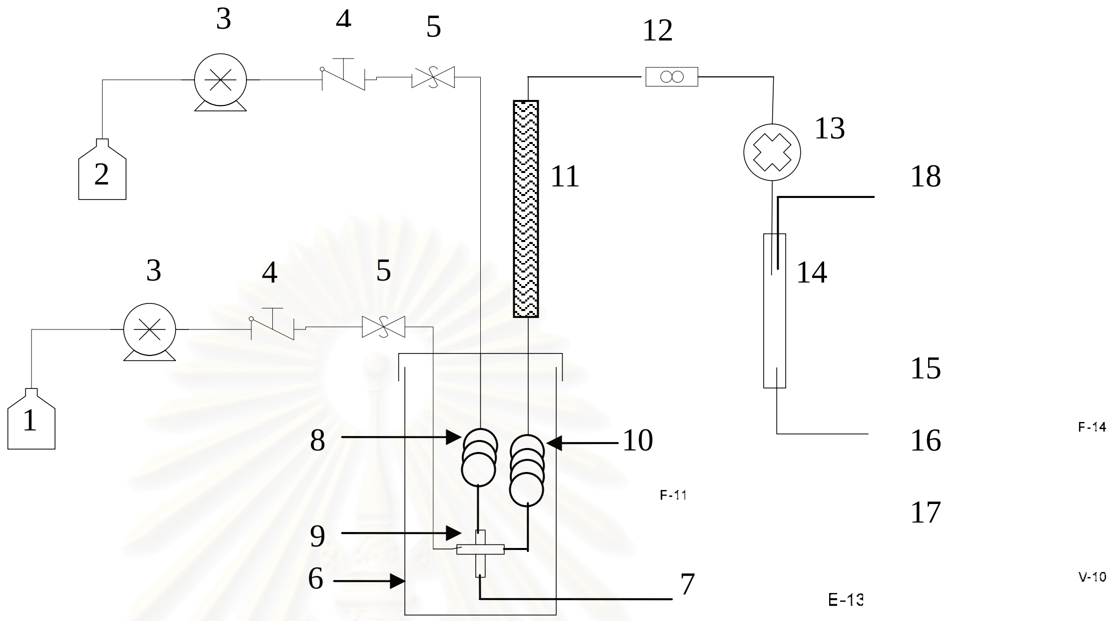

Figure 3.1 Experimental apparatus for non-catalytic study in SCWO of formaldehyde

E-12

1. HCHO solution

F-7

2. H_2O_2 solution tank was built by Taiatsu techno corporation

F-1 F-8

3. HPLC pump type PU-980 by Jasco company

V-4 V-8

4. Lift check valve E-6

5. Stop valve

6. Fluidized sand bath was built by Mastuki kayaku company

E-2

7. Thermocouple of reactor

8. H_2O_2 pre-heater stainless steel outside diameter 0.16 cm length 10 m

9. Union cross

10. Reactor is made of Hastelloy C-276 tubing, inside diameter 0.11 cm, outside diameter 0.16 cm and length 4 m volume of reactor is 3.66 cm^3.

11. Heat exchanger

12. Inline filter

13. Automatic Back Pressure Regulator type 880-81 by Jasco

14. Separator

15. Flame Ionization Detector Gas Chromatography (GC-FID) for analyze methanol in liquid phase: column Porapak Q 80-100 C-0473.

16. Thermal Conductivity Detector Gas Chromatography (GC-TCD) column APS-201 20% FlusinT 60-80 for analyzed formaldehyde in liquid product.

17. Total Organic Carbon analyzer (TOC) for analyzed total organic carbon in liquid product

18. Thermal Conductivity Detector Gas Chromatography (GC-TCD) column unibead S C 60-80 for analyzed CO, CO_2 in gas product.

3.1.2 Materials

1. **Water** is commercially obtained distilled water and deoxygenated by N_2 gas bubbling prior to use.

2. **The oxidant** is oxygen which was produced by the thermal decomposition of H_2O_2, the solution of which was prepared from 30 wt % H_2O_2/water initial stock solutions.

3. **The formaldehyde solution** is prepared from 37 wt % commercial aqueous solutions which also contained about 8 % of methanol as a preservative.

4. **Methanol solution** is prepared from 99 wt % commercial aqueous solutions.

3.1.3 Experimental procedures

1. H_2O_2 solution, which is completely decomposed into O_2 and H_2O in a preheating line, and formaldehyde solution are separately fed into the reactor using two HPLC pumps. To keep the contribution of the preheating stage where the hydrolysis reaction of HCHO may proceed to some extent as small as possible, the solution of HCHO is directly introduced into the reactor without preheating. The flow rate of preheated H_2O_2 solution is always at least 4 times larger than that of the solution of HCHO so as to heat up the solution of HCHO very quickly to the reaction temperature after mixing two streams.
2. The fluid emitted from the reactor is cooled and depressurized, followed by the gas-liquid separation.
3. The gas products as well as formaldehyde and methanol as preservative in liquid are analyzed by GC-TCD. Methanol in liquid phase is quantified by GC-FID. Total organic carbon in liquid phase is measured by TOC analyzer.
4. The initial formaldehyde concentration is depending on each study,

- **The effect of temperature on formaldehyde conversion**: 0.08 mol/L at ambient condition can calculate for concentration at reactor entrance dependence on temperature and pressure. Reaction temperature and pressure are 400, 450 and 500^{o}C, 25 MPa, respectively

- **The effect of initial formaldehyde concentrations on formaldehyde conversion**: 0.04 and 0.08 mol/L at ambient condition can calculate for concentration at reactor entrance dependence on temperature and pressure. Reaction temperature and pressure are 400, 450 and 500^{o}C, 25 MPa, respectively

- **The effect of methanol concentration as a stabilizer on formaldehyde conversion**: formaldehyde/methanol ratios, 1:0.2, 1:0.4, 1:1 and concentration of formaldehyde/methanol: 0.08:0.016, 0.08:0.032, 0.08:0.08, respectively. Reaction temperature and pressure are 450 and 500^{o}C, 25 MPa, respectively.

3.2 Catalytic compact sized reactor by SCWO technique

For the catalytic study, a simple and compact reaction system is used, the size of which is 0.5 × 0.5 × 1.0 m^3. The flow sheet of the apparatus is shown in Figure 3.2. The fixed bed reactor (Stainless steel 0.95 cm o.d. volume 4.3 mL) with loading 10 g of MnO_2, surrounded by the electric heater is used in this experiment. The effects of reaction temperature, initial formaldehyde concentration, percent excess of oxygen and mixture of organic compounds decomposition in catalytic SCWO compact sized reactor are investigated.

3.2.1 Equipments

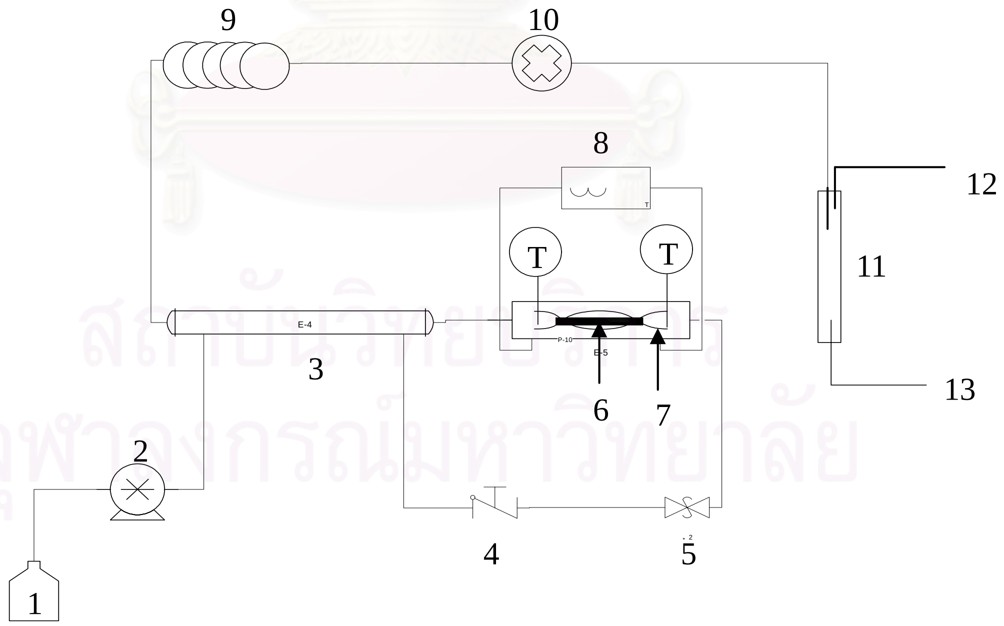

Figure 3.2 Experimental apparatus for catalytic SCWO compact sized reactor

Figure 3.3 Catalytic SCWO compact sized reactor for laboratory waste treatment

1. Organic and hydrogen peroxide solution
2. HPLC pump NP-AX-15
3. Heat exchanger
4. Check valve
5. Relief valve
6. Fixed bed reactor
7. Vial heater
8. Temperature controller set
9. Cooler by air contact
10. Back pressure regulator, GO REGULATOR: BP-66
11. Separator
12. Thermal Conductivity Detector Gas Chromatography (GC-TCD) column unibead S C 60-80 for analyzed CO, CO_2 in gas product.

13. Total Organic Carbon analyzer (TOC) for analyzed total organic carbon in liquid product

3.2.2 Materials

1. **Water** is commercially obtained distilled water and deoxygenated by N_2 gas bubbling prior to use.
2. **The oxidant** is oxygen which is produced by the thermal decomposition of H_2O_2, the solution of which is prepared from 30 wt % H_2O_2/water initial stock solutions.
3. **Formaldehyde solution** is prepared from 37 wt % commercial aqueous solutions which also contained about 8 % of methanol as a preservative.
4. **Methanol solution** is prepared from 99 wt % commercial aqueous solutions.
5. **Ethanol solution** is prepared from 95 wt % commercial aqueous solutions.
6. **Acetic acid solution** is prepared from 99 wt % commercial aqueous solutions.
7. **MnO_2** is prepared from commercial catalyst (160 – 500 µm) 10 g

3.2.3 Experimental procedures

1. H_2O_2 solution and organic solution are fed into the reactor using one HPLC pump. Volumetric flow rate of solution is 3.2-10.2 mL/min.
2. The fluid emitted from the reactor is cooled and depressurized, followed by the gas-liquid separation.
3. The gas product is analyzed by GC-TCD and liquid product is measured by TOC analyzer.

4. The condition of the experiments are depending on each study,

- **Effect of reaction temperature on conversion**: initial formaldehyde concentration is 0.3 mol/L at ambient condition, excess oxygen 100%. Reaction temperature and pressure is 350, 380 and 400^{o}C, 25 MPa.
- **Effect of initial formaldehyde concentration on conversion**: initial formaldehyde concentration is 0.1, 0.3, 0.6 mol/L at ambient condition, excess oxygen 100 %. Reaction temperature and pressure is 400^{o}C, 25 MPa.
- **Effect of percent oxygen excess on conversion**: initial formaldehyde concentration is 0.3 mol/L at ambient condition, excess oxygen 8, 65, 100 %. Reaction temperature and pressure is 400^{o}C, 25 MPa.
- **Effect of mixture of organic compounds on conversion**: initial concentration of each compounds: formaldehyde, methanol, ethanol, acetic acid is 0.1 mol/L at ambient condition, excess oxygen 100 %. Reaction temperature and pressure is 400^{o}C, 25 MPa.

3.3 Elimination hydrochloric acid before SCWO reactor

In design of the cascade process where hydrolysis and oxidation are consecutively combined, it is necessary to eliminate HCl between these two stages, because HCl is the major product in the hydrolysis dichloromethane and provides very corrosive atmosphere in sub- and supercritical water. The two different methods are introduced; one is high pressure method: the addition of $Pb(CH_3COO)_2$ as a precipitating reagent, and the other is low pressure method: the removal of HCl by ion exchange resin. The diagram of precipitation technique is shown in Figure 3.4 and the ion exchange resin experimental apparatus is shown in Figure 3.5.

3.3.1 High pressure method: precipitation of hydrochloric acid

3.3.1.1 Equipments

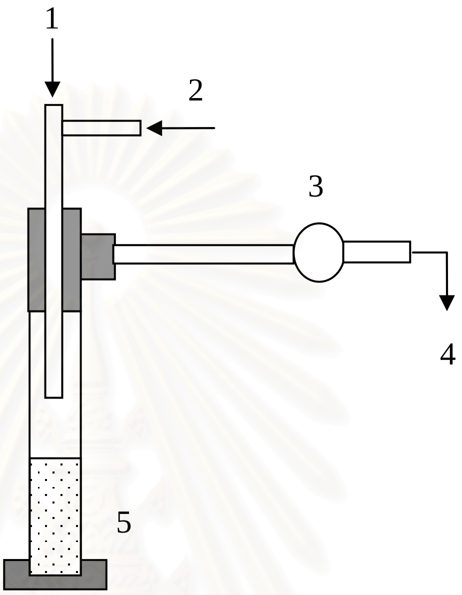

Figure 3.4 The diagram of precipitation technique

1. $Pb(CH_3COO)_2$ solution
2. HCl solution
3. Back pressure regulator
4. Effluent analyzed by Ion Chromatography (IC)
5. Precipitation zone

3.3.1.2 Materials

1. **Water** is commercially obtained distilled water and deoxygenated by N_2 gas bubbling prior to use.

2. **Hydrochloric acid** is prepared from 2 mol/L. commercial aqueous solutions.

3. **Lead (Pb)** is prepared from lead acetate ($Pb(CH_3COO)_2$) commercial.

3.3.1.3 Experimental procedures

1. Reaction temperature is ambient and pressure is 0.1-25 MPa. The HCl and $Pb(CH_3COO)_2$ concentration in the original solution is 0.1-0.2 and 0.5 mol/L, respectively.
2. The solution of HCl and $Pb(CH_3COO)_2$ are separately fed by two HPLC pumps.
3. Chloride ion emitted from the reactor is analyzed by ion chromatography equipped with a Shodex ICI-524A column.

3.3.2 Low pressure method: Ion Exchange resin technique

Because of their limited properties, the resins should be used at the temperature below 100°C and atmospheric pressure. In this experiment ion exchange resin is applied to remove HCl before SCWO reactor at low pressure. The experimental setup is shown in Figure 3.5. Strong base ion exchange resins ($R\text{-}N(CH_3)_3 \cdot OH$) are used in this experiment.

3.3.2.1 Equipments

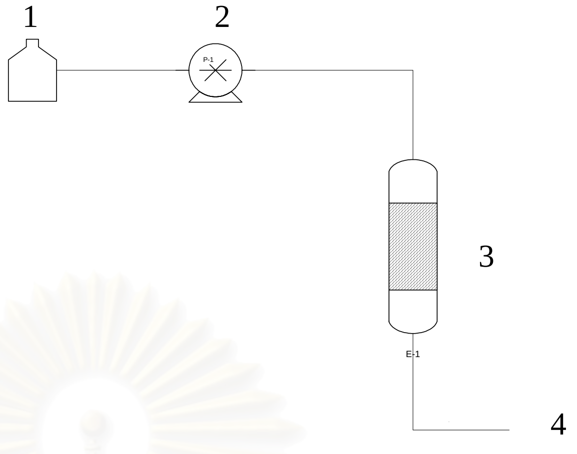

Figure 3.5 The diagram of ion exchange resin technique

1. HCl solution
2. HPLC pump
3. Fixed bed with ion exchange resin volume 4.3 mL
4. Effluent analyzed by Ion Chromatography (IC)

3.3.2.2 Materials

1. **Water** is commercially obtained distilled water and deoxygenated by N_2 gas bubbling prior to use.

2. **Hydrochloric acid** is prepared from 2 mol/L. commercial aqueous solutions.

3. **Ion exchange resin** is strong base resin commercial. [R-N$(CH_3)_3$.OH]

3.3.2.3 Experimental procedures

1. Reaction temperature is ambient and pressure is 0.1 MPa. The HCl concentration in the original solution is 0.1-0.2 mol/L 3.14 and 6.25 g of ion exchange resins are used.
2. The solution of HCl is fed by one HPLC pump, and passes to ion exchange resin column.
3. Chloride ion emitted from the column is analyzed by ion chromatography equipped with a Shodex ICI-524A column.

CHAPTER IV

NON-CATALYTIC STUDY OF FORMALDEHYDE OXIDATION IN SUPERCRITICAL WATER

There have been many previous studies on the hydrolysis of dichloromethane in sub-critical water, which the main products are known to be formaldehyde and HCl [6-9]. Compared with the abundance of the previous researches on dichloromethane hydrolysis, the kinetic of formaldehyde oxidation in supercritical water has been less investigated. Therefore, the SCWO of formaldehyde in order to obtain the kinetic information is investigated. In this section, the effects of temperature, initial formaldehyde concentrations and methanol concentration as a stabilizer on formaldehyde conversion are investigated and the mechanism of formaldehyde oxidation in SCW is also discussed. Besides, the lengths of plug flow reactor for complete destruction of formaldehyde on these conditions are presented.

4.1 Effect of temperature reaction on formaldehyde conversion

The experiments are conducted using a plug flow reactor (PFR). The experimental apparatus is shown in Figure 3.1. The conversion profiles of formaldehyde at temperature of 400, 450 and 500^{o}C, and pressure of 25 MPa are shown in Figure 4.1. Initial formaldehyde concentration of 0.08 mol/L at ambient condition can be used to calculate for concentration at reactor entrance dependence on temperature and pressure. The initial concentrations of formaldehyde at the reactor entrance are 2.7, 1.7 and 1.3 mmol/L at 400, 450 and 500^{o}C, respectively. An excess amount of H_2O_2 (325 % of stoichiometric requirement) is supplied. Based on the studies of Croiset et al. [47], it has been evidenced that H_2O_2 completely decomposed in the pre-heaters even at high flow rate and low temperature.

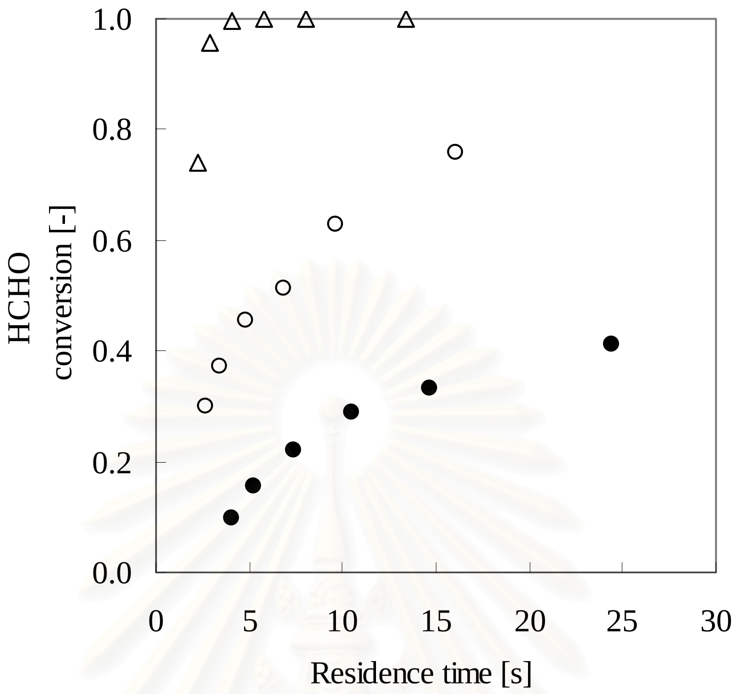

Figure 4.1 Formaldehyde conversion of non-catalytic study in SCWO at 400°C (●), 450°C (○) and 500°C (Δ), at 25 MPa

In Figure 4.1, there is obviously suggested that the conversion of formaldehyde increased with increase in temperature. Formaldehyde conversion at 400°C and 24 s of residence time can be decomposed 41 %. Approximately, 77 % can be achieved at 450°C and 16 s, and formaldehyde is completely decomposed at 500°C, 4 s of residence time.

The global reaction network for SCWO of formaldehyde can be written as follows, by assuming that each step in the scheme follows first order kinetics.

$$\mathrm{HCHO} \xrightarrow{k_1} \mathrm{CO} \xrightarrow{k_2} \mathrm{CO_2} \qquad (4.1)$$

Equation 4.2 shows formaldehyde decomposition depends on residence time.

$$\frac{d[HCHO]}{dt} = -k_1[HCHO] \tag{4.2}$$

From equation 4.2,

$$-\ln(1-X) = k\tau \tag{4.3}$$

X = Formaldehyde conversion

τ = Residence time (s)

The first-order plot of ln (1-X) versus residence time (τ), where X is the formaldehyde conversion, is shown in Figure 4.2. The experimental data can be plotted on a straight line at each temperature and slopes provide estimation of the rate constants. The plots indicating pseudo first-order kinetic is applicable to the non-catalytic oxidation of formaldehyde in supercritical water.

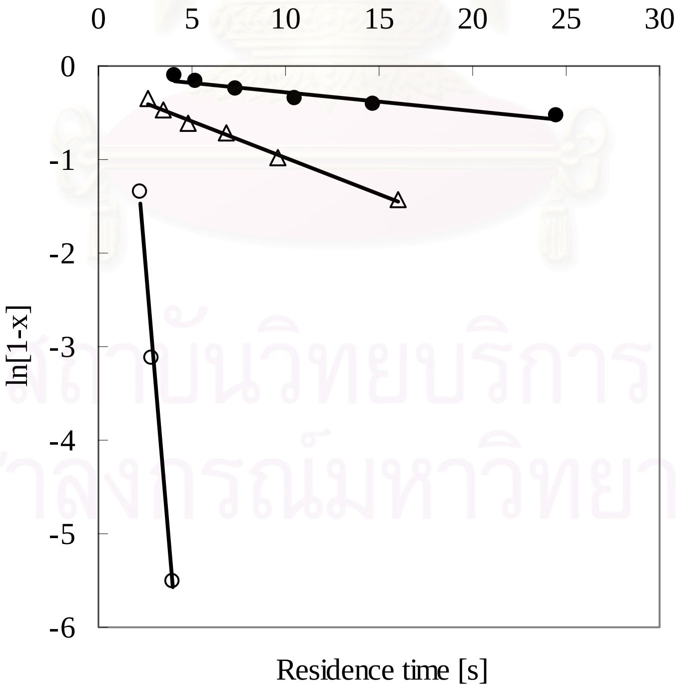

Figure 4.2 First order plot of formaldehyde oxidation in supercritical water at 400°C (●), 450°C (Δ) and 500°C (○), at 25 MPa

Assume a pseudo first order reaction of formaldehyde in the kinetic analysis. The pseudo first order rate constants calculated from the data are shown in Table 4.1.

Table 4.1 The pseudo first order rate constants of formaldehyde oxidation in supercritical water at 400-500°C [74]

Temperature (°C)	**Rate constant (s^{-1})**
400	0.02
450	0.08
500	2.30

The global rate constant (k) has Arrhenius-type temperature dependence as follows,

$$k = A \exp\left(-\frac{E_a}{RT}\right) \tag{4.3}$$

A = pre-exponential factor (s^{-1})

E_a = activation energy (cal. mol $^{-1}$)

R = gas constant (mol. cal^{-1}.K^{-1})

T = temperature (K)

From equation 4.3,

$$\ln k = \frac{-E_a}{RT} + \ln A \tag{4.4}$$

Arrhenius plot which is the relationship between ln k and $\frac{1}{T}$ is presented in Figure 4.3. From this relation, Arrhenius kinetic parameters of formaldehyde in SCWO in this study are calculated to be $A = (5.70 \pm 6.11)\times10^{14}$ s^{-1} and $E_a = 51.35 \pm 0.99$ kcal/mol while $R = 1.98\times10^{-3}$ kcal mol^{-1} K^{-1}.

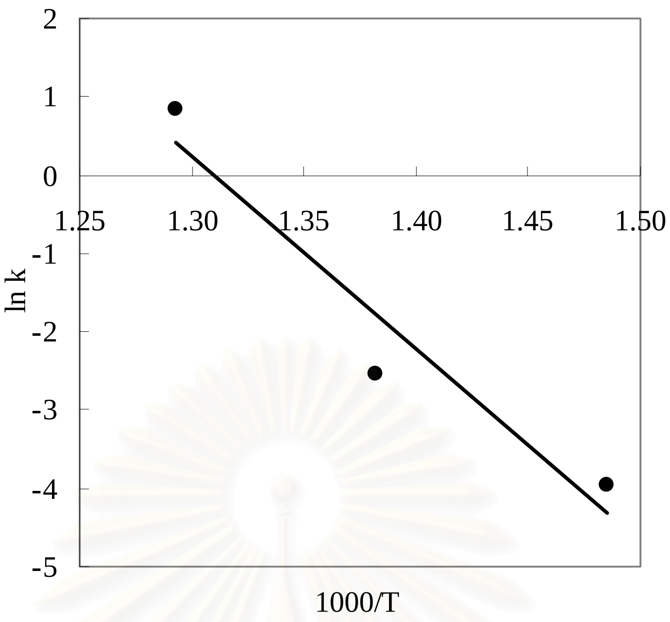

Figure 4.3 Arrehenius plot of formaldehyde oxidation in supercritical water

The global reaction rate of organic compounds oxidation in SCW can be described as follows:

$$rate = A\exp\left(\frac{-E_a}{RT}\right)[substrate]^a[\mathrm{O}_2]^b[\mathrm{H}_2\mathrm{O}]^c \qquad (4.5)$$

Where *a*, *b*, *c* are the reaction order of organic compound, oxygen and H_2O, respectively. The reaction can be regarded as pseudo *a* th order with respect to organic compound, because O_2 is always present in much excess of the stoichiometric requirement [1]. Water can actively participate in the reactions and it is not merely an inert medium for oxidation reactions. As a result, Arrhenius equation of formaldehyde oxidation in SCW in this study is shown in equation 4.6.

$$rate = 5.70 \pm 6.11 \times 10^{14} \exp\left(\frac{-51.35 \pm 0.99}{RT}\right)[HCHO] \qquad (4.6)$$

From the temperature dependence of the rate constants in Table 4.1, the calculated activation energy and pre-exponential factor of formaldehyde oxidation in supercritical water are about 51.35±0.99 kcal/mol and $5.70 \pm 6.11 \times 10^{14}$ s^{-1}, respectively. In the previous literatures, there has not been carried out the direct experimental measurement of the activation energy and pre-exponential factor of this reaction, and the only available values to be compared with our data are 90.6±42.9 kcal/mol and $1 \times 10^{25.1 \pm 11.3}$ s^{-1}, respectively obtained in the oxidation of methanol by Brock et al.[45]. The rate constant of formaldehyde oxidation was estimated with such assumption that the carbon mass balance was dependent only on CO, CO_2, methanol and formaldehyde, though formaldehyde was not quantitatively analyzed by their experimental method [45]. In spite of the large uncertainty in the reported activation energy and pre-exponential factor, the values obtained in this paper are still in agreement with the previous one within the stated uncertainty.

The global reaction network for SCWO of formaldehyde can be written by assuming that each step in the scheme follows first order kinetics. Obviously, the higher yields for CO and CO_2 are obtained at the longer residence times and the higher temperatures, but complete oxidation could not be achieved even at 500^{o}C and 13.4 s. Figure 4.4 shows the carbon yields balance of formaldehyde oxidation in supercritical water at each reaction temperature which is closely to unity within experimental error ± 5 %. The carbon yield balance based on TOC concentration of formaldehyde oxidation in SCW is also measured and shown in Figure 4.5.

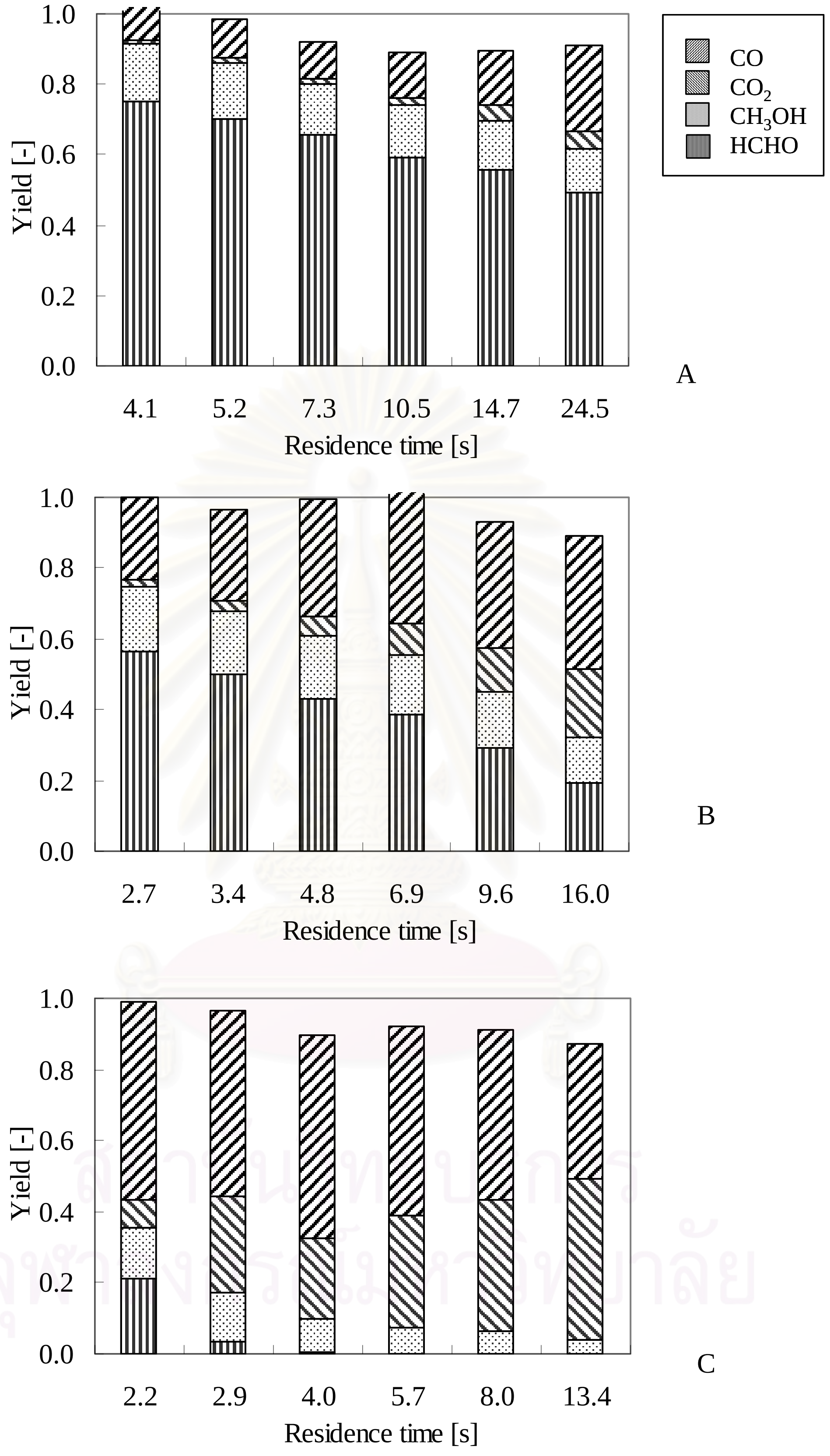

Figure 4.4 Carbon yields distribution of formaldehyde oxidation in SCW in non-catalytic study at 400°C (A), 450°C (B) and 500°C (C), at 25 MPa

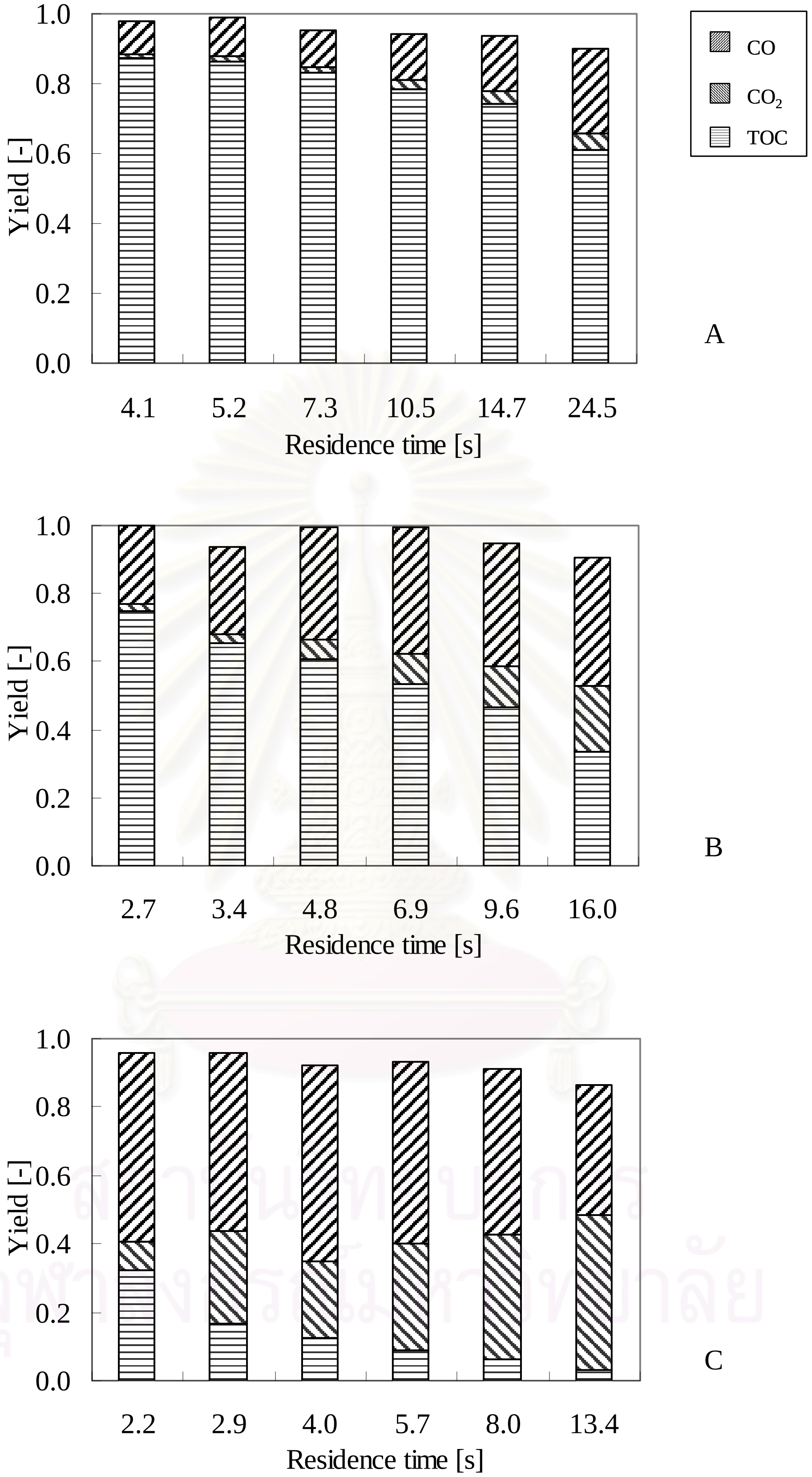

Figure 4.5 Carbon yields (TOC) distribution of formaldehyde oxidation in SCW in non-catalytic study at 400°C (A), 450°C (B) and 500°C (C), 25 MPa

4.2 Effect of initial formaldehyde concentration on formaldehyde conversion

Formaldehyde oxidation is conducted at 400-500°C and 25 MPa in an isothermal, isobaric tubular reactor using various formaldehyde feed concentrations ranging from 0.6 to 2.7 mmol/L. The O_2 concentration is always at least 3 times greater than the stoichiometric requirement for complete oxidation of organics. Formaldehyde conversion depending on the initial formaldehyde concentrations at 400°C, 450°C and 500°C are shown in Figures 4.6-4.8, respectively.

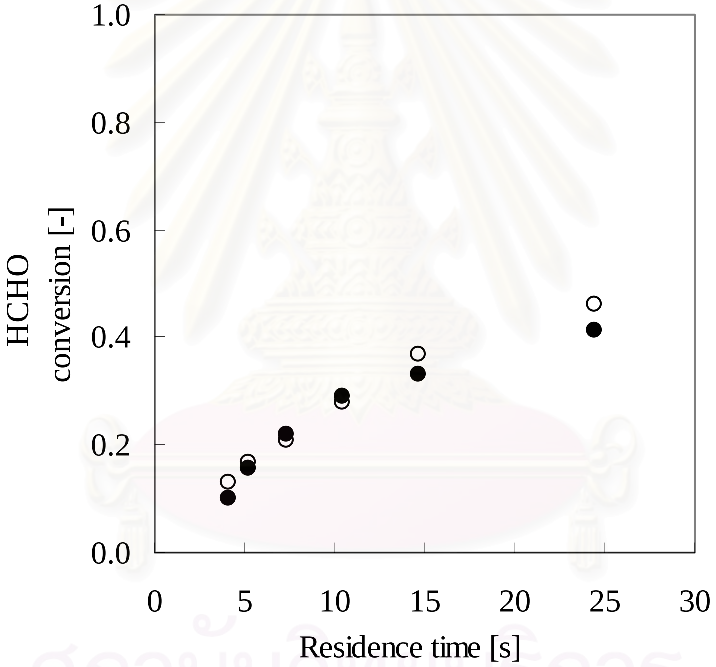

Figure 4.6 Formaldehyde conversion of non-catalytic study in SCWO at 400°C, 25 MPa, $[HCHO]_0$ at reactor entrance 1.3 (○) and 2.7 (●) mmol/L

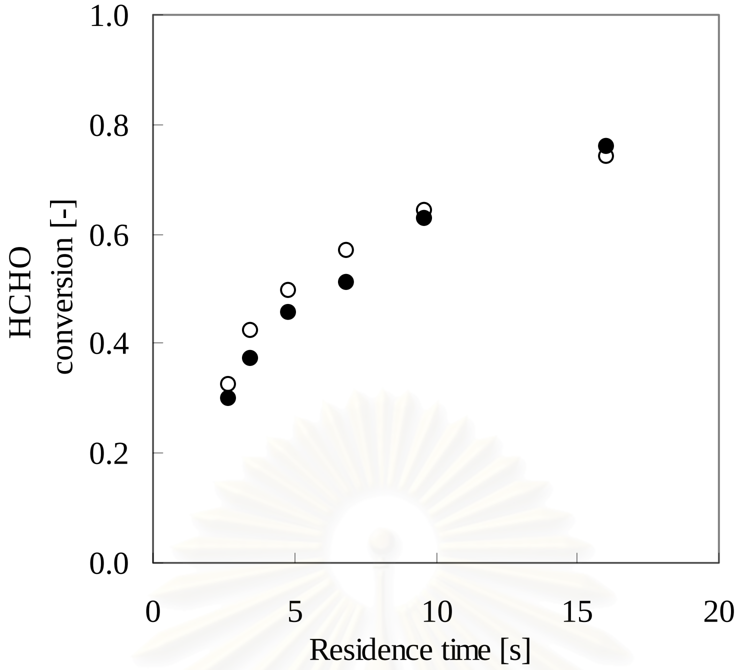

Figure 4.7 Formaldehyde conversion of non-catalytic study in SCWO at 450°C, 25 MPa, $[HCHO]_0$ at reactor entrance 0.8 (○) and 1.7 (●) mmol/L

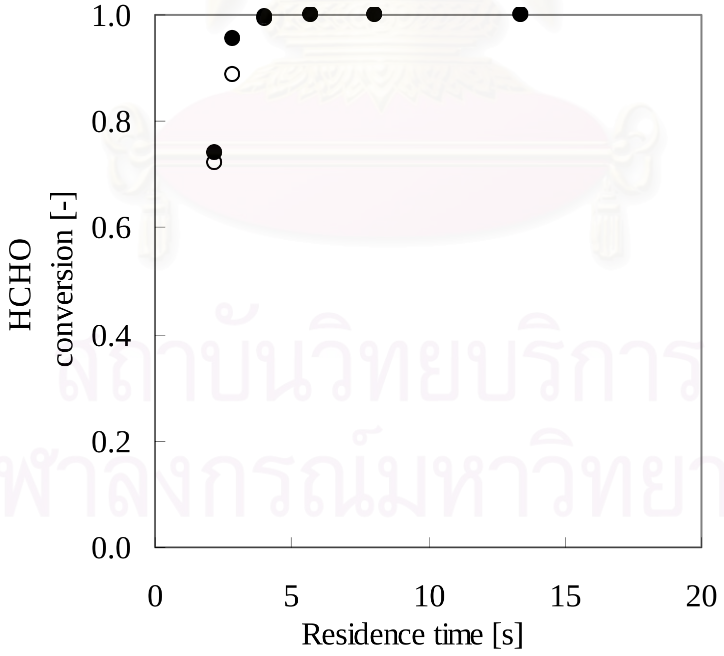

Figure 4.8 Formaldehyde conversion of non-catalytic study in SCWO at 500°C, 25 MPa, $[HCHO]_0$ at reactor entrance 0.6 (○) and 1.3 (●) mmol/L

The results from Figures 4.6-4.8 suggested that the formaldehyde conversion has no significant effect on initial formaldehyde concentration. Moreover, the first-order plots of formaldehyde oxidation in SCW in different initial formaldehyde concentrations at each temperature are also plotted and shown in Figure 4.9.

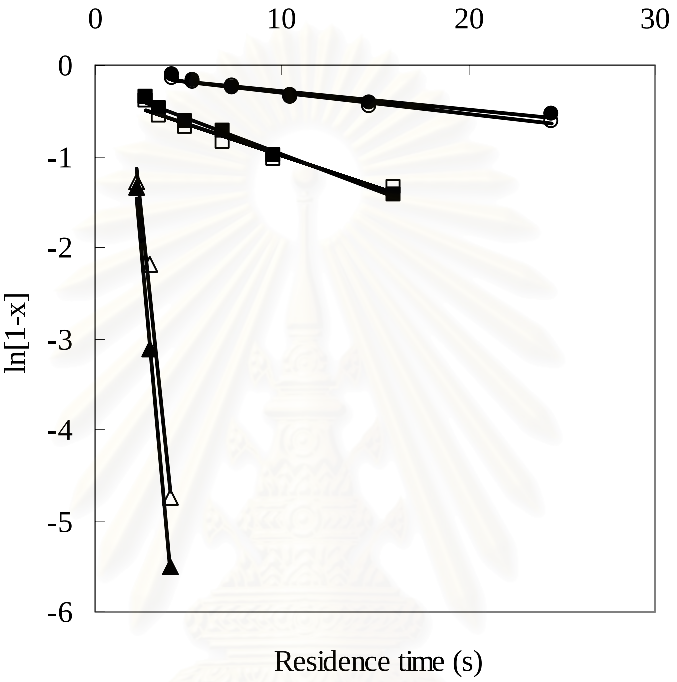

Figure 4.9 First order plot of formaldehyde oxidation in supercritical water at 25 MPa, 400^{o}C, [HCHO]$_0$ at reactor entrance 1.3 (○), 2.7 (●) mmol/L, at 450^{o}C [HCHO]$_0$ at reactor entrance 0.8 (□), 1.7 (■) mmol/L and 500^{o}C, [HCHO]$_0$ at reactor entrance 0.6 (Δ), 1.3 (▲) mmol/L

The results from Figure 4.9, the pseudo first order plots of formaldehyde disappearance in SCW at each initial formaldehyde concentration are straight line and almost the same for each formaldehyde concentration at the same temperature. The pseudo first order rate constants which depend on initial formaldehyde concentration are shown in Table 4.2.

Table 4.2 The pseudo first order rate constants of formaldehyde oxidation in SCW at $[HCHO]_0$ 0.04 and 0.08 mol/L at ambient condition

Temperature (^{o}C)	**Rate constant (k_1) (s^{-1})**	
	$[HCHO]_0$ 0.04 mol/L	$[HCHO]_0$ 0.08 mol/L
400	0.02	0.02
450	0.07	0.08
500	1.98	2.30

The rate constants of formaldehyde decomposition agree very well at different initial formaldehyde concentrations, suggesting that the pseudo first-order kinetic can be applied to the non-catalytic supercritical water oxidation of formaldehyde.

4.3 Effect of methanol concentration as a stabilizer on formaldehyde conversion

The commercial formaldehyde solution in this study contained about 8 % of methanol as a preservative. Therefore, the effect of contained methanol on formaldehyde conversion is studied. Oxidation experiments of the formaldehyde/methanol mixture at 450^{o}C and 500^{o}C, 25 MPa are conducted using several formaldehyde/methanol molar ratios, with formaldehyde concentration at 1.3 - 1.7 mmol/L and adding methanol at two different concentrations. The commercial formaldehyde solution 37 % which is used in this study and contained about 8 % of methanol as a preservative is also studied.

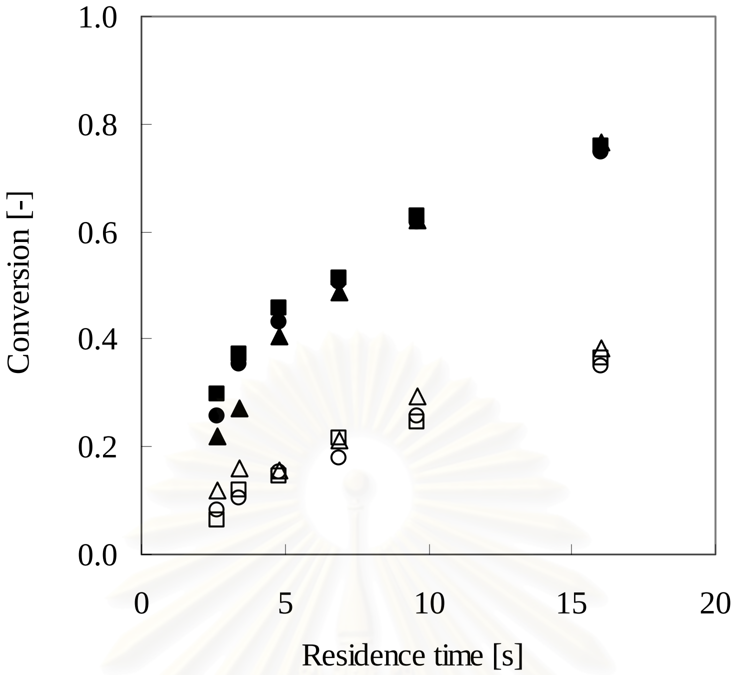

Figure 4.10 Formaldehyde and methanol conversion in supercritical water oxidation at the molar ratio of HCHO: CH_3OH 1:0.2 (▲, △), 1:0.4 (●, ○) and 1:1 (■, □) (HCHO conversion, CH_3OH conversion) at 450°C, 25 MPa

The ratio of formaldehyde and methanol in each experiment are 1:0.2, 1:0.4, and 1:1. The experimental result of methanol effect on formaldehyde and methanol conversion at 450°C and 500°C, 25 MPa are shown in Figures 4.10 and 4.11, respectively.

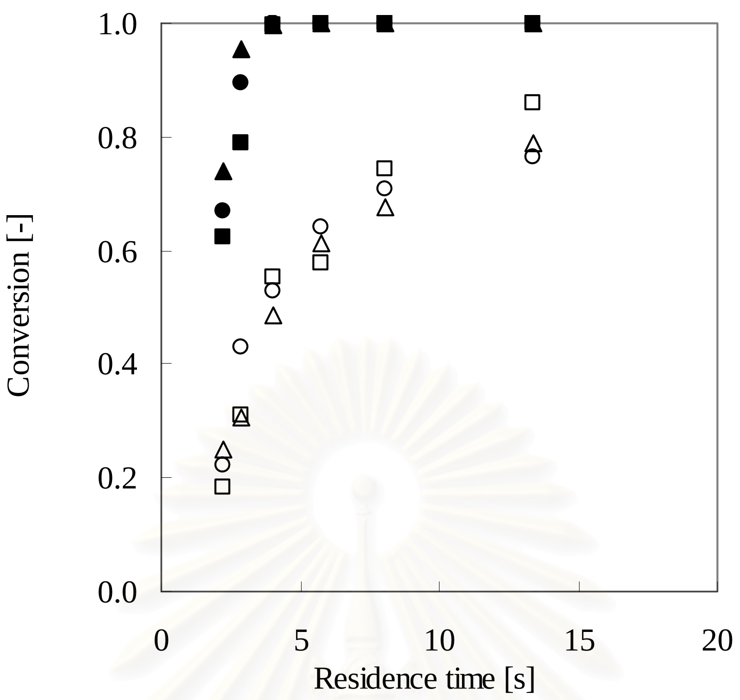

Figure 4.11 Formaldehyde and methanol conversion in supercritical water oxidation in ratio of HCHO: CH_3OH 1: 0.2 (▲, Δ), 1:0.4 (●, ○) and 1:1 (■, □) (HCHO conversion, CH_3OH conversion) at 500°C, 25 MPa

From Figures 4.10 and 4.11, formaldehyde conversion decreases with increase in methanol concentration at each temperature and residence time. It is suggested that the formaldehyde formation as an intermediate of methanol oxidation in SCW [45] is produced more when the concentration of methanol increases. It might be apparent that the formaldehyde conversion decreases with increase methanol concentration. Formaldehyde in the effluent which detected comes from not only reactant formaldehyde but also formaldehyde product from methanol oxidation. However, formaldehyde conversion has no significant difference in this range of formaldehyde to methanol. Therefore, in this study assume that the methanol concentration as a stabilizer in commercial formaldehyde solution is not so significant for formaldehyde conversion and kinetic parameters. The methanol conversions in the mixture of formaldehyde/methanol in each ratio are almost similarly tendency. The results show that formaldehyde concentration has no effect of methanol conversion.

Rice et al. [46] reported that methanol could produce formaldehyde with a maximum yield of about 20 % in the temperature range of 440-500^{o}C. Since the ratio of formaldehyde in the original solution to methanol was about 1: 0.2, the maximum yield of formaldehyde from methanol oxidation would be estimated to be less than 4 % of initial formaldehyde concentration. Thus, the contribution of formaldehyde production from methanol oxidation is assumed to be negligibly small.

4.4 Mechanism of formaldehyde oxidation in SCW

The global network for supercritical water oxidation of formaldehyde can be written as equation 4.1.

$$\mathrm{HCHO}\,(1) \xrightarrow{k_1} \mathrm{CO}(2) \xrightarrow{k_2} \mathrm{CO_2}\,(3) \qquad (4.1)$$

By assuming that each step in this scheme follows pseudo-first order kinetics, one can derive analytical expressions for the concentration profile for each compound by solving the governing differential equations as follows,

$$\frac{d[HCHO]}{dt} = -k_1[HCHO] \qquad (4.2)$$

$$\frac{d[CO]}{dt} = k_1[HCHO] - k_2[CO] \qquad (4.7)$$

$$\frac{d[CO_2]}{dt} = k_2[CO] \qquad (4.8)$$

As a result, molar yield of each compounds are shown in equation 4.9-4.11 [48, 75].

$$Y_1 = 1\text{-}X_1 = C_1/C_{1,\,0} = \exp(-k_1\tau) \qquad (4.9)$$

$$Y_2 = C_2/C_{1,\,0} = k_1\,[\exp(-k_1\tau) - \exp(-k_2\tau)]/\,(k_2\text{-}k_1) \qquad (4.10)$$

$$Y_3 = C_3/C_{1,\,0} = 1\text{-}[k_2 \exp(-k_1\tau) - k_1 \exp(-k_2\tau)]/\,(k_2\text{-}k_1) \qquad (4.11)$$

C_1 = Concentration of formaldehyde at each residence time
C_2 = Concentration of carbon monoxide in product
C_3 = Concentration of carbon dioxide in product
$C_{1,\,0}$ = Initial concentration of formaldehyde
Y_1 = Yield of formaldehyde
Y_2 = Yield of carbon monoxide
Y_3 = Yield of carbon dioxide

The global first-order rate constants can be obtained by fitting experimental data to the equations. The global rate constant for formaldehyde disappearance, k_1, is obtained by plotting ln(1 - X) against the residence time, as discussed in Table 4.2. The rate constants k_2 is obtained by unweighted nonlinear regression. The pseudo first rate constant of formaldehyde oxidation in SCW is shown in Table 4.3.

Table 4.3 The pseudo first order rate constants of formaldehyde oxidation in SCW at 25 MPa, $[HCHO]_0$ 0.08 mol/L at ambient condition

	Rate constant (s^{-1})	
Temperature (^oC)	**k_1**	**k_2**
400	0.02	0.05
450	0.08	0.09
500	2.30	0.33

Arrhenius plot of carbon monoxide oxidation in supercritical water is shown in Figure 4.12. Arrhenius kinetic parameters of CO in SCWO in this study are A = 2.28 $\times 10^4$ s^{-1}, E_a = 17.41 kcal/mol while R = 1.98×10^{-3} kcal mol^{-1} K^{-1}.

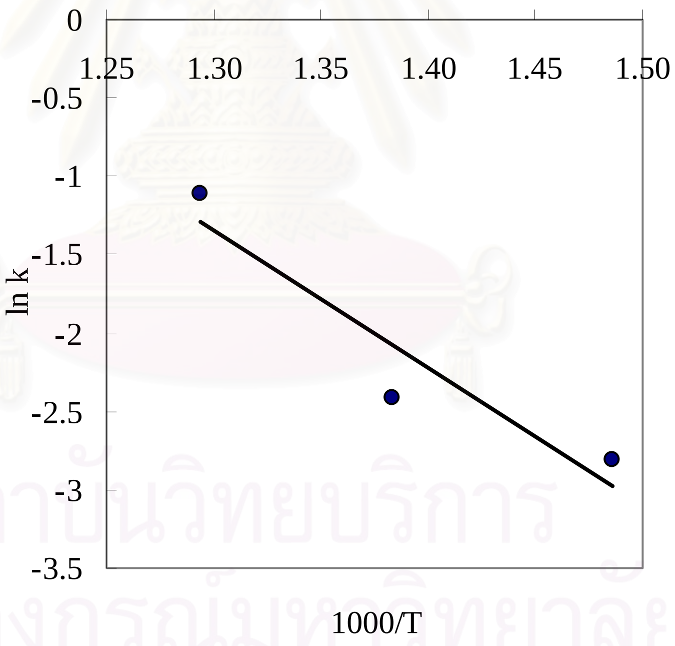

Figure 4.12 Arrehenius plot of carbon monoxide oxidation in supercritical water

From the rate constants, k_2 is obtained by unweighted nonlinear regression in Table 4.3, the calculated activation energy and pre-exponential factor of CO oxidation in supercritical water are about 17.41 kcal/mol and $2.28\times10^{4}\,s^{-1}$. In the previous literatures, there has not been carried out the direct experimental measurement of the activation energy and pre-exponential factor of this reaction, and the only available value to be compared with our data are 59.2 ± 39.1 kcal/mol and $1\times10^{15.6\pm10.3}$ s^{-1}, respectively obtained in the oxidation of methanol by Brock et al.[45]. Although, the values of activation energy and pre-exponential factor obtained in this study are not in the range of their study but also nearly still in agreement within the uncertainty.

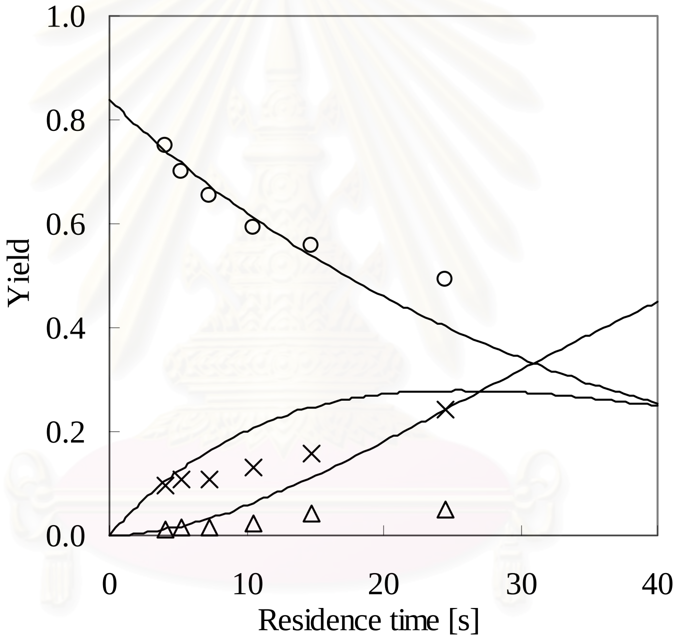

Figure 4.13 Experimental yields distribution of formaldehyde (○), CO (×) and CO_2 (Δ) and calculation by first order reaction (—) at 400°C, 25 MPa

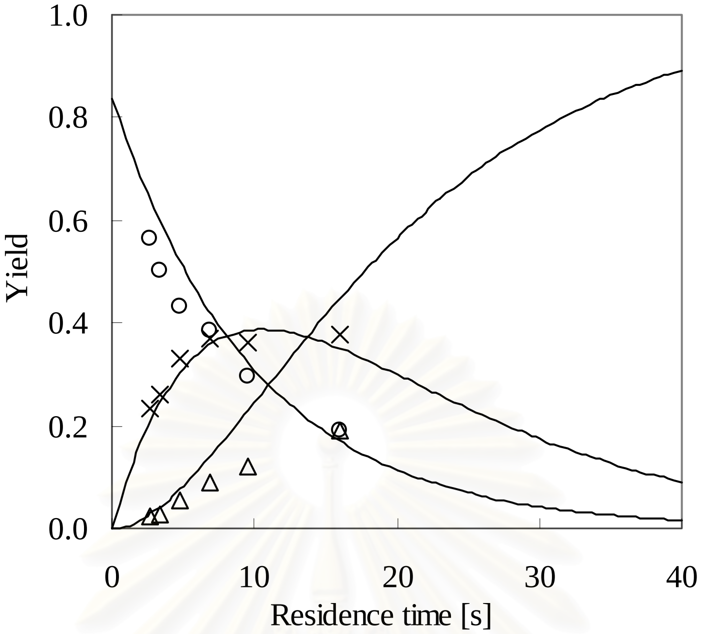

Figure 4.14 Experimental yields distribution of formaldehyde (○), CO (×) and CO_2 (Δ) and calculation by first order reaction (—) at 450°C, 25 MPa

The experimental data are well described by this simple model, as shown in Figures 4.13-4.14, which suggests that the essential features of formaldehyde SCWO can be explained using simple first-order kinetics**.**

The global reaction of formaldehyde oxidation is presented as follow:

$$HCHO + O_2 \rightarrow CO_2 + H_2O \tag{4.12}$$

In case of incomplete reaction,

$$HCHO + \frac{1}{2}O_2 \rightarrow CO + H_2O \tag{4.13}$$

$$CO + \frac{1}{2}O_2 \rightarrow CO_2 \tag{4.14}$$

Including, hydrogen peroxide (as oxygen resource) decomposition in SCW is shown as follow,

$$H_2O_2 \rightarrow \frac{1}{2}O_2 + H_2O \qquad (4.15)$$

There have been many previous studies explained the reaction mechanism of H_2O_2 decomposition in SCWO [47, 53, 54]. They described H_2O_2 decomposition pathway in SCWO by the following reaction, M is water.

$$H_2O_2 + (M) \rightarrow 2 \bullet OH + (M) \qquad (R1)$$

$$\bullet OH + H_2O_2 \rightarrow H_2O + HO_2 \qquad (R2)$$

$$\bullet OH + HO_2 \rightarrow H_2O + O_2 \qquad (R3)$$

$$HO_2 + HO_2 \rightarrow H_2O_2 + O_2 \qquad (R4)$$

The mechanism of formaldehyde decomposition in supercritical water oxidation is discussed below. Brock et al. [44] reported that the detailed chemical kinetic model based on elementary reaction, OH radical was very important reaction for oxidation of organic compound in SCW. Moreover, Feng et al. [51] also presented the mechanism of saturated and unsaturated organic compounds reacting with hydroxyl radicals by hydrogen abstraction to form water and a carbon radical. The mechanism is shown in equation (4.16).

$$RH + \bullet OH \rightarrow R \bullet + H_2O \qquad (4.16)$$

In this study, the mechanism of formaldehyde oxidation in SCW with OH radical reaction can described as follows:

$$HCHO + \bullet OH \rightarrow HCO \bullet + H_2O \qquad (4.17)$$

Ploeger et al. [53] presented the C-1 submechanism reactions involving all single-carbon compounds and the H_2/O_2 submechanism governs the reactions of hydrogen, water, oxygen, hydrogen peroxide, and HO_x radicals (H●, OH● and HO_2●). For methane oxidation in SCW, hydroxyl (OH●) and hydroperoxy (HO_2●) radicals hold the central role in the oxidation of hydrogen, carbon monoxide, methane, and other intermediates. The global pathway of methane is shown in equation 4.18.

$$CH_4 \to CH_3\bullet \to CH_3O\bullet \to \boxed{CH_2O \to HCO\bullet \to CO \to CO_2} \qquad (4.18)$$

Besides, Brock et al. [45] described methanol oxidation in supercritical water by the global reaction sequence $CH_3OH \to CH_2O \to CO \to CO_2$. The mechanism of methanol decomposition in SCWO is shown in equation 4.19.

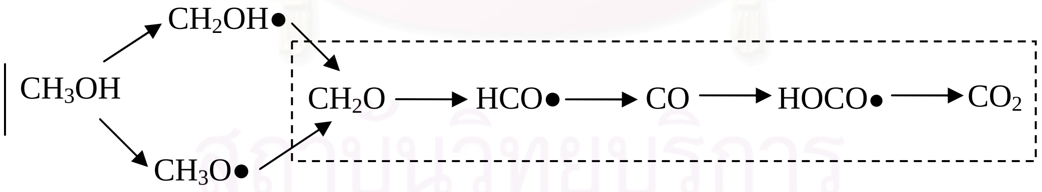

$$\begin{tikzcd}
 & CH_2OH\bullet \arrow[dr] & & & & & \\
CH_3OH \arrow[ur] \arrow[dr] & & CH_2O \arrow[r] & HCO\bullet \arrow[r] & CO \arrow[r] & HOCO\bullet \arrow[r] & CO_2 \\
 & CH_3O\bullet \arrow[ur] & & & & &
\end{tikzcd} \qquad (4.19)$$

Methanol was consumed in two parallel paths by OH radicals, which abstract hydrogen to form either CH_3O or CH_2OH. Both radicals reacted to produce formaldehyde: the CH_3O radical reacted mostly by eliminating a hydrogen atom, whereas the CH_2OH radical mostly reacts with O_2. Formaldehyde mostly reacted with OH to produce HCO radicals, which reacted with O_2 to yield CO. The CO then combined with OH to form a chemically activated HOCO radical, which was quickly stabilized by intermolecular energy transfer. The stabilized HOCO then very quickly reacted with O_2 to form CO_2.

From equations 4.18 and 4.19, formaldehyde is intermediate of both methane and methanol oxidation. The mechanisms of formaldehyde oxidation in both studies are almost similar and reasonable. Therefore, in this study the mechanism of formaldehyde oxidation in SCW can be assumed from equations R1-R4 and 4.17-4.19.

$$CH_2O \rightarrow HCO\bullet \rightarrow CO \rightarrow HOCO\bullet \rightarrow CO_2 \qquad (4.20)$$

The mechanisms of formaldehyde decomposition can be written as follows,

H_2O_2 decomposition $$H_2O_2 \rightarrow \bullet OH + \bullet OH \qquad (4.21)$$

CH_2O decomposition $$CH_2O + \bullet OH \rightarrow HCO\bullet + H_2O \qquad (4.17)$$

$$HCO\bullet + O_2 \rightarrow CO + HO_2\bullet \qquad (4.22)$$

$$CO + 2\bullet OH \rightarrow HOCO\bullet + H_2O \qquad (4.23)$$

$$HOCO\bullet + O_2 \rightarrow CO_2 + HO_2\bullet \qquad (4.24)$$

A common theme in formaldehyde SCWO is that an OH radical attacks a stable carbon-containing molecule (CH_2O, and CO) to form a carbon-containing radical intermediate. CH_2O forms HCO, and CO forms HOCO. All of these carbon-containing radicals reacted with O_2 to form a stable molecule plus HO_2. HO_2

is the ultimate radical product in all of these steps [45]. One HO_2 then reacts with a second HO_2 to form H_2O_2, which is a reservoir species for the HO_2 and OH radicals. H_2O_2 can then undergo to form two OH radicals, which can begin the oxidation cycle again.

4.5 Plug flow reactor for complete destruction of formaldehyde

One area of intense study is the determination of kinetic parameters for model SCWO compounds that are interest in university, industrial and military waste treatment applications.

From pseudo first order kinetic rate constant in Table 4.1, the size of plug flow reactor for complete destruction of non-catalytic formaldehyde oxidation in SCW at 25 MPa is calculated.

From equation 4.3

$$-\ln(1-X) = k\tau$$

On assumption

Conversion of formaldehyde (X) = 0.9999

Flow rate of solution (F_t) = 4.7 mL/min

Pressure = 25 MPa

I.D. of tube = 0.108 cm.

The calculation of non-catalytic reactor for complete destruction of formaldehyde in SCW condition is shown in Table 4.4.

Table 4.4 Design of plug flow reactor for complete destruction of non-catalytic formaldehyde oxidation in SCW at 25 MPa

Temperature (^{o}C)	**Plug Flow Reactor for complete destruction**		
	Residence time (min)	Volume of reactor (cm^3)	Length of reactor (m)
400	7.68	216.79	236.70
450	1.92	82.52	90.07
500	0.07	3.60	3.93

For the calculation from Table 4.4, conclude that for complete decomposition of formaldehyde oxidation in SCW by non-catalytic system need very long reactor at 400^{o}C, long residence time and require high temperature for achieve 100 % formaldehyde conversion. It is suggested that further modification of the system to achieve 100 % conversion of formaldehyde at a lower temperature and shorter residence time is required for the practical application of SCWO technology to laboratory waste treatment. The catalytic oxidation in SCW system is interested for next investigation.

CHAPTER V

CATALYTIC COMPACT SIZED REACTOR BY SUPERCRITICAL WATER OXIDATION TECHNIQUE

From the experimental results of non-catalytic study in the chapter 4, it is suggested that further modification of the system to achieve 100 % conversion of formaldehyde at a lower temperature and shorter residence time is required for the practical application of SCWO technology to laboratory waste treatment. Recently, heterogeneous catalysis in supercritical water has been proposed as a technique that can increase the yields of the complete oxidation products such as CO_2 and decrease the process temperature require.

In this study, the heterogeneous catalysis to enhance the formaldehyde decomposition is next investigated. A compact sized reactor for the on-site treatment of laboratory wastewater, which expect to meet the two important and fundamental concepts of such waste treatment, "treatment at the origin" and "self-responsibility for waste" have been recently developed. For the catalytic study, a simple and compact reaction system is used, the size of which is $0.5 \times 0.5 \times 1.0$ m^3. The effects of reaction temperature, initial formaldehyde concentration and percent excess of oxygen on complete destruction of formaldehyde and mixture of organic compounds decomposition in the catalytic SCWO compact sized reactor are investigated.

The schematic drawing is shown in Figure 3.2. The reaction setup for the catalytic reaction is almost the same as the case of non-catalytic reaction, except for the fixed bed reactor with 10 g of MnO_2 as catalyst. The initial concentration of formaldehyde in solution is 0.1 - 0.6 mol/L in original solution, the temperature range is 350 - 400°C and hydrogen peroxide as oxygen resource is 8 - 100 % excess. Pressure is kept constant at 25 MPa.

5.1 Effect of reaction temperature on conversion

The experimental results at 350 - 400°C and 25 MPa are shown in Figure 5.1. The initial concentration of formaldehyde which contained about 8 % of methanol as a preservative in original solution is 0.3 mol/L at ambient condition and excess oxygen is 100 %. The powdered MnO_2 catalyst is prepared by grinding the commercial pellets. The contact time is defined as catalyst bulk volume divided by fluid volumetric flow rate as equation 5.1, on assumption that the flows in the reactor are isothermal.

$$\tau = \frac{\text{Catalytic bulk volume}}{\text{Fluid volumetric flow rate at the reactor entrance}} \qquad (5.1)$$

Total Organic Carbon (TOC) conversion (X) is used to evaluate the extent of oxidative conversion. X defines as follows:

$$\text{TOC conversion}: X = 1 - \frac{[\text{TOC}]_t}{[\text{TOC}]_0} \qquad (5.2)$$

Where $[\text{TOC}]_0$ is the initial TOC concentration and $[\text{TOC}]_t$ is the residual TOC concentration after reaction.

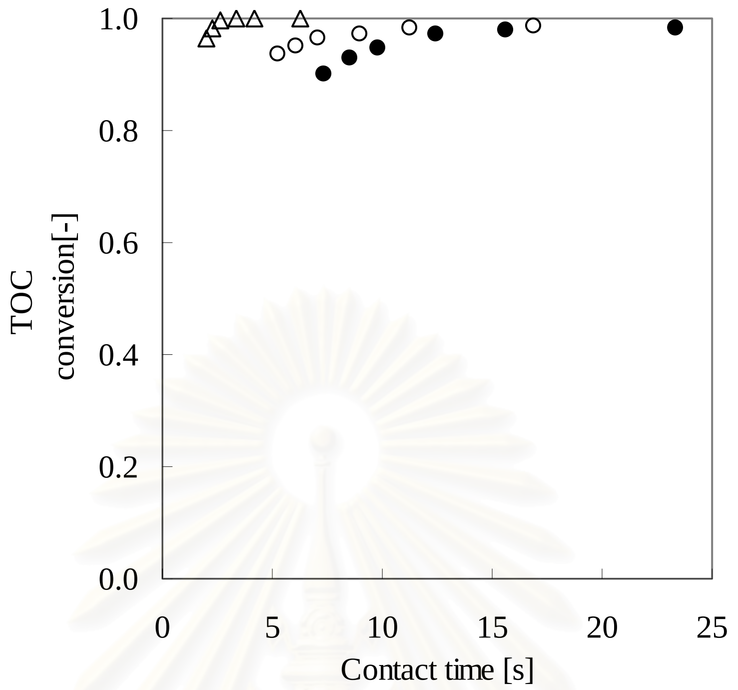

Figure 5.1 Total organic carbon conversion in catalytic SCWO compact sized system at 350°C (●), 380°C (○) and 400°C (Δ), 25 MPa, $[HCHO]_0$ 0.3 mol/L at ambient condition

The results in Figure 5.1 show that formaldehyde conversion exceeds 90 % at 350 and 380°C at contact times of 7.3 and 5.3 s, respectively. At 400°C, formaldehyde can be completely destructed in a shorter contact time less than 2 s. Figure 5.2 shows the carbon yield balance of formaldehyde oxidation in catalytic SCWO reactor which is close to unity within experimental error ± 5 %. CO_2 is the most abundant reaction product and CO can not be detected because of CO is very fast achieved to CO_2 under these conditions.

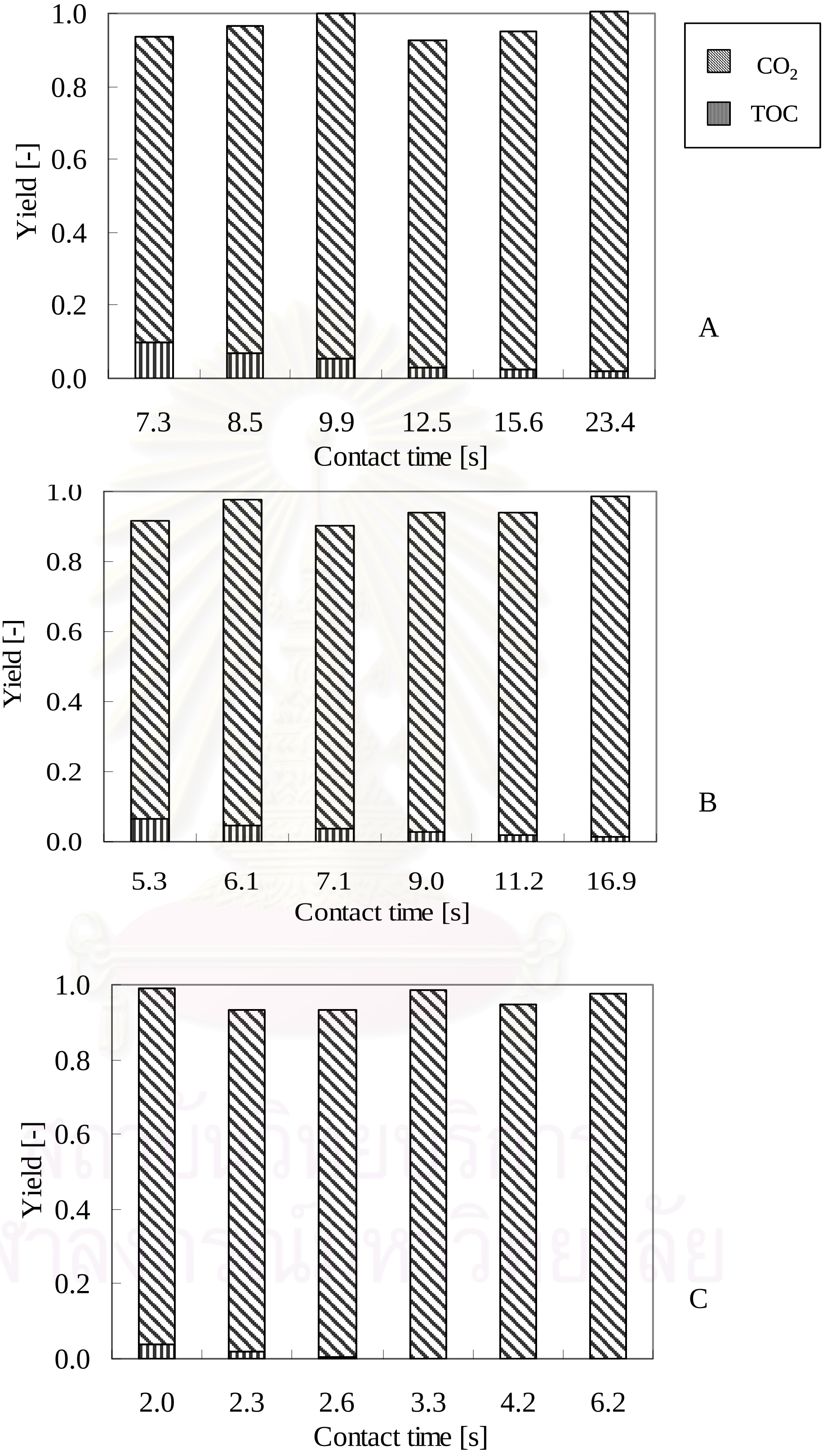

Figure 5.2 Carbon yields distribution of formaldehyde in catalytic SCWO compact sized system at 350^{o}C (A), 380^{o}C (B), 400^{o}C (C)

5.2 Effect of initial formaldehyde concentration on conversion

The experimental results of initial formaldehyde concentration effect on TOC conversion is shown in Figure 5.3. The range of formaldehyde concentration is 0.1-0.6 mol/L at ambient conditions and excess oxygen is 100 %. Temperature and pressure are 400^{o}C and 25 MPa, respectively. The concentration of formaldehyde in this experiment is based on the effluent product of dichloromethane hydrolysis reaction. The data of dichloromethane concentration in pharmaceutical laboratory wastewater is shown in Table 2.9.

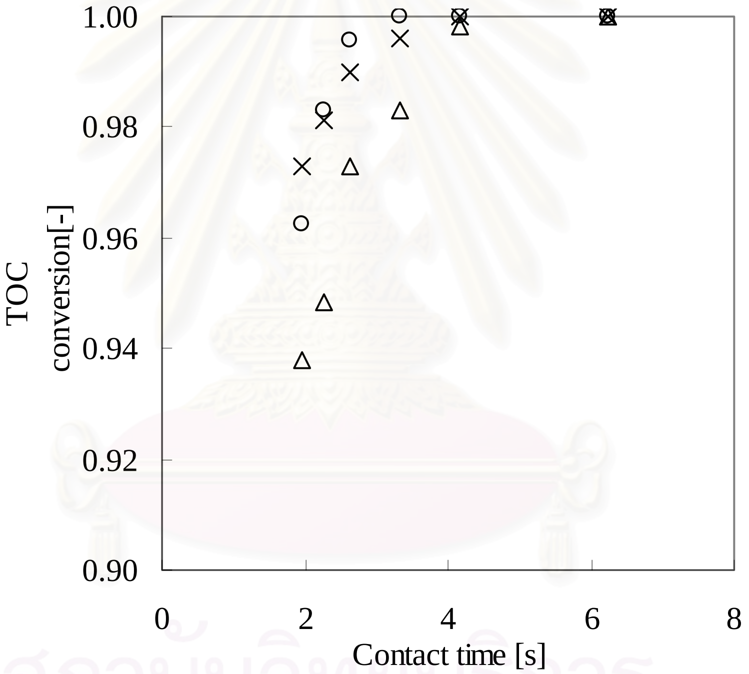

Figure 5.3 Total organic carbon conversion in catalytic SCWO compact sized system at 400^{o}C, 25 MPa, $[HCHO]_0$ at ambient condition 0.1 mol/L (×), 0.3 mol/L (○), and 0.6 mol/L (Δ)

From the experimental results in Figure 5.3, formaldehyde conversion exceeds 93 % at 400^{o}C, 25 MPa in each initial formaldehyde concentration 0.1, 0.3, 0.6 mol/L at contact times of 4.2 s. The formaldehyde conversion decreases with increase of formaldehyde concentration at contact time of 2.0-3.3 s and very fast complete decomposition is achieved at 4.2 s in the condition of each initial formaldehyde concentration. It is suggested that the effect of initial formaldehyde concentration is small on TOC conversion at longer contact time of formaldehyde decomposition in catalytic SCWO compact sized reactor. The carbon yields balance of formaldehyde oxidation in catalytic SCWO reactor at 400^{o}C, 25 MPa at each initial formaldehyde concentration which is close to unity within experimental error ± 5 % are shown in Figure 5.4. CO_2 is the most abundant reaction product and CO can not be detected because CO is very fast achieved to CO_2 under these conditions.

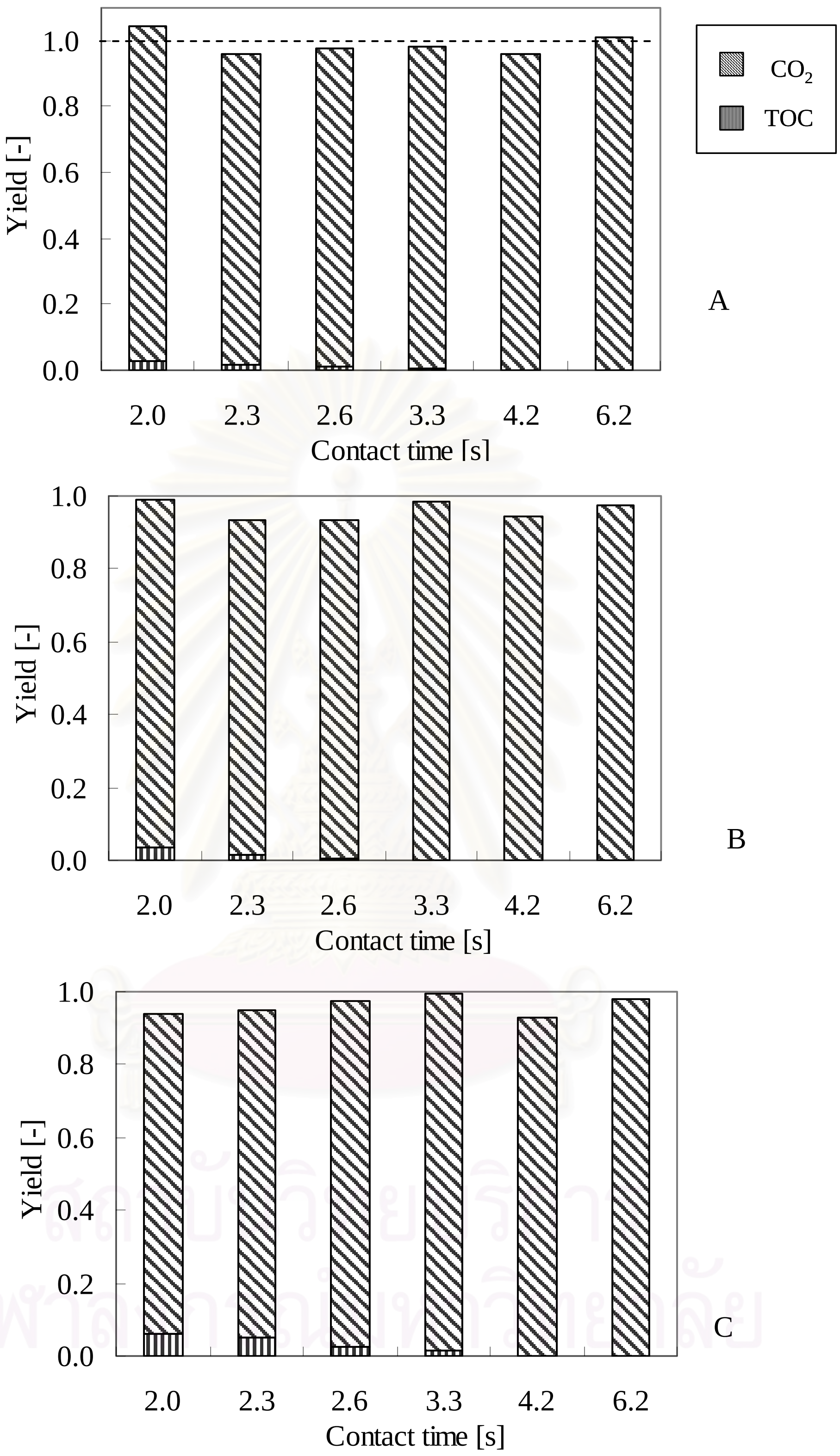

Figure 5.4 Carbon yields distribution of formaldehyde in catalytic SCWO compact sized system at 400^{o}C, 25 MPa, $[HCHO]_0$ at ambient condition 0.1 mol/L (A), 0.3 mol/L (B), 0.6 mol/L (C)

5.3 Effect of excess oxygen on conversion

The effect of the amount of hydrogen peroxide on formaldehyde decomposition to obtain the optimal condition of excess oxygen concentration in catalytic SCWO compact sized system is examined. The experimental results at excess oxygen of 8 %, 65 % and 100 % are shown in Figure 5.5. Initial formaldehyde concentration in original solution is 0.3 mol/L at ambient condition. Temperature and pressure are 400°C and 25 MPa.

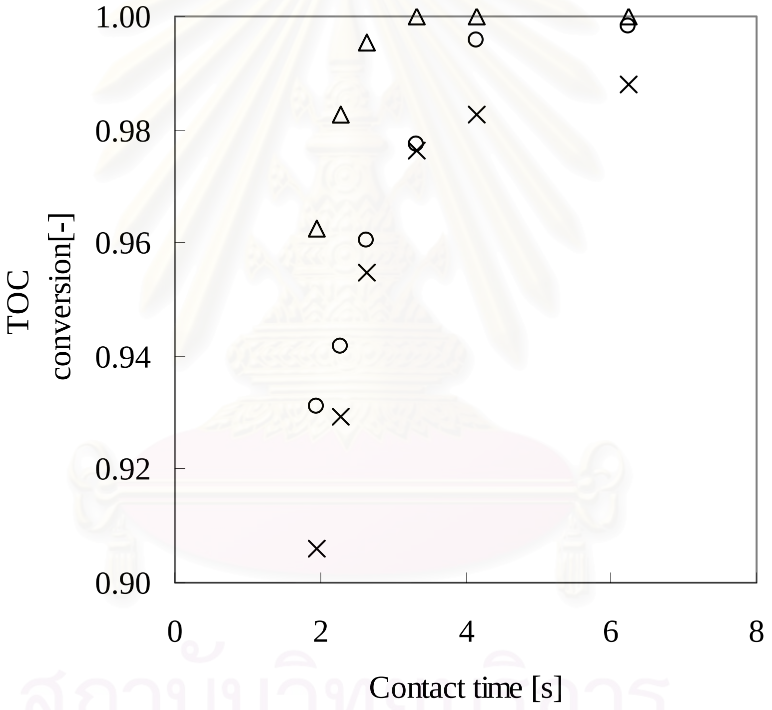

Figure 5.5 Total organic carbon conversion in catalytic SCWO compact sized system at 400°C, 25 MPa and excess oxygen of 8 % (×), 65 % (○), and 100 % (Δ)

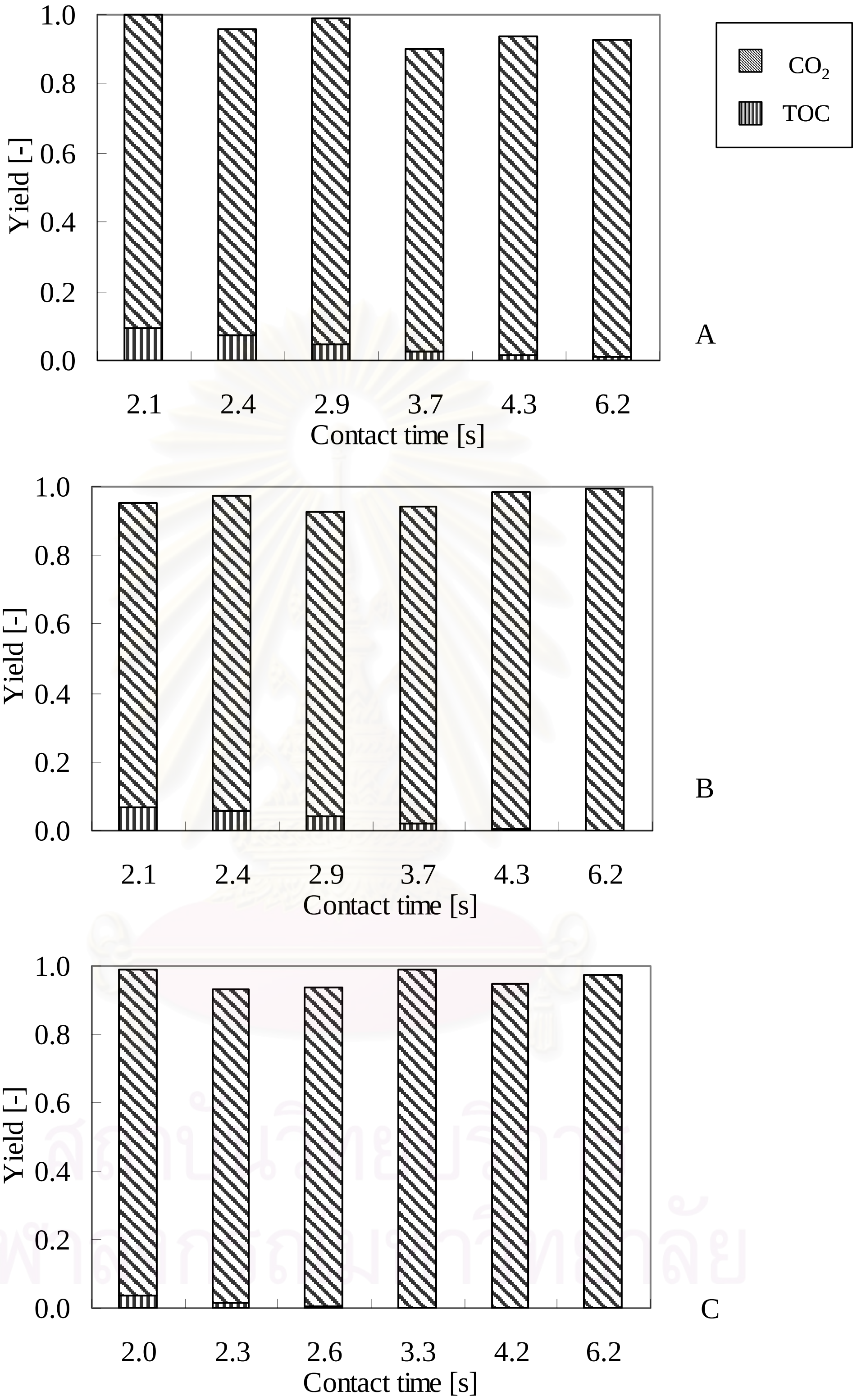

Figure 5.6 Carbon yields distribution of formaldehyde in catalytic SCWO compact sized system at excess oxygen of 8% (A), 65% (B), 100% (C), 400°C, 25 MPa.

From the experimental results in Figure 5.5, formaldehyde conversion exceeds 90, 92, 96 % at 400°C, 25 MPa at excess oxygen 8 %, 65 %, 100 % respectively at 2 s of contact time. The formaldehyde conversion increases with increase of excess oxygen and complete destruction is achieved at 4.2 s in the experiments of 100% excess oxygen. It is suggested that the amount of hydrogen peroxide which is a resource of oxygen has effect on TOC conversion of formaldehyde decomposition at shorter contact time. However, the effect can be negligible at longer contact time. The carbon yields balance of formaldehyde oxidation in catalytic SCWO reactor at 400°C, 25 MPa at difference excess oxygen which is close to unity within experimental error ± 5 % are shown in Figure 5.6. CO_2 is the most abundant reaction product and CO can not be detected because CO is very fast achieved to CO_2 under these conditions. As a result, the optimal condition of excess oxygen concentration in catalytic SCWO compact sized system is excess oxygen 100 % at 4.2 s of contact time.

5.4 Effect of mixture organic compounds on conversion

The artificial pharmaceutical laboratory wastewater and also would be intermediate products from dichloromethane hydrolysis process are examined in catalytic SCWO compact sized reactor. The experimental results of total organic carbon conversion of organic mixture in this system compounds which contains formaldehyde of 0.1 mol/L, methanol of 0.1 mol/L, ethanol of 0.1 mol/L and acetic acid of 0.1 mol/L are shown in Figure 5.7. Temperature and pressure are 400°C and 25 MPa, respectively and excess oxygen is 100 %.

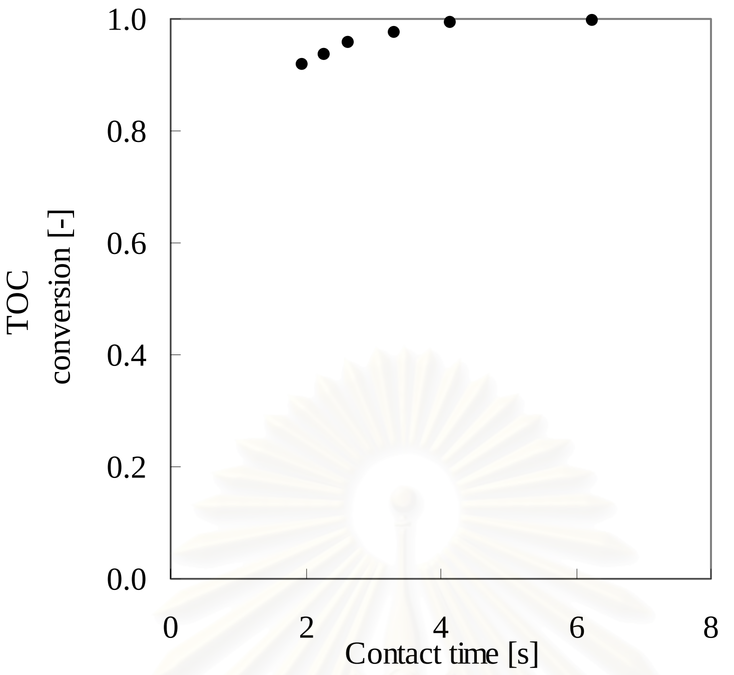

Figure 5.7 Total organic carbon conversion in catalytic SCWO compact sized system at 400°C, 25 MPa, mixture of organic compounds

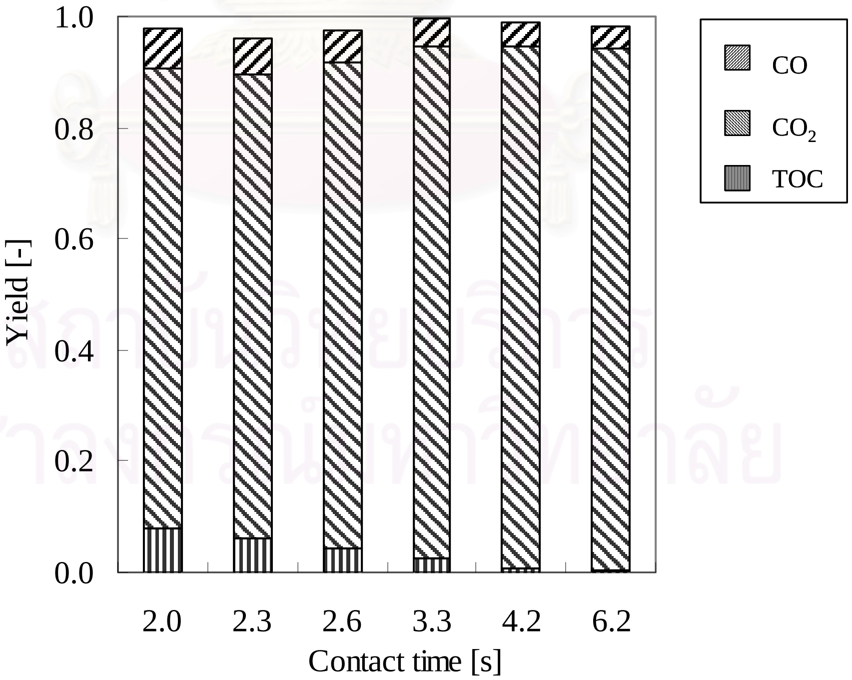

Figure 5.8 Carbon yields distribution of mixed organic compounds in catalytic SCWO compact sized system at 400°C, 25 MPa, excess oxygen 100 %

From the experimental results in Figure 5.7, total organic carbon conversion of organic mixture exceeds 90 % at 400^{o}C, 25 MPa and contact time of 4.2 s at 100% excess oxygen. Figure 5.8 shows that carbon yields balance of mixed organic compounds oxidation in catalytic SCWO compact sized reactor at 400^{o}C, 25 MPa is close to unity within experimental error ± 5 %. Small amount of CO is produced meanwhile CO_2 is the most abundant reaction gas product.

5.5 Comparison of formaldehyde decomposition in non-catalytic and catalytic SCWO

According to experimental study of formaldehyde oxidation in SCW with and without catalyst, formaldehyde conversion and CO_2 yield which is the product for complete oxidation of each study are observed. For non-catalytic SCWO study, formaldehyde conversion less than 40% is obtained from under 400^{o}C, 25 MPa. The formaldehyde conversion is always much higher and exceeded 95 % due to the presence of the MnO_2 as catalyst. Non-catalytic SCWO of formaldehyde produced CO_2 molar yields less than 5 %, but during catalytic SCWO of formaldehyde the CO_2 molar yields are over 91 %. Clearly, both the formaldehyde conversion and the CO_2 molar yield are much higher for catalytic oxidation in supercritical water using MnO_2 as catalyst.

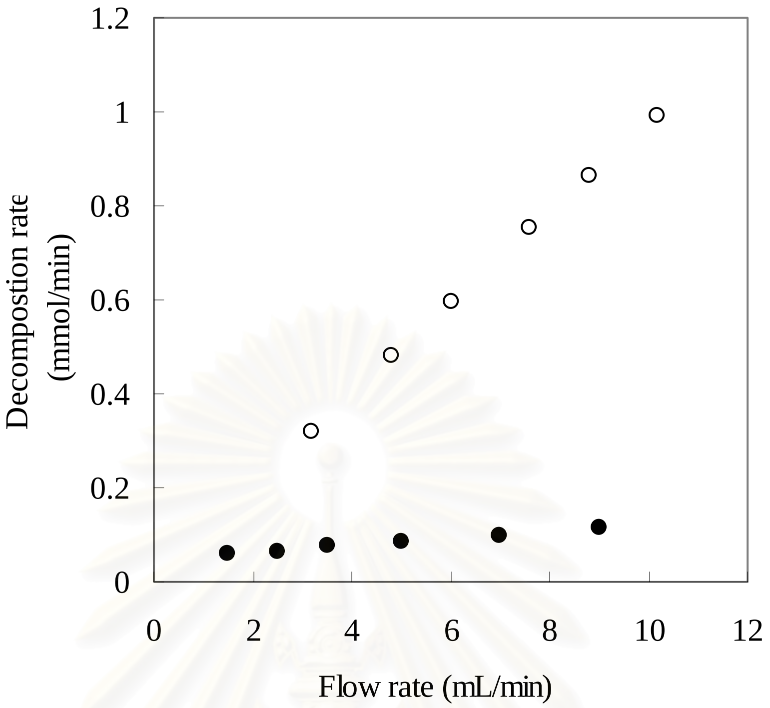

Figure 5.9 Total organic carbon decomposition rate of formaldehyde in non-catalytic (●) and catalytic (○) SCWO at 400°C and 25 MPa

The comparison of decomposition rates between catalytic and non-catalytic studies is shown in Figure 5.9. For example, when the reactant solution is fed to the reactor at the same flow rate of 3 mL/min, the decomposition rate of non-catalytic study is 0.06 mmol/min. Meanwhile the decomposition rate of 0.32 mmol/min is obtained from catalytic system. From the slope of each line in Figure 5.9, it is suggested that organic carbon can be destructed in catalytic compact sized system at least 5 times faster that non-catalytic system at the same reaction condition.

CHAPTER VI

ELIMINATION OF HYDROCHLORIC ACID BEFORE SUPERCRITICAL WATER OXIDATION REACTOR

In recent years supercritical water oxidation has emerged as a promising new technology for the destruction of hazardous organic waste. The SCWO process involves heating and pressurizing aqueous organic waste, to conditions above the critical point of water in the presence of an oxidizer. Organic materials and wastes can easily be oxidized in supercritical water and converted to CO_2 and H_2O. The two main disadvantages posed by the use of SCWO are corrosion and salt precipitation in the equipment.

In this study, dichloromethane is chosen as a representative model of chlorinated compounds. In order to avoid the corrosion problem by chloride, the two reactors are consecutively combined, aiming at hydrolysis in the first reactor followed by SCWO in the second reactor, for the complete destruction of dichloromethane. The schematic drawing of the design of multi-stage process for the treatment of dichloromethane is shown in Figure 6.1.

Figure 6.1 Design of the multi-stage system for treatment of dichloromethane

Because the hydrolysis of dichloromethane in the first reactor of the proposed system has already been intensively investigated [6-9], and the SCWO of formaldehyde which is known to be the main product of the hydrolysis of dichloromethane is investigated. Additionally, the results on the methods to eliminate HCl before entering the oxidation stage are reported in this chapter. In design of the cascade process where hydrolysis and oxidation are consecutively combined, it is necessary to eliminate HCl between these two stages, because HCl is the major product in the hydrolysis of dichloromethane, and provides very corrosive atmosphere in sub- and supercritical water. The two different methods are examined; one is the addition of $Pb(CH_3COO)_2$ as a precipitated reagent, and the other is the removal of HCl by ion exchange resin.

6.1 High pressure method: precipitation method

The experimental setup is shown in Figure 3.4. The HCl precipitating reaction by $Pb(CH_3COO)_2$ as a precipitant is shown in equation 6.1

$$\mathrm{Pb(CH_3COO)_2}\,(aq) + \mathrm{2HCl}\,(aq) \rightarrow \mathrm{PbCl_2}\,(s) + \mathrm{2CH_3COOH}\,(l) \qquad (6.1)$$

The concentration of hydrochloric acid in this experiment is based on the effluent product of dichloromethane hydrolysis reaction. The data of dichloromethane concentration in pharmaceutical laboratory wastewater is shown in Table 2.9. $Pb(CH_3COO)_2$ as precipitated reagent of HCl at excess 5 times of stoichiometric requirement is examined. The HCl and $Pb(CH_3COO)_2$ concentrations in the original solution are 0.2 and 0.5 mol/L, respectively. The aqueous solution of HCl and $Pb(CH_3COO)_2$ are separately fed by HPLC pumps at flow rate of 1 mL/min. Time profile of the concentration ratio of HCl in the effluent at time t = t (C_t) divided by HCl initial concentration at t=0 (C_0) at 0.1 MPa, 25^{o}C is shown in Figure 6.2.

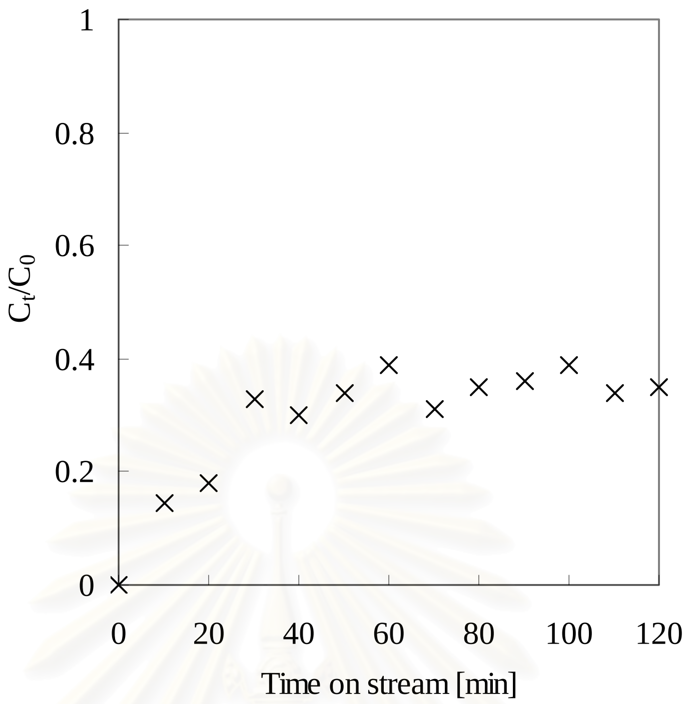

Figure 6.2 Time profile of HCl concentration in the effluent of the precipitation method at 25°C, 0.1 MPa

This result shows that about 60-80 % of HCl could be removed along with 120 minutes of time on stream by precipitation technique at 0.1 MPa and 25°C.

Next, at higher pressure condition to apply this technique for the consecutive combination system without depressurization is also investigated. Time profile of HCl concentration in the effluent at 25 MPa, 25°C is shown in Figure 6.3.

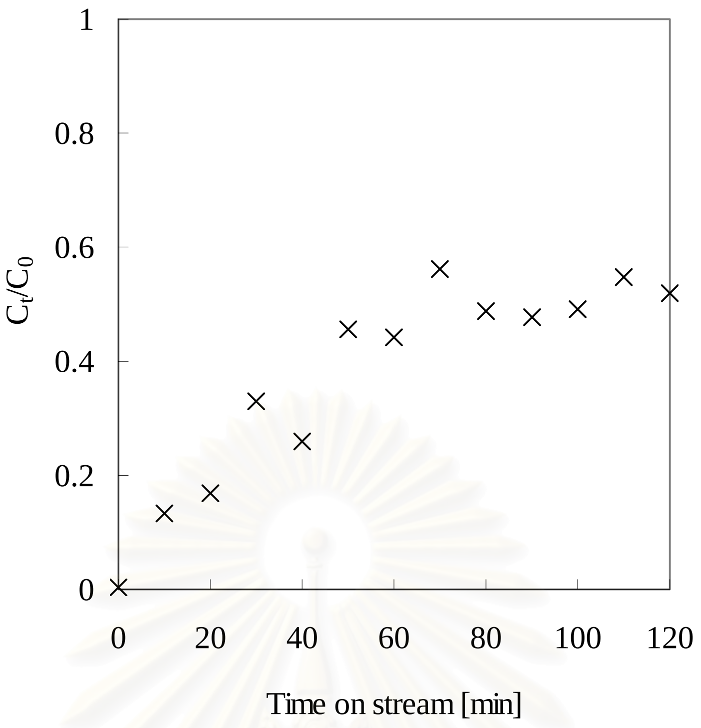

Figure 6.3 Time profile of HCl concentration in the effluent in the precipitation method at 25^{o}C, 25 MPa

This result shows that about 50-70 % of HCl could be removed along with 120 minutes of time on stream by precipitation technique at 25 MPa, ambient temperature. This technique is attractive for HCl removal because it is applicable to the high pressure condition.

6.2 Low pressure method: Ion exchange resin

An ion exchange resin is composed of high-molecular-weight polyelectrolytes that can exchange their mobile ions for ions of similar charge from the surrounding medium. Because of their limitation properties, the resins should be used at the temperature below 100^{o}C and atmospheric pressure. In this experiment ion exchange resin is applied to remove HCl before SCWO reactor at low pressure. The experimental set up is shown in Figure 3.5. Strong base ion exchange resins (R-N

$(CH_3)_3 \cdot OH$) are used in this experiment. The HCl concentration in the original solution is 0.2 mol/L for all experiments in this section. Volume of resin column is 4.3 mL and flow rate of HCl aqueous solution is also constant at 1 mL/min for all experiments in this section. The amounts of resin used for these experiments are 3.14 - 6.25 g. Time profile of HCl concentration in the effluent by using 3.14 g ion exchange resin is shown in Figure 6.4. Strong base resins are used in the hydroxide (OH) form. They will react with anions in solution and can convert an acid solution to pure water. The absorption reaction of HCl on ion exchange resin is shown in equation 6.2.

$$\mathrm{R\text{ - }N(CH_3)_3 \bullet OH + HCl \rightarrow R\text{ - }N(CH_3)_3Cl + H_2O} \qquad (6.2)$$

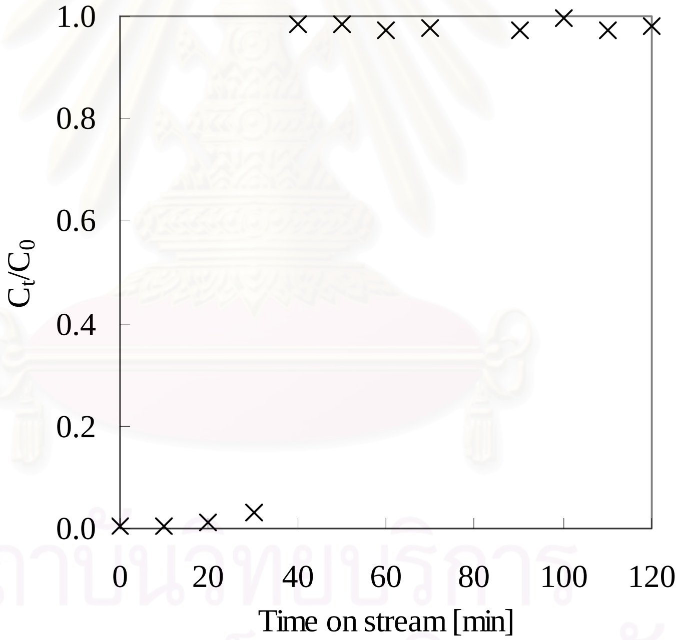

Figure 6.4 Time profile of HCl concentration in the effluent of the ion exchange resin 3.14 g at 25°C, 0.1 MPa

As a result, chloride ions are almost completely adsorbed by the resins before 20 min, but suddenly breakthrough of HCl occurs in 30 min. From the experimental result, adsorption rate of this resin is 0.03 mmol/g resin. min.

Additionally, increased amount of resins in order to extend the duration time is examined. Time profile of HCl concentration in the effluent by using 6.25 g ion exchange resin at 25°C, 0.1 MPa is shown in Figure 6.5.

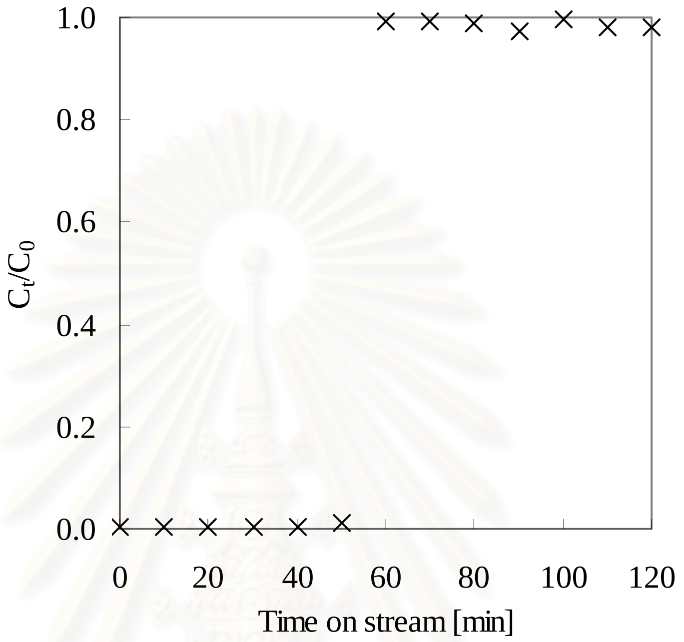

Figure 6.5 Time profile of HCl concentration in the effluent of the ion exchange resin 6.25 g at 25°C, 0.1 MPa

Chloride ions are almost completely adsorbed by the resins before 40 min, but suddenly breakthrough of HCl occurs after 50 min. Figure 6.5 shows that duration time can be extended by increase of the amount of ion exchange resin. The same method is also examined to apply for the mixture of HCl and formaldehyde solution. The concentration of formaldehyde in the aqueous solution is 0.1 mol/L which methanol as a preservative, the solution of mixture of organics and HCl aqueous solution is fed into the system by one HPLC pump. The amount of resin in this experiment is 6.25 g. The time profile of HCl concentration and TOC concentration in the case of mixture are shown in Figures 6.6 and 6.7, respectively.

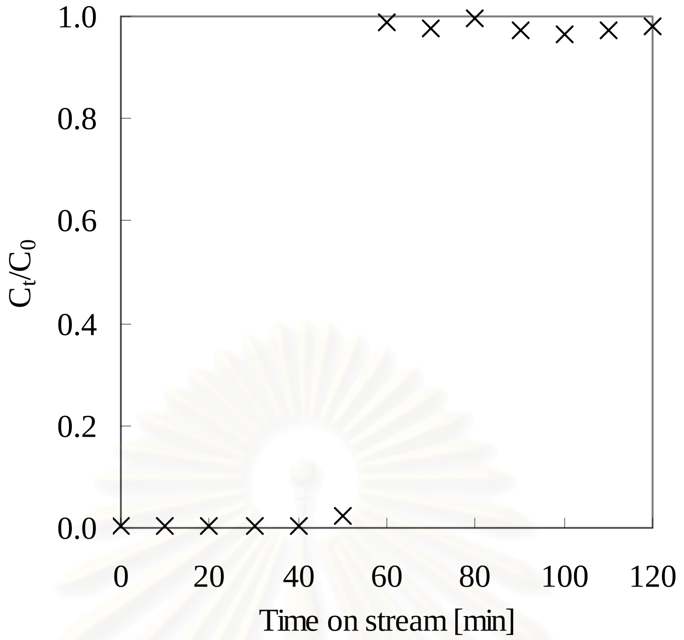

Figure 6.6 Time profile of HCl concentration in the effluent which operate mixture of HCl and HCHO in original solution, 6.25 g of resins at 25^{o}C, 0.1 MPa

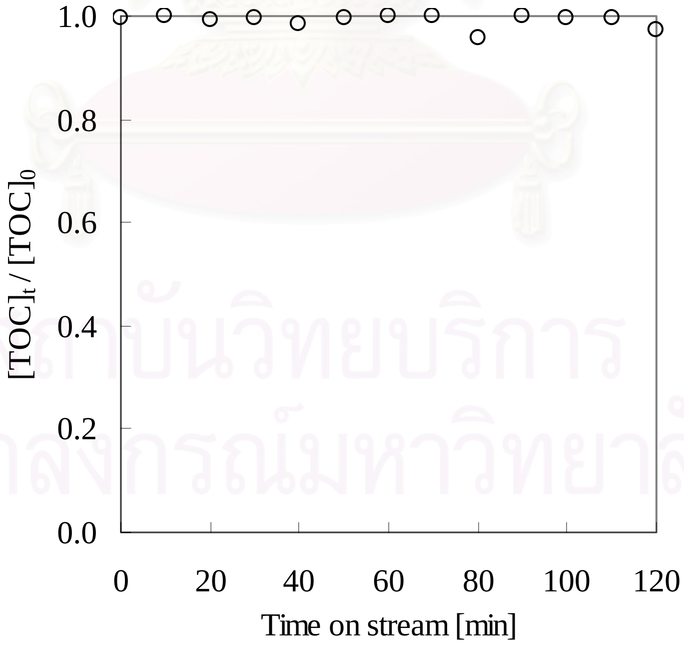

Figure 6.7 Time profile of total organic carbon concentration in the effluent which operate mixture of HCl and HCHO in original solution, 6.25 g of resins at 25^{o}C, 0.1 MPa

The results from Figures 6.6 and 6.7 show that organics aqueous solution does not affect adsorption ability of ion exchange resin in this experimental condition. Taking into consideration of the fact that even very small concentration of HCl may cause the corrosion problem in SCWO, ion exchange resin method would be promising as long as it is used before breakthrough time. However, it should also be noted that the use of resin needs the system pressure to be reduced to atmospheric pressure, which would be disadvantage for the entire system due to loss of efficiency.

6.3 Design of whole system for dichloromethane destruction by consecutive combination of hydrolysis and supercritical water oxidation process

In this study, dichloromethane is chosen as a representative model of chlorinated compounds. In order to avoid the problem of corrosion by chloride, the whole system of a new cascade process where two reactors are consecutively combined, aiming at hydrolysis in the first reactor followed by SCWO in the second reactor which ion exchange resin is used as HCl elimination method before SCWO reactor, for the complete destruction of halogenated organic compounds is designed. The schematic apparatus of proposed cascade process with consecutive combination of hydrolysis and SCWO for pharmaceutical laboratories wastewater is shown in Figure 6.8. In order to design the hydrolysis reactor of dichloromethane, the extensive previous study of Oshima et al. [9] is referred. From Table 2.10, on assumptions as follows: a) temperature at 300^{o}C, b) pressure at 25 MPa, c) rate constant (k) of 7.16×10^{-2} s^{-1}, d) initial concentration of dichloromethane at 0.1 mol/L for ambient condition, e) conversion of dichloromethane at 0.9999, f) flow rate of 1 mL/min and d) I.D. of titanium reactor at 0.18 cm. According to these assumptions, the length of hydrolysis reactor (block A) should be 1.11 m. The ion exchange resin column (block B), on assumptions as 50 minute of time on stream, flow rate at 1 mL/min, initial HCl concentration at 0.2 mol/L, the amount of ion exchange resin should be 6.25 g. Finally, the initial formaldehyde concentration from dichloromethane hydrolysis would be 0.1 mol/L at solution tank of compact sized system (block C). This study demonstrated that formaldehyde will be completely destructed to produce CO_2 and H_2O.

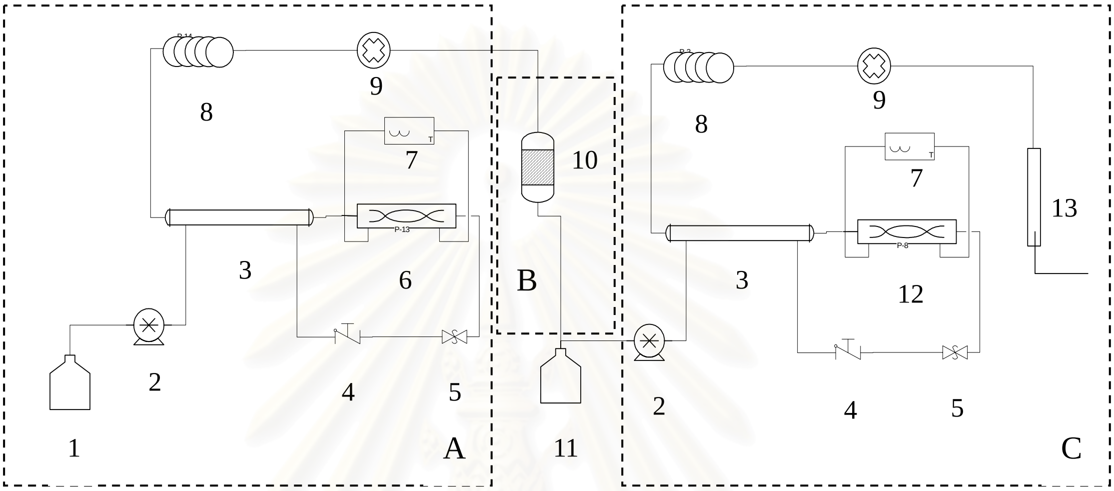

1) hydrolysis system solution tank, 2) HPLC pump, 3) Heat exchanger, 4) Check valve, 5) Relief valve, 6) hydrolysis reactor, 7) Temperature controller set, 8) Cooler by air contact, 9) Back pressure regulator, 10) Ion exchange resin column, 11) SCWO system solution tank, 12) SCWO reactor, 13) Separator

Figure 6.8 Schematic apparatus of proposed cascade process with consecutive combination of hydrolysis and SCWO for pharmaceutical laboratories wastewater treatment. Blocks A, B and C are dichloromethane hydrolysis, ion exchange resin and SCWO of organic compounds, respectively.

CHAPTER VII

CONCLUSIONS AND RECOMMENDATIONS

7.1 Conclusions

7.1.1 Non-catalytic study of formaldehyde oxidation in SCW

Formaldehyde oxidation without catalyst in SCW, and carry out kinetic analyses to find out the optimal condition for the complete destruction of formaldehyde is examined. The global reaction network for SCWO of formaldehyde can be written by assuming that each step in the scheme follows first order kinetics.

$$\mathrm{HCHO} \rightarrow \mathrm{CO} \rightarrow \mathrm{CO}_2$$

Arrhenius equation of formaldehyde oxidation in SCW is shown as follow:

$$rate = 5.70 \pm 6.11 \times 10^{14} \exp\left(\frac{-51.35 \pm 0.99}{RT}\right)[HCHO]$$

In the non-catalytic oxidation of formaldehyde in supercritical water about 77 % conversion of formaldehyde is achieved at 450^{o}C and 16 s, conversions is complete at 500^{o}C, 25 MPa within a residence time of 4 s.

7.1.2 Catalytic compact sized system by SCWO technique

For the catalytic study, a simple and compact reaction system is used. MnO_2 is used as a catalyst; formaldehyde conversion exceeds 95 % in 2 s and completely destructs at 400^{o}C, 25 MPa at 4.2 s of contact time. The experimental results suggest that the catalytic SCWO is a promising technique for the complete destruction of formaldehyde. The optimal condition for complete destruction of formaldehyde oxidation in SCW by catalytic compact sized system is 400^{o}C, 25 MPa, excess oxygen of 100 % for initial formaldehyde concentration range of 0.1-0.6 mol/L at 4.2 s of contact time and volumetric flow rate of solution at 4.7 mL/min. Besides, this compact sized reactor can be used for treatment of other organic compounds such as methanol, ethanol and acetic acid.

7.1.3 Elimination of hydrochloric acid before SCWO reactor

In design of the cascade process where hydrolysis and oxidation are consecutively combined, it is necessary to eliminate HCl between the two stages, because HCl is the major product in the hydrolysis of dichloromethane which provides very corrosive atmosphere in sub- and supercritical water. Two methods, precipitating method and ion exchange method, for eliminating HCl are experimentally examined. The results show that both methods would work for the removal of HCl. Considering the fact that even very small concentration of HCl may cause the corrosion problem in SCWO; ion exchange resin method would be promising for the design of new cascade process as long as it is used before breakthrough time.

7.2 Recommendations

1. The investigation of optimal conditions for hydrochloric acid precipitation method before SCWO reactor such as flow rates, concentration of precipitant are necessary in the design of new cascade process for complete destruction of dichloromethane.

2. The suitable types of precipitant for hydrochloric acid precipitation before SCWO reactor at high pressure which complete remove HCl and kind for environment such as $Ba(OH)_2$ should be investigated.

3. The HCl absorbent at high temperature and pressure such as activated carbon should be investigated to reduce loss of energy between two stages.

4. The ion exchange resin should be improved by regeneration of the resin for increase in duration time to keep continuous flow system. The schematic outline of regenerating ion exchange resin column is shown in Figure 7.1.

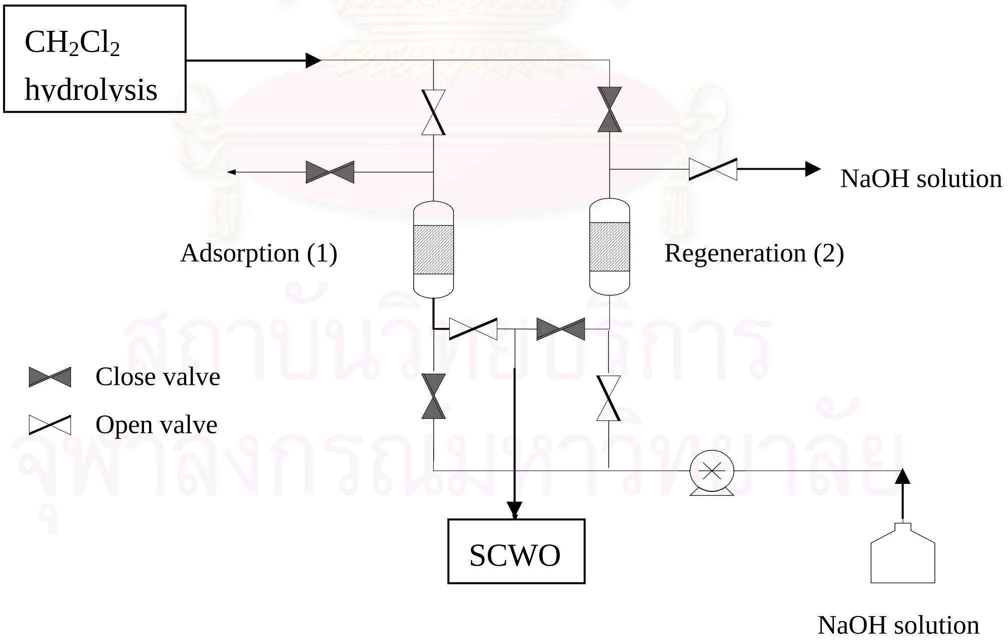

Figure 7.1 The schematic outline of regeneration ion exchange resin column by NaOH solution. Column 1 is adsorption process and column 2 is regeneration process.

Figure 7.1 shows the application of ion exchange resin method for continuous process. Example, when column 1 is applied for adsorption process of HCl from CH_2Cl_2 hydrolysis, meanwhile column 2 is applied for regeneration process of saturated resins by NaOH solution. After resins in column 1 are saturated, control valves should be switched from close to open and open to close positions. Then, the process of column 1 will be changed to regeneration process and column 2 will be adsorption process.

REFERENCES

[1] Arai, Y., Sato, T., and Takebayashi, Y. Supercritical Fluids: Molecular Interaction, Physical Properties, and New Applications. German: Springer-verlag Berlin Heidelber. 2002.

[2] Edogan, K. and Brennecke, J.F. Supercritical Fluid Engineering Science Washington DC: American Chemical Society. 1993.

[3] McHugh, M. Supercritical Fluid Extraction. Butterworth Heiemann. 2nd. 1994

[4] Lee, M.L., Markides, K.E. Analytical Supercritical Fluid Chromatography and Extraction, Chromatography Conferences. UT: Provo Inc. 1990.

[5] Katritzky, A.R., Nichols, D.A., Siskin, M., Murugan, R. and Balasubramanian, M. Reactions in High-Temperature Aqueous Media. Chem. Rev. 101 (2001) 837-892.

[6] Marrone, P.A., Gschwend, P.M., Swallow, K.C., Peters, W.A. and Tester, J.W. Product distribution and reaction pathways for methylene chloride hydrolysis and oxidation under hydrothermal conditions. J. of Supercritical Fluids 12 (1998): 239-254.

[7] Marrone, P.A., Arias, T.A., Peters, W.A. and Tester, J.W. Solvation effects on kinetics of methylene chloride sub-and supercritcal water: Theory, experiment, and Ab initio calculations. J. Phys. Chem A 102 (1998): 7013-7028.

[8] Salvatierra, D., Taylor, J.D., Marrone, P.A. and Tester, J.W. Kinetic study of hydrolysis of methylene chloride from 100 to 500 °C. Ind.Eng.Chem.Res. 38 (1999): 4169-4174.

[9] Oshima, Y., Bijanto, B. and Koda, S. Kinetics of methylene chloride hydrolysis and the salt effect under hydrothermal conditions. Industrial and Engineering chemistry Research. 40(4) (2001): 1026-1031.

[10] Savage, P.E., Gopalan, S., Tahmid, I.M., Martino, C.J. and Brock, E.E. Reactions at supercritical conditions: Applications and Fundamentals. AIChE. 41(7) 1995: 1723-1778.

[11] Watanabe, M., Sato, T., Inomata, H., Smith, R.L., Jr., Arai, K., Kruse, A. and Dinjus, E. Chemical reactions of C_1 compounds in near-critical and supercritical water. Chem.Rev. 104 (2004): 5803-5821.

[12] Akiya, N. and Savage, P.E. Roles of water for chemical reactions in high-temperature water. Chem. Rev. 102 (2002): 2725-2750.

[13] Savage, P.E. Heterogeneous catalysis in supercritical water. Catalysis Today 62 (2000): 167-173.

[14] Savage, P.E. Organic chemical reactions in supercritical water. Chem.Rev. 99 (1999): 603-621.

[15] Ding, Z.Y., Frisch, M.A., Li, L. and Gloyna, E.F. Catalytic oxidation in supercritical water. Ind.Eng.Rev. 35 (1996): 3257-3279.

[16] Savage, P.E., Dunn, J.B. and Yu, J. Recent advances in catalytic oxidation in supercritical water. Combust. Sci. and Tech. 178 (2006): 443-465.

[17] Bermejo, M.D. and Cocero, M.J. Journal reviews: Supercritical water oxidation: A Technical Reviews. AIChE. 52 (2006): 3933-3951.

[18] Hayward, T.M., Svishchev, I.M. and Makhija, R.C. Stainless steel flow reactor for supercritical water oxidation: corrosion tests. J. of Supercritical Fluids 27 (2003): 275-281.

[19] Kritzer, P. Corrosion in high-temperature and supercritical water and aqueous solutions: a review. J. of Supercritical Fluid. 29 (2004): 1-29.

[20] Delville, M.H., Botella, Ph., Jaszay, Th. and Frayret. Electrochemical study of corrosion in aqueous high pressure, high temperature media and measurements of materials corrosion rates: applications to the hydrothermal treatments of organic wastes by SCWO. J. of Supercritical Fluids 26 (2003): 169-179.

[21] Wikipedia, the free encyclopedia. Formaldehyde [online]. Available from: http://en.wikipedia.org/wiki/Formaldehyde [2007, June 2].

[22] Environmental Health Criteria 89. Formaldehyde [online]. Available from: http://www.inchem.org/documents/ehc/ehc/ehc89.htm#SectionNumber:2.1 [2007, November 1].

[23] Agency for Toxic Substances and Disease Registry, Division of Toxicology, Atlanta. Formaldehyde [online]. Available from: http://www.health-report.co.uk/formaldehyde-fact-sheet.htm [2007, December 27].

[24] University of North Carolina at Chapel Hill, Environment, Health & Safety. Formaldehyde Online Training Course [online]. Available from: http://ehs.unc.edu/training/self_study/formaldehyde/index.shtml [2007, December 25].

[25] Control and Treatment Technology for the Metal Finishing Industry. Ion Exchange [online]. Available from: http://www.remco.com/ix.htm [2007, November 26].

[26] Wikipedia, the free encyclopedia. Ion exchange resin [online]. Available from: http://en.wikipedia.org/wiki/Ion_exchange_resin [2007, December 25]

[27] ChemIndustry.com, Inc. Ion exchange resin [online]. Available from: http://www.chemindustry.com/chemnames/i/ion_exchange_resin.html [2007, December 26].

[28] N.C. Division of Pollution Prevention and Environmental Assistance and Waste Reduction Resource Center. Laboratories (Research and Testing) [online]. Available from: http://wrrc.p2pays.org/industry/indsectinfo.asp. [2007 December 28].

[29] Waddell, D. Laboratory Waste Management Guide, Final Report. Seattle, WA: Local Hazardous Waste Management Program in King County. 2005.

[30] Yamasaki, Y., Enomoto, H., Yamasaki, N. and Nakahara, M. NMR study of hydrothermal reactions of dichloromethane with and without Alkali. Bull.Chem.Soc.Jpn 73 (2000): 2687-2693.

[31] Yamasaki, Y., Enomoto, H., Yamasaki, N. and Nakahara, M. Methanol formation from dichloromethane under hydrothermal conditions. Chemistry Letters (1999): 83-84.

[32] Yamasaki, Y., Yamasaki, N. and Enomoto, H. Dechlorination of concentrated monochloroalkanes under various hydrothermal conditions. J.of Chemical Engineering of Japan. 37(10) (2004): 1252-1258.

[33] Sinquin, G., Petit, C., Libs, S., Hinderman, J.P. and Kienhemann, A. Catalytic destruction of chlorinated C_1 volatile organic compounds (CVOCs) reactivity, oxidation and hydrolysis mechanisms. Applied Catalysts B: Envirinmental 27 (2000): 105-115.

[34] Pinard, L., Mijoin, J., Ayrault, P., Canaff, C. and Magnoux, P. On the mechanism of the catalytic destruction of dichloromethane over Pt Zeolite catalysts. Applied Catalysts B: Envirinmental 51 (2004): 1-8.

[35] Pinard, L., Mijoin, J., Magnoux, P. and Guisnet, M. Dichlromethane transformation over bifunctional PtFAU catalysts influence of acidobasicity of the zeolite. Comptes Rendus Chimie. 8 (2005): 457-463.

[36] Klein, R., Scheer, M.D. and Schoen, L.J. The pyrolysis of formaldehyde. Bureau of mines. 78 (1955): 50-52.

[37] Saito, K., Kakumoto, T., Nakanishi, Y. and Imamura, A. Thermal decomposition of formaldehyde at high temperatures. J. Phys.Chem. 89 (1985): 3109-3113.

[38] Tsujino, Y., Wakai, C., Matubayashi, N. and Nakahara, M. Non catalytic cannizaro-type reaction of formaldehyde in hot water. Chemistry Letters. (1999): 287-288.

[39] Takahashi, H., Takei, S., Hori, T. and Nitta, T. A real-space-grid QM/MM study on the ionic/radical association reaction in aqueous phase: HCHO + OH → HCHO – OH. J. of Molecular Structure (Theochem). 632 (2003): 185-195.

[40] Takahashi, H., Hori, T., Wakabayashi, T. and Tomoshige, N. Real space Ab initio molecular dynamics simulations for the reactions of OH radical/OH anion with formaldehyde. J. Phys. Chem. A. 105 (2001): 4351-4358.

[41] Watanabe, M., Osada, M., Inomata, H., Arai, K. and Kruse, A. Acidity and basicity of metal oxide catalysts for formaldehyde reaction in supercritical water at 673 K. Applied Catalysis A: General. 245 (2003): 333-341.

[42] Osada, M., Watanabe, M., Sue, K., Adchiri, T. and Arai, K. Water density dependence of formaldehyde reaction in supercritical water. J. of Supercritical Fluids. 28 (2004): 219-224.

[43] Boock, L.T. and Klein, T. Lumping strategy for modeling the oxidation of C_1-C_3 alcohols and acetic acid in high temperature water. Ind.Eng.Chem.Res. 32 (1993): 2464-2473.

[44] Brock, E.E. and Savage, P.E. Detailed chemical kinetics model for supercritical water oxidation of C_1 compounds and H_2. AIChE. 41(8) (1995): 1874-1888.

[45] Brock, E.E., Oshima, Y., Savage, P.E. and Barker, J.R. Kinetics and mechanism of methanol oxidation in supercritical water. J.Phys.Chem. 100 (1996): 15834-15842.

[46] Rice, S.F., Hunter, T.B., Ryden, A.C. and Hanush, R.G. Raman spectroscopic measurement of oxidation in supercritical water. 1. Conversion of methanol to formaldehyde. Ind.Eng.Chem.Res. 35 (1996): 2161-2171.

[47] Croiset, E. Rice, S.F. and Hanush, R.G. Hydrogen peroxide decomposition in supercritical water. AIChE. 43(9) (1997): 2343-2352.

[48] Anitescu, G., Zhang, Zhang, Z. and Tavlarides, L.L. A kinetic study of methanol oxidation in supercritical water. Ind.Eng.Chem.Res. 38 (1999): 2231-2237.

[49] Oshima, Y., Bijanto, B. and Koda, S. PFR and CSTR analyses of supercritical water oxidation of methanol. J. of Chemical Engineering of Japan. 33(3) (2000): 507-513.

[50] Rice, S.F. and Croiset, E. Oxidation of simple alcohol on supercritical water III. Formation of intermediates from ethanol. Ind.Eng.Chem.Res. 40 (2001): 86-93.

[51] Feng, J., Aki, S.N.V.K., Chateauneuf, J.E. and Brennecke, J.F. Abstraction of hydrogen from methanol by hydroxyl radical in subcritical and supercritical water. J. Phys.Chem. A. 107 (2003): 11043-11048.

[52] Henrikson, J.T., Grice, C.R. and Savage, P.E. Effect of water density on methanol oxidation kinetics in supercritical water. J. Phys.Chem. A. 110 (2006): 3627-3632.

[53] Ploeger, J.M., Bielenberg, P.A., Dinaro-Blanchard, J.L., Lachance, R.P., Taylor, J.D., Green, W.H. and Tester, J.W. Modeling oxidation and hydrolysis reactions in supercritical water—free radical elementary reaction networks and their applications. Combust. Sci. and Tech. 178 (2006): 363-398.

[54] Hayashi, R., Onishi, M., Sugiyama, M., Koda, S. and Oshima, Y. Kinetic analysis on alcohol concentration and mixture effect in supercritical water oxidation of methanol and ethanol by elementary reaction model. J. of Supercritical Fluid. 40(1) (2007): 74-83.

[55] Oshima, Y., Hori, K., Toda, M., Chommanad, T. and Koda, S. Phenol oxidation kinetics in supercritical water. J. of Supercritical Fluid. 13 (1998): 241-246.

[56] Portela, J.R., Nebot, E. and Martinez, O.E. Kinetic comparison between subcritical and supercritical water oxidation of phenol. Chemical Engineering Journal. 81 (2001): 287-299.

[57] Perez, I.V., Rogak, S. and Branion, R. Supercritical water oxidation of phenol and 2, 4- dinirtophenol. J. of Supercritical Fluid. 30 (2004): 71-87.

[58] Goto, M., Nada, T., Kodama, A. and Hirose, T. Kinetic analysis for destruction of municipal sewage sludge and alcohol distillery wastewater by supercritical water oxidation. Ind.Eng.Chem.Res. 38 (1999): 1863-1865.

[59] Jin, F.M., Kishita, A., Moriya, T. and Enomoto, H. Kinetics of oxidation of food waste with H_2O_2 in supercritical water. J. of Supercritical Fluid. 19 (2001): 251-262.

[60] Fang, Z., Xu, S., Butler, I.S., Smith, R.L. and Kozinski, J.A. Destruction of decachlorobiphenyl using supercritical water oxidation. Energy & Fuels. 18 (2004): 1257-1265.

[61] Wang, T. and Zhu, X. Conversion and kinetics of the oxidation of coal in supercritical water. Energy & Fuels. 18 (2004): 1569-1572.

[62] Fauvel, E. Dubien, C.J., Tanneur, V. and Moussiere, S. A porous reactor for supercritical water oxidation: Experimental results on salty compounds and corrosive solvents oxidation. Ind.Eng.Chem.Res. 44 (2005): 8968-8971.

[63] Bermejo, M.D., Polanco, F.F. and Cocero, M.J. Effect of the transpiring wall on the behavior of a supercritical water oxidation reactor: Modeling and experimental results. Ind.Eng.Chem.Res. 45 (2006): 3438-3446.

[64] Prikopsky, K., Wellig, B. and Rohr, R.V. SCWO of salt containing artificial wastewater using a transpiring-wall reactor: Experimental results. J. of Supercritical Fluid. 40 (2007): 246-257.

[65] Yu, J. and Savage, P.E. Catalytic oxidation of phenol over MnO_2 in supercritical water. Ind.Eng.Chem.Res. 38 (1999): 3793-3801.

[66] Yu, J. and Savage, P.E. Kinetics of MnO_2-catalyzed acetic acid oxidation in supercritical water. Ind.Eng.Chem.Res. 39 (2000): 4014-4019.

[67] Yu, J. and Savage, P.E. Phenol oxidation over CuO/Al_2O_3 in supercritical water. Applied Catalysis B: Environmental. 28 (2000): 275-288.

[68] Oshima, Y., Tomita, K. and Koda, S. Kinetics of the catalytic oxidation of phenol over manganese oxide in supercritical water. Ind.Eng.Chem.Res. 38 (1999): 4183-4188.

[69] Armbruster, U., Martin, A. and Krepel, A. Hydrolysis and oxidation decomposition of ethyl acetate in sub- and super-critical water. Applied Catalysis B: Environmenntal. 31 (2001): 263-273.

[70] Yu, J. and Savage, P.E. Catalyst activity, stability, and transformations during oxidation supercritical water. Applied Catalysis B: Environmental. 31 (2001): 123-132.

[71] Suppes, G.J., Roy, S. and Ruckman, J. Calcium carbonate catalysis of alcohol oxidation in near-critical water. AIChE. 47(9) (2001): 2102-2110.

[72] Matsumura, Y., Urase, T., Yamamoto, K. and Nunoura T. Carbon catalyzed supercritical water oxidation of phenol. J. of Supercritical Fluid. (2002): 149-156.

[73] Tomita, K. and Oshima, Y. Stability of manganese oxide in catalytic supercritical water oxidation of phenol. Ind.Eng.Chem.Res. 43 (2004): 7740-7743.

[74] Ruamchat, T., Hayashi, R., Ngamprasertsith, S. and Oshima, Y. A novel on-site system for the treatment of pharmaceutical laboratory wastewater by supercritical water oxidation. Environmental Sciences 13(5) (2006): 297-304.

[75] Levenspiel, O. Chemical Reaction Engineering. New York: John wiley and sons. 1999.

APPENDICES

Appendix A

Pharmaceutical Laboratory Wastewater

The data of organic laboratory wastewater have been collected for 3 months from Quality Assurance Division, Government Pharmaceutical Organization (GPO), Thailand. There are 4 types of wastewater classification as follow:

1. Halogenated organic compounds such as dichloromethane, chloroform, bromine solution.
2. Non-Halogenated organic compounds such as methanol, ethanol, acetone, acetonitrile, cyclohexane.
3. Glacial acid such as acetic acid, hydrochloric acid, sulfuric acid, nitric acid.
4. Heavy metal such as lead nitrate solution, arsenic trioxide solution, silver nitrate solution.

In this study, total amount of wastewater in laboratory and amount of each solution are collected per week. Methanol, ethanol, acetone, acetonitrile and cyclohexane are obtained as non-halogenated organic compounds. Dichloromethane and chloroform are obtained as halogenated organic compounds. The data of non-chlorinated organic compounds is located in Table A-1

Table A-1 Data of non-halogenated organic compounds in pharmaceutical laboratory wastewater

Week	**Total amount of wastewater** (L)	**Amount of non-halogenated organic compounds (L)**				
		Methanol	Ethanol	Acetone	Acetonenitrile	cyclohexane
1	45	3	3	5	1	2
2	40	2	4	2	2	2
3	45	1	1	1	1	2
4	40	2	3	3	2	1
5	40	2	2	4	1	2
6	40	4	3	2	1	1
7	40	3	1	3	2	1
8	45	2	2	4	3	2
9	40	3	3	1	1	1
10	40	2	2	1	2	2
11	45	1	1	2	1	1
12	40	3	2	1	2	2

The data of halogenated organic compounds is located in Table A-2

Table A-2 Data of halogenated organic compounds in pharmaceutical laboratory wastewater

Week	**Total amount of wastewater (L)**	**Amount of halogenated organic compounds (L)**	
		Dichloromethane	Chloroform
1	30	2	1
2	45	1	1
3	40	1	1
4	20	1	2
5	45	2	2
6	30	1	1
7	20	2	1
8	25	1	3
9	20	1	1
10	25	2	2
11	30	1	1
12	25	1	1

Calculation of average concentration of organic compounds in wastewater

Example A-1 The data from Table A-1

On week 1, a total amount of waste water (V_{total}) is 45 L. and amount of methanol (V_{CH_3OH}) is 3 L.

Concentration of methanol in wastewater = $\dfrac{V_{CH_3OH}(L) \times \rho_{CH_3OH}(g/mL) \times 1000}{MW_{CH_3OH} \times V_{total}(L)}$

$$= \frac{3 \times 0.79 \times 1000}{32 \times 45}$$

= 1.65 mol/L

Assumption: 5 days per week

As a result, concentration of methanol in wastewater per day is 1.65/5 = 0.33 mol/L

Density (ρ) and Molecular Weight (MW) of representative organic laboratory wastewater compounds are shown in Table A-3.

Table A-3 Density (ρ) and Molecular Weight (MW) of organic compounds

Compounds	**Density** (ρ)	**Molecular Weight** (MW)
Methanol	0.79	32
Ethanol	0.78	46
Acetone	0.79	58
Acetonitrile	0.79	41
Cyclohexane	0.78	84
Dichloromethane	1.33	84
Chloroform	1.48	119

The average concentrations of non-halogenated organic compounds are shown in Table A-4.

Table A-4 The average concentrations of non-halogenated organic compounds in pharmaceutical laboratory wastewater

Week	**Average concentrations (mol/L)**				
	Methanol	Ethanol	Acetone	Acetonitrile	Cyclohexane
1	0.33	0.23	0.30	0.09	0.08
2	0.25	0.34	0.14	0.19	0.09
3	0.11	0.08	0.06	0.09	0.08
4	0.25	0.25	0.20	0.19	0.05
5	0.25	0.17	0.27	0.10	0.09
6	0.49	0.25	0.14	0.10	0.05
7	0.37	0.08	0.20	0.19	0.05
8	0.22	0.15	0.24	0.26	0.08
9	0.37	0.25	0.07	0.10	0.05
10	0.25	0.17	0.07	0.19	0.09
11	0.11	0.08	0.12	0.09	0.04
12	0.37	0.17	0.07	0.19	0.09
Average	**0.28**	**0.19**	**0.16**	**0.15**	**0.07**

The average concentrations of halogenated organic compounds are shown in Table A-5.

Table A-5 The average concentrations of halogenated organic compounds in pharmaceutical laboratory wastewater

Week	**Average concentrations (mol/L)**	
	Dichloromethane	Chloroform
1	0.21	0.08
2	0.07	0.06
3	0.08	0.06
4	0.16	0.25
5	0.14	0.11
6	0.10	0.08
7	0.31	0.30
8	0.13	0.30
9	0.16	0.12
10	0.25	0.20
11	0.10	0.08
12	0.13	0.10
Average	0.15	0.13

Appendix B

Effluent analysis

B.1 Formaldehyde analysis

Analyzer	Thermal Conductivity Detector Gas Chromatography (GC-TCD)
Type	GC-8A Shimadzu
Column	SUS, 2 m., Flusin/T, 60/80, APS-201
Carrier gas	He
Flow rate	30 mL/min
Volume of injected sample	2 µL
Temperature of injector	150 ^{o}C
Prog. rate	5^{o}C/min
Temperature of column	110-140^{o}C
Current	100 mA

B.2 Methanol analysis

Analyzer	Flame Ionization Detector Gas Chromatography (GC-FID)
Column	Porapak Q, 80/100, C-0473
Carrier gas	N_2
Volume of injected sample	1 mL
Temperature of injector	130^{o}C
Temperature of detector	200^{o}C

B.3 Total organic carbon analysis

Analyzer	Total Organic Carbon (TOC)
Type	SHIMADZU TOC-5000A
Carrier gas	Air (For combustion),
Carrier gas flow rate	150 mL/min
Combustion temperature	680^{o}C

B.4 Gas product analysis

Analyzer	Thermal Conductivity Detector Gas Chromatography (GC-TCD)
Type	GC-8A Shimadzu
Column	SUS, 2 m., Unibead s c, 60/80
Carrier gas	He
Flow rate	30 mL/min
Volume of injected sample	4 μL
Temperature of injector	120^{o}C
Temperature of column	80^{o}C
Current	100 mA

B.5 Hydrochloric acid analysis

Analyzer	Ion Chromatography (IC)
Type	Shodex IC
Column	Shodex IC, I-524 A
Guard column	Shodex IC, I-A-G
Buffer	Phthalic acid 2.5 mM and 2-amino-2-hydroxymethyl-1, 3-propanedial pH 4
Flow rate	1.2 mL/min
Temperature of column	40^{o}C
Temperature of cell	45^{o}C
Conductivity measurement	Shodex CD-5
Polarity	+
Sensitivity	10
Range	1.24 μ scm^{-1}

Appendix C

Calculations

C.1 Non-catalytic study

C.1.1 Volume of reactor (V_R)

$$V_R = \frac{\pi D^2 L}{4}$$

V_R = Volume of reactor (m^3)
D = Inside diameter of reactor (m)
L= Length of reactor (m)

In this study, the reactor is made of Hastelloy C-276 tubing (0.160 cm o.d., 0.108 cm i.d.), Length 4 m.

$$V_R = \frac{\pi (0.00108)^2 (4)}{4}$$

$$= 3.66 \times 10^{-6}\ m^3 \quad = 3.66\ mL$$

Volume of Plug flow reactor in this study is 3.66 mL

C.1.2 Residence time (τ)

$$\tau = \frac{V_R}{F_t \times \frac{\rho_a}{\rho_T}}$$

τ = Residence time (min)

V_R = Volume of reactor (mL)

ρ_T = Density of water at each condition (kg/m^3)
ρ_a = Density of water at ambient condition (kg/m^3)

F_t = Total volumetric flow rate of solution (mL/min)

Example C-1 Data from table D-2, formaldehyde oxidation in SCW by PFR reactor at temperature 400^{o}C and pressure 25 MPa. Volumetric flow rate of formaldehyde and hydrogen peroxide are 1 mL/min and 4 mL/min, respectively.

$$\tau = \frac{V_R}{(F_{HCHO} + F_{H_2O_2}) \times \frac{\rho_a}{\rho_T}}$$

$$\tau = \frac{3.66mL}{(1mL/\min + 4mL/\min) \times \frac{997.05kg/m^3}{166.54kg/m^3}}$$

$$\tau = 0.12\min = 7.34\sec.$$

Residence time of this condition is 7.34 second

C.1.3 Conversion (X)

$$X = 1 - \frac{C_t}{C_0}$$

X = Conversion of organic compound

C_t = Concentration of organic compound at time profile (mol/L)

C_0 = Initial concentration of organic compound (mol/L)

Example C-2 Data from table D-2, formaldehyde oxidation in SCW by PFR reactor at temperature 400°C and pressure 25 MPa. Volumetric flow rate of formaldehyde and hydrogen peroxide are 1 mL/min and 4 mL/min, respectively. Concentration of formaldehyde at residence time 7.34 s. is 0.014 mol/L (HCHO peak area 2113.5), methanol 0.003 mol/L (CH_3OH peak area 586253) and initial concentration of formaldehyde in original solution is 0.08 mol/L (HCHO peak area 13537), methanol is 0.016 mol/L (CH_3OH peak area 3256365).

To keep the contribution of the preheating stage where the hydrolysis reaction of HCHO may proceed to some extent as small as possible, the solution of HCHO is directly introduced into the reactor without preheating. The flow rate of preheated H_2O_2 solution is always at least 4 times larger than that of the solution of HCHO so as to heat up the solution of HCHO very quickly to the reaction temperature after mixing two streams.

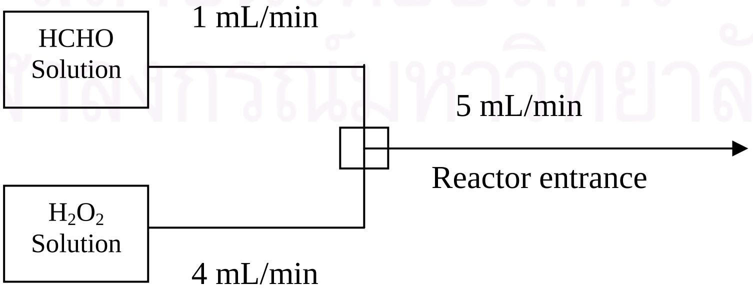

Figure C-1 Flow chart of formaldehyde and hydrogen peroxide solution at mixing point of PFR study in SCWO

From Figure C-1, formaldehyde and methanol conversion are calculated as follow:

Formaldehyde conversion (X_{HCHO}) = $1-\left(\frac{2113.5}{\left(13537\times \frac{1}{5}\right)}\right)$

$$X_{HCHO} = 0.22$$

Formaldehyde conversion of this condition is 0.22

Methanol (as stabilizer) conversion = $1-\left(\frac{586253}{\left(3256365\times \frac{1}{5}\right)}\right)$

$$X_{CH3OH} = 0.10$$

Methanol conversion of this condition is 0.10

C.1.4 Concentration of organic solution at reactor entrance

$$C_R = C_0 \times \frac{\rho_T}{\rho_a} \times \frac{1}{5}$$

C_R = Concentration of organic solution at reactor entrance (mol/L)

C_0 = Initial concentration of organic compound (mol/L)

ρ_T = Density of water at each condition (kg/m^3)

ρ_a = Density of water at ambient condition (kg/m^3)

Example C-3 from example C-2, concentration of formaldehyde and methanol at the reactor entrance at 400^{o}C, 25 MPa are calculated as follow:

$$[HCHO]_R = [HCHO]_0 \times \frac{\rho_T}{\rho_a} \times \frac{1}{5}$$

$$[HCHO]_R = 0.08 mol/L \times \frac{166.54 kg/m^3}{997.05 kg/m^3} \times \frac{1}{5}$$

$$[HCHO]_R = 0.0027 \text{ mol/L}$$

Concentration of formaldehyde at the reactor entrance in this condition is 0.0027 mol/L.

$$[CH_3OH]_R = [CH_3OH]_0 \times \frac{\rho_T}{\rho_a} \times 1/5$$

$$[CH_3OH]_R = 0.016 mol/L \times \frac{166.54 kg/m^3}{997.05 kg/m^3} \times 1/5$$

$$[CH_3OH]_R = 0.0005 \text{ mol/L}$$

Concentration of methanol at the reactor entrance in this condition is 0.0005 mol/L.

C.1.5 Excess oxygen

$$\% \text{ Oxygen excess} = \frac{[O_2] \text{ at reactor entrance} - [O_2] \text{ stoichiometric}}{[O_2] \text{ stoichiometric}} \times 100$$

Example C-4 from example C-3,

Formaldehyde oxidation reaction is

$$\mathrm{HCHO} + \mathrm{O_2} \rightarrow \mathrm{CO_2} + \mathrm{H_2O}$$

And methanol oxidation reaction is

$$\mathrm{CH_3OH} + \frac{3}{2}\mathrm{O_2} \rightarrow \mathrm{CO_2} + 2\mathrm{H_2O}$$

From example C-3, $[HCHO]_R = 0.0027$ mol/L and $[CH_3OH]_R = 0.0005$ mol/L

So **stoichiometric O_2 concentration =** $0.0027 + \left(\frac{3}{2} \times 0.0005\right)$ **= 0.004 mol/L**

From experimental result, volumetric flow rate of oxygen (V_{O_2}) is calculated as follow:

From ideal gas law $PV = nRT$

$$\therefore n = \frac{PV}{RT}$$

P = 1 atm

T = Room temperature (300 K)

V = volumetric flow rate of oxygen (V_{O_2}) (mL/min)

R = 0.082 (L)(atm)/(mole)(K)

n = Molar flow rate of oxygen (mol/min)

$$\text{Molar flow rate of oxygen} = \frac{1atm \times \left(13.05mL \big/ 1000mL\right) / \min}{0.082 \, (L)(atm) \big/ (mole)(K) \times 300K}$$

Molar flow rate of oxygen = 0.0005 mol/min

$$\text{Volumetric flow rate of oxygen at reactor entrance} = V_T \times \frac{\rho_a}{\rho_T}$$

Volumetric flow rate of oxygen at reactor entrance

$$= \left(5mL \times \frac{L}{1000mL}\right) / \min \times \frac{997.05kg / \min}{166.54kg / \min}$$

Volumetric flow rate of oxygen at reactor entrance = 0.029 L/min

$$O_2 \text{ concentration at reactor entrance} = \frac{\text{Molar flow rate of } O_2}{\text{Volumetric flow rate of } O_2 \text{ at reactor entrance}}$$

$$= \frac{0.0005mol / \min}{0.029L / \min}$$

O_2 concentration at reactor entrance = 0.017 mol/L

$$\textbf{\% excess oxygen} = \frac{0.017 mol/L - 0.004 mol/L}{0.004 mol/L} \times 100 = 325\ \%$$

% excess oxygen in this condition is 325 %

C.1.6 Yield of formaldehyde and methanol

$$Y = (1 - X)$$

Y = Yield of organic compound

X = Conversion of organic compound

Example C-5 from example C-2, yield of formaldehyde and methanol are calculated as follow:

$$Y_{HCHO} = (1 - X_{HCHO}) \times \left(\frac{[HCHO]_0}{[HCHO]_0 + [CH_3OH]_0} \right)$$

$$Y_{HCHO} = (1 - 0.22) \times \left(\frac{0.08}{0.08 + 0.016} \right)$$

$$Y_{HCHO} = 0.66$$

Formaldehyde yield of this condition is 0.66

$$Y_{CH3OH} = (1 - X_{CH_3OH}) \times \left(\frac{[CH_3OH]_0}{[HCHO]_0 + [CH_3OH]_0} \right)$$

$$Y_{CH3OH} = (1 - 0.10) \times \left(\frac{0.016}{0.08 + 0.016} \right)$$

$$Y_{CH3OH} = 0.14$$

Methanol yield of this condition is 0.14

C.1.5 Percent mole of gas products

$$\%\text{ mole of CO} = \frac{\%\text{ mole STD CO}}{\text{Peak area of STD CO}} \times \text{peak area CO in gas product}$$

$$\%\text{ mole of CO}_2 = \frac{\%\text{ mole STD CO}_2}{\text{Peak area of STD CO}_2} \times \text{peak area CO}_2\text{ in gas product}$$

Example C-6 from example C-2,

$$\%\text{ mole of CO} = \frac{3.96}{67234} \times 33707$$

% mole of CO = 1.98

$$\%\text{ mole of CO}_2 = \frac{4.02}{110923} \times 5927$$

% mole of CO_2 = 0.21

C.1.6 Molar flow rate of gas product

From idea gas law $PV = nRT$

$$\therefore n = \frac{PV}{RT}$$

P = 1 atm

T = Room temperature (300 K)

V = Gas flow rate (mL/min) × % mole of gas product

R = 0.082 (L)(atm)/(gmole)(K)

n = Molar flow rate of gas product

Example C-7 Data from table, Gas flow rate 13.05 mL/min

$$\text{Molar flow rate of CO} = \frac{1atm\times\left(13.05mL\Big/_{1000mL}\right)/\min\times1.98\%}{0.082\,{}^{(L)(atm)}\Big/_{(gmole)(K)}\times300K}$$

Molar flow rate of CO = 0.00001 mol/min

$$\text{Molar flow rate of CO}_2 = \frac{1atm\times\left(13.05mL\Big/_{1000mL}\right)/\min\times0.21\%}{0.082\,{}^{(L)(atm)}\Big/_{(gmole)(K)}\times300K}$$

Molar flow rate of CO_2 = 0.000001 mol/min

C.1.7 Gas product yield in gas phase ($Y_{(g)}$)

$$Y_{(g)} = \left(\frac{\text{Molar flow rate of gas product}}{([HCHO]_0+[CH_3OH]_0)\times F_{HCHO}}\right)$$

$Y_{(g)}$ = Gas product yield

$[HCHO]_0$ = Initial concentration of formaldehyde (mol/L)

$[CH_3OH]_0$ = Initial concentration of methanol (mol/L)

F_{HCHO} = Volumetric flow rate of formaldehyde solution (mL/min)

Example C-8 from example C-7,

$$Y_{(CO)} = Y_{(CO,\ g)}$$

$$Y_{(CO,\ g)} = \frac{0.00001mol/\min}{(0.08+0.016)mol/L\times\left(1mL\times\dfrac{L}{1000mL}\right)/\min}$$

$$Y_{(CO,\ g)} = 0.11$$

CO yield in this condition = 0.11

C.1.8 Gas product yield in liquid phase ($Y_{CO_2,l}$)

CO_2 is easily soluble in liquid phase. So yield of CO_2 should be calculated both in gas phase and liquid phase. Henry's Law is used as equilibrium equation between gas phase and liquid phase.

$$P_{CO_2} = X_{CO_2} \times H$$

P_{CO_2} = Partial pressure = %mole of CO_2 in gas product × Total pressure

Total pressure = 0.101 MPa

X_{CO_2} = Molar fraction of CO_2 in liquid product

H = Henry's law constant = 165.8 MPa at T =300 K, P= 0.101 MPa

Molar flow rate of CO_2 in liquid phase (mol/min) = $\dfrac{F_t \times X_{CO_2} \times \rho_{H_2O}}{MW_{H_2O}}$

Molar flow rate of CO_2 in liquid phase (mol/min) =

$$= \frac{\left(\frac{1mL/\min + 4mL/\min}{1000mL/L}\right) \times \left(\frac{0.0021 \times 0.101MPa}{165.8MPa}\right) \times 1000g/L}{18}$$

= 3.56 ×10^{-7}mol/min

$$(Y_{CO_2,l}) = \left(\frac{\text{Molar flow rate of } \mathrm{CO}_2 \text{ in liquid phase}}{([HCHO]_0 + [CH_3OH]_0) \times F_{HCHO}}\right)$$

$$= \frac{3.56 \times 10^{-7}\, mol/\min}{(0.08mol/L + 0.016mol/L) \times \left(1mL \times \frac{L}{1000mL}\right)/\min}$$

= 0.004

Yield of CO_2 in liquid product of this condition is 0.004

$$Y_{(CO_2,g)} = \frac{0.000001 mol/\min}{(0.08+0.016) mol/L \times \left(1mL \times \frac{L}{1000mL}\right)/\min}$$

$$Y_{(CO_2,g)} = 0.012$$

Yield of CO_2 in gas product of this condition is 0.012

$$Y_{(CO_2)} = Y_{(CO_2,g)} + Y_{(CO_2,l)}$$

$$Y_{(CO_2)} = 0.012 + 0.004 = 0.016 = 0.02$$

Yield of CO_2 in this condition is 0.02

C.1.9 Plug flow reactor for complete destruction of formaldehyde

$$-\ln(1 - X) = k\tau$$

X = Formaldehyde conversion

τ= Residence time (min)

On assumption

Conversion of formaldehyde (X) = 0.9999

Flow rate of solution (F_t) = 4.7 mL/min

Pressure = 25 MPa

I.D. of tube = 0.108 cm.

At 400^{o}C, 25 MPa: k_1= 0.02 s^{-1}

$$-\ln(1-0.9999) = (0.02)\tau$$

$$\tau = \frac{-\ln(1-0.9999)}{0.02} = 460.52 \text{ s} = 7.68 \text{ min}$$

Residence time for complete destruction of HCHO in this condition is 7.68 minute

From residence time
$$\tau = \frac{V_R}{F_t \times \dfrac{\rho_a}{\rho_T}}$$

$$\therefore V_R = \tau \times \left(F_t \times \frac{\rho_a}{\rho_{400^o C}} \right)$$

$$\therefore V_R = 7.68\min \times \left(4.7mL/\min \times \frac{997.05kg/m^3}{166.54kg/m^3} \right)$$

$$\therefore V_R = 216.79mL = 216.79cm^3$$

Volume of reactor in this condition is 216.79 mL

From volume of reactor

$$V_R = \frac{\pi D^2 L}{4}$$

$$\therefore L = \frac{V_R}{\pi D^2 / 4}$$

$$\therefore L = \frac{216.79cm^3}{\pi (0.108cm)^2 / 4}$$

$$L = 236.65\ \mathrm{m}$$

Length of reactor for complete destruction of HCHO in this condition is 236.65 meter

C.1.10 Calculation of pseudo first order rate constant of carbon monoxide (k_2) oxidation in SCW

The rate constants k_2 is obtained by unweighted nonlinear regression. From equation 4.12 and 4.13

$$Y_{CO} = k_1\,[\exp(-k_1\tau) - \exp(-k_2\tau)]/\,(k_2-k_1) \qquad (4.12)$$

$$Y_{CO2} = 1-[k_2\exp(-k_1\tau) - k_1\exp(-k_2\tau)]/\,(k_2-k_1) \qquad (4.13)$$

From equation 4.12

$$k_1 = \frac{Y_{CO}(k_2 - k_1)}{[\exp(-k_1\tau) - \exp(-k_2\tau)]} \qquad (D.1)$$

From equation 4.13

$$Y_{CO2} = 1 - \frac{[k_2\exp(-k_1\tau) - k_1\exp(-k_2\tau)]}{(k_2 - k_1)} \qquad (D.2)$$

From Table 4.3, 450^{o}C, k_1 = 0.08,

From Table D-2, 450^{o}C, 25 MPa : Y_{CO} = 0.23, Y_{CO2} = 0.02, τ = 2.7

Trial and error value of k_2 at τ = 2.7 in equations D.1 and D.2 which give approximately value of k_1 = 0.08, Y_{CO} = 0.23, Y_{CO2} = 0.02

As a result, in this condition k_2 = 0.09

C.2 Catalytic SCWO compact sized reactor study

C.2.1 Contact time

$$\text{Contact time} = \frac{\text{Catalyst bulk volume (mL)}}{\text{Fluid volumetric flow rate (mL/min)}}$$

$$\text{Contact time} = \frac{V_{MnO_2} \times g_{MnO_2}}{F_t \times \dfrac{\rho_a}{\rho_T}}$$

V_{MnO_2} = Pore volume of MnO_2 = 0.20 mL/g

g_{MnO_2} = Amounts of MnO_2 (g)

Example C-9 data from Table D-6, flow rate of solution 8.8 mL/min, temperature and pressure are 400^{o}C and 25 MPa, respectively.

$$\text{Contact time} = \frac{0.20 mL/g \times 10 g.}{8.8 mL/\min \times \dfrac{997.05 kg/m^3}{166.54 kg/m^3}}$$

$$= 0.038 \text{ min} = 2.27 \text{ second}$$

Contact time in this condition is 2.27 second

C.2.2 Total organic carbon (TOC) conversion

$$X_{[TOC]} = \left(1 - \frac{[TOC]_t}{[TOC]_0}\right)$$

$X_{[TOC]}$ = TOC conversion

$[TOC]_t$ = Concentration of TOC at time profile (mol/L)

$[TOC]_0$ = Initial concentration of TOC in original solution (mol/L)

Example C-10 Data from table D-6 at the same condition of example C-9, $[TOC]_t$ = 0.008 mol/L, $[TOC]_0$ = 0.3 mol/L

$$X_{[TOC]} = \left(1 - \frac{0.008}{0.3}\right)$$

$$X_{[TOC]} = 0.98$$

Total organic carbon (TOC) conversion in this condition is 0.98

C.2.3 Decomposition rate

$$\text{Decomposition rate} = X \times [TOC]_0 \times F_t$$

Example C-11 Data from table D-7 at 400^{o}C, 25 MPa, formaldehyde initial concentration 0.1 mol/L, flow rate 4.8 mL/min

$$\text{Decomposition rate} = 1 \times 0.1 \frac{mol}{L} \times 4.8 \frac{mL}{\min} \times \frac{L}{1000 mL}$$

$$= 4.8 \times 10^{-4} \text{ mol/min} = 0.48 \text{ mmol/min}$$

Decomposition rate of this condition is 0.48 mmol/min.

Appendix D

Experimental data

Table D-1 Water density at each condition

Temperature (^oC) at 25 MPa	**Water density (kg/m^3)**
Ambient (25^oC)	997.05
350	625.45
380	450.82
400	166.54
450	108.98
500	91.18

Table D-2 Experimental data of non-catalytic formaldehyde oxidation in SCW, $[HCHO]_0$ = 0.08 mol/L at ambient condition

Condition	**Flow rate (mL/min)**		**Resident time (sec)**	**Gas product flow rate (mL/min)**	**Conversion**			**Yield (C-base)**					**Carbon yield balance**	
	Organic	H_2O_2			HCHO	CH_3OH	TOC	HCHO	CH_3OH	TOC	CO_2	CO	Org+Y_{gas}	TOC +Y_{gas}
T 400°C, 25 MPa	0.3	1.2	24.48	3.56	0.41	0.23	0.39	0.49	0.13	0.61	0.05	0.24	0.91	0.90
	0.5	2.0	14.69	6.25	0.33	0.15	0.26	0.56	0.14	0.74	0.04	0.16	0.90	0.94
	0.7	2.8	10.49	9.04	0.29	0.11	0.21	0.59	0.15	0.78	0.02	0.13	0.89	0.94
	1.0	4.0	7.34	13.05	0.22	0.10	0.17	0.66	0.14	0.83	0.02	0.11	0.92	0.95
	1.4	5.6	5.24	19.04	0.16	0.05	0.14	0.69	0.16	0.86	0.02	0.11	0.99	0.99
	1.8	7.2	4.08	25.26	0.10	0.02	0.13	0.75	0.16	0.87	0.01	0.09	1.02	0.98
T 450°C, 25 MPa	0.3	1.2	16.02	3.83	0.76	0.37	0.66	0.19	0.13	0.34	0.19	0.38	0.89	0.90
	0.5	2.0	9.61	6.83	0.63	0.25	0.54	0.29	0.16	0.46	0.12	0.36	0.93	0.95
	0.7	2.8	6.86	9.72	0.51	0.22	0.47	0.39	0.17	0.53	0.09	0.37	1.01	0.99
	1.0	4.0	4.81	13.95	0.46	0.15	0.39	0.43	0.18	0.61	0.06	0.33	0.90	0.99
	1.4	5.6	3.43	17.83	0.37	0.12	0.35	0.50	0.18	0.65	0.03	0.26	0.97	0.94
	1.8	7.2	2.67	25.32	0.30	0.06	0.25	0.56	0.18	0.75	0.02	0.23	1.00	1.00
T 500°C, 25 MPa	0.3	1.2	13.40	4.07	1.00	0.78	0.97	0.00	0.04	0.03	0.45	0.37	0.87	0.86
	0.5	2.0	8.04	7.79	1.00	0.67	0.94	0.00	0.06	0.06	0.36	0.48	0.91	0.91
	0.7	2.8	5.74	10.41	1.00	0.61	0.91	0.00	0.07	0.09	0.31	0.53	0.92	0.93
	1.0	4.0	4.02	14.27	0.99	0.49	0.88	0.00	0.09	0.12	0.23	0.57	0.89	0.92
	1.4	5.6	2.87	20.37	0.95	0.31	0.83	0.03	0.14	0.17	0.27	0.52	0.97	0.96
	1.8	7.2	2.23	25.21	0.74	0.25	0.68	0.21	0.14	0.32	0.08	0.55	0.99	0.96

Table D-3 Experimental data of non-catalytic formaldehyde oxidation in SCW, $[HCHO]_0 = 0.04$ mol/L at ambient condition

Condition	**Flow rate (mL/min)**		**Resident time (sec)**	**Gas product flow rate (mL/min)**	**Conversion**			**Yield (C-base)**					**Carbon yield balance**	
	Organic	H_2O_2			HCHO	CH_3OH	TOC	HCHO	CH_3OH	TOC	CO_2	CO	Org+Y_{gas}	TOC +Y_{gas}
T 400°C, 25 MPa	0.3	1.2	24.48	3.63	0.46	0.20	0.42	0.47	0.11	0.59	0.14	0.24	0.96	0.97
	0.5	2.0	14.69	6.28	0.37	0.10	0.30	0.55	0.12	0.71	0.07	0.18	0.93	0.97
	0.7	2.8	10.49	9.15	0.28	0.06	0.21	0.63	0.13	0.78	0.06	0.12	0.93	0.96
	1.0	4.0	7.34	13.16	0.21	0.14	0.20	0.68	0.12	0.79	0.03	0.12	0.95	0.94
	1.4	5.6	5.24	18.58	0.17	0.06	0.17	0.72	0.13	0.83	0.03	0.07	0.95	0.94
	1.8	7.2	4.08	28.57	0.13	0.07	0.15	0.75	0.13	0.85	0.03	0.08	0.98	0.96
T 450°C, 25 MPa	0.3	1.2	16.02	3.71	0.74	0.26	0.69	0.22	0.10	0.31	0.28	0.29	0.92	0.88
	0.5	2.0	9.61	6.86	0.64	0.26	0.61	0.31	0.10	0.39	0.21	0.29	0.94	0.89
	0.7	2.8	6.86	9.63	0.57	0.24	0.50	0.37	0.10	0.49	0.17	0.28	0.93	0.95
	1.0	4.0	4.81	13.94	0.50	0.22	0.42	0.43	0.11	0.57	0.08	0.27	0.89	0.92
	1.4	5.6	3.43	19.13	0.42	0.10	0.39	0.49	0.12	0.61	0.06	0.24	0.90	0.91
	1.8	7.2	2.67	24.54	0.32	0.06	0.27	0.58	0.13	0.72	0.04	0.19	0.91	0.95
T 500°C, 25 MPa	0.3	1.2	13.40	4.12	1.00	0.64	0.90	0.00	0.07	0.09	0.38	0.44	0.90	0.93
	0.5	2.0	8.04	7.89	1.00	0.54	0.89	0.00	0.09	0.11	0.37	0.43	0.89	0.91
	0.7	2.8	5.74	10.52	1.00	0.46	0.87	0.00	0.11	0.13	0.34	0.47	0.92	0.94
	1.0	4.0	4.02	14.91	0.99	0.45	0.83	0.00	0.11	0.17	0.31	0.49	0.92	0.97
	1.4	5.6	2.87	20.91	0.88	0.40	0.72	0.09	0.12	0.28	0.26	0.39	0.86	0.93
	1.8	7.2	2.23	26.20	0.72	0.39	0.62	0.24	0.12	0.38	0.20	0.31	0.85	0.89

Table D-4 Experimental data of non-catalytic formaldehyde oxidation in SCW of, effect of methanol concentration on formaldehyde conversion, $[HCHO]_0$ = 0.08 mol/L at ambient condition, 450°C, 25 MPa

Ratio HCHO: CH_3OH	**Flow rate (mL/min)**		**Resident time (sec)**	**Gas product flow rate (mL/min)**	**Conversion**			**Yield (C-base)**					**Carbon yield balance**	
	Organic	H_2O_2			HCHO	CH_3OH	TOC	HCHO	CH_3OH	TOC	CO_2	CO	Org+Y_{gas}	TOC +Y_{gas}
1:0.2	0.3	1.2	16.02	3.82	0.76	0.37	0.66	0.20	0.13	0.34	0.20	0.38	0.89	0.90
	0.5	2.0	9.61	6.84	0.63	0.25	0.54	0.30	0.16	0.46	0.12	0.37	0.93	0.95
	0.7	2.8	6.86	9.72	0.51	0.22	0.47	0.40	0.17	0.53	0.09	0.38	1.01	0.99
	1.0	4.0	4.81	13.95	0.46	0.15	0.39	0.44	0.18	0.61	0.06	0.34	0.99	1.00
	1.4	5.6	3.43	17.83	0.37	0.12	0.34	0.52	0.18	0.65	0.03	0.27	0.96	0.94
	1.8	7.2	2.67	25.32	0.29	0.06	0.25	0.57	0.18	0.75	0.02	0.24	1.00	1.00
1:0.5	0.3	1.2	16.02	3.69	0.75	0.35	0.59	0.16	0.23	0.41	0.21	0.31	0.91	0.92
	0.5	2.0	9.61	6.58	0.62	0.26	0.51	0.25	0.25	0.49	0.16	0.32	0.98	0.97
	0.7	2.8	6.86	9.04	0.51	0.18	0.41	0.32	0.29	0.59	0.10	0.23	0.95	0.93
	1.0	4.0	4.81	13.78	0.43	0.15	0.30	0.37	0.29	0.69	0.07	0.20	0.94	0.97
	1.4	5.6	3.43	18.96	0.35	0.11	0.24	0.42	0.31	0.75	0.04	0.16	0.94	0.96
	1.8	7.2	2.67	23.43	0.26	0.08	0.21	0.48	0.31	0.79	0.02	0.14	0.97	0.95
1:1	0.3	1.2	16.02	3.92	0.76	0.38	0.49	0.12	0.30	0.51	0.13	0.27	0.83	0.91
	0.5	2.0	9.61	6.78	0.62	0.29	0.42	0.19	0.34	0.58	0.09	0.22	0.85	0.90
	0.7	2.8	6.86	9.67	0.48	0.21	0.36	0.25	0.40	0.64	0.08	0.22	0.96	0.95
	1.0	4.0	4.81	13.79	0.40	0.16	0.30	0.30	0.42	0.69	0.05	0.17	0.94	0.92
	1.4	5.6	3.43	19.14	0.27	0.16	0.22	0.37	0.42	0.78	0.03	0.14	0.95	0.96
	1.8	7.2	2.67	23.95	0.22	0.12	0.14	0.40	0.44	0.86	0.03	0.08	0.94	0.97

Table D-5 Experimental data of non-catalytic formaldehyde oxidation in SCW, effect of methanol concentration on formaldehyde conversion, $[HCHO]_0$ = 0.08 mol/L at ambient condition, 500°C, 25 MPa

Ratio HCHO: CH_3OH	**Flow rate (mL/min)**		**Resident time (sec)**	**Gas product flow rate (mL/min)**	**Conversion**			**Yield (C-base)**					**Carbon yield balance**	
	Organic	H_2O_2			HCHO	CH_3OH	TOC	HCHO	CH_3OH	TOC	CO_2	CO	Org+Y_{gas}	TOC +Y_{gas}
1:0.2	0.3	1.2	13.40	4.07	1.00	0.78	0.97	0.00	0.04	0.03	0.45	0.37	0.87	0.86
	0.5	2.0	8.04	7.79	1.00	0.67	0.94	0.00	0.06	0.06	0.37	0.48	0.91	0.91
	0.7	2.8	5.74	10.41	1.00	0.61	0.91	0.00	0.07	0.09	0.31	0.53	0.92	0.93
	1.0	4.0	4.02	14.27	0.99	0.48	0.88	0.00	0.09	0.12	0.22	0.57	0.89	0.92
	1.4	5.6	2.87	20.37	0.95	0.30	0.83	0.04	0.14	0.17	0.27	0.52	0.97	0.96
	1.8	7.2	2.23	25.21	0.74	0.25	0.68	0.21	0.14	0.32	0.08	0.55	0.99	0.96
1:0.5	0.3	1.2	13.40	3.96	1.00	0.76	0.91	0.00	0.08	0.09	0.53	0.36	0.98	0.98
	0.5	2.0	8.04	7.38	1.00	0.71	0.88	0.00	0.10	0.12	0.39	0.49	0.99	1.00
	0.7	2.8	5.74	9.84	1.00	0.64	0.87	0.00	0.13	0.13	0.32	0.59	1.05	1.04
	1.0	4.0	4.02	14.48	1.00	0.53	0.81	0.00	0.16	0.19	0.23	0.52	0.91	0.94
	1.4	5.6	2.87	19.29	0.89	0.43	0.77	0.07	0.21	0.23	0.15	0.65	1.08	1.04
	1.8	7.2	2.23	20.91	0.67	0.22	0.59	0.22	0.26	0.41	0.09	0.49	1.06	0.99
1:1	0.3	1.2	13.40	4.01	1.00	0.86	0.91	0.00	0.06	0.09	0.42	0.40	0.89	0.92
	0.5	2.0	8.04	7.78	1.00	0.74	0.86	0.00	0.11	0.14	0.30	0.47	0.88	0.91
	0.7	2.8	5.74	10.46	1.00	0.58	0.80	0.00	0.18	0.20	0.24	0.55	0.97	0.99
	1.0	4.0	4.02	14.01	0.99	0.55	0.76	0.00	0.21	0.24	0.21	0.55	0.96	0.99
	1.4	5.6	2.87	20.85	0.78	0.31	0.59	0.12	0.30	0.40	0.11	0.47	1.00	0.99
	1.8	7.2	2.23	25.10	0.62	0.18	0.49	0.21	0.37	0.51	0.08	0.40	1.06	0.99

Table D-6 Experimental data of catalytic compact sized reactor by SCWO technique, $[HCHO]_0$ = 0.3 mol/L at ambient condition, 25 MPa, excess oxygen 100%

Temperature (^oC)	**Flow rate of solution (mL/min)**	**Contact time (sec)**	**TOC conversion**	**Yield**			**Carbon yield balance**
				TOC	CO_2	CO	
350	3.2	23.40	0.98	0.02	0.99	0.00	1.01
	4.8	15.60	0.98	0.02	0.93	0.00	0.95
	6.0	12.48	0.97	0.03	0.90	0.00	0.93
	7.6	9.85	0.95	0.05	0.94	0.00	1.00
	8.8	8.51	0.93	0.07	0.89	0.00	0.97
	10.2	7.34	0.90	0.10	0.84	0.00	0.94
380	3.2	16.87	0.99	0.01	0.97	0.00	0.99
	4.8	11.25	0.98	0.02	0.92	0.00	0.94
	6.0	9.00	0.97	0.03	0.91	0.00	0.94
	7.6	7.10	0.96	0.04	0.86	0.00	0.90
	8.8	6.13	0.95	0.05	0.94	0.00	0.99
	10.2	5.29	0.94	0.06	0.85	0.00	0.92
400	3.2	6.24	1.00	0.00	0.98	0.00	0.98
	4.8	4.16	1.00	0.00	0.95	0.00	0.95
	6.0	3.33	1.00	0.00	0.99	0.00	0.99
	7.6	2.63	1.00	0.00	0.93	0.00	0.93
	8.8	2.27	0.98	0.02	0.91	0.00	0.93
	10.2	1.96	0.96	0.04	0.95	0.00	0.99

Table D-7 Experimental data of catalytic compact sized reactor by SCWO technique, 400°C, 25 MPa, excess oxygen 100%

$[HCHO]_0$ (mol/L)	**Flow rate of solution (mL/min)**	**Contact time (sec)**	**TOC conversion**	**Yield**			**Carbon yield balance**
				TOC	CO_2	CO	
0.1	3.2	6.24	1.00	0.00	1.01	0.00	1.01
	4.8	4.16	1.00	0.00	0.96	0.00	0.96
	6.0	3.33	1.00	0.00	0.98	0.00	0.98
	7.6	2.63	0.99	0.01	0.96	0.00	0.97
	8.8	2.27	0.98	0.02	0.94	0.00	0.96
	10.2	1.96	0.97	0.03	1.02	0.00	1.04
0.3	3.2	6.24	1.00	0.00	0.98	0.00	0.98
	4.8	4.16	1.00	0.00	0.95	0.00	0.95
	6.0	3.33	1.00	0.00	0.99	0.00	0.99
	7.6	2.63	1.00	0.00	0.93	0.00	0.93
	8.8	2.27	0.98	0.02	0.91	0.00	0.93
	10.2	1.96	0.96	0.04	0.95	0.00	0.99
0.6	3.2	6.24	1.00	0.00	0.98	0.00	0.98
	4.8	4.16	1.00	0.00	0.93	0.00	0.93
	6.0	3.33	0.98	0.02	0.98	0.00	1.00
	7.6	2.63	0.97	0.03	0.95	0.00	0.97
	8.8	2.27	0.95	0.05	0.90	0.00	0.95
	10.2	1.96	0.94	0.06	0.88	0.00	0.94

Table D-8 Experimental data of catalytic compact sized reactor by SCWO technique, 400^{o}C, 25 MPa, $[HCHO]_0$ = 0.3 mol/L at ambient condition.

% excess oxygen	**Flow rate of solution (mL/min)**	**Contact time (sec)**	**TOC conversion**	**Yield**			**Carbon yield balance**
				TOC	CO_2	CO	
8	3.2	6.24	0.99	0.01	0.92	0.00	0.93
	4.8	4.16	0.98	0.02	0.92	0.00	0.94
	6.0	3.33	0.98	0.02	0.88	0.00	0.90
	7.6	2.63	0.95	0.05	0.94	0.00	0.99
	8.8	2.27	0.93	0.07	0.89	0.00	0.96
	10.2	1.96	0.91	0.09	0.91	0.00	1.00
65	3.2	6.24	1.00	0.00	0.99	0.00	0.99
	4.8	4.16	1.00	0.00	0.98	0.00	0.98
	6.0	3.33	0.98	0.02	0.92	0.00	0.94
	7.6	2.63	0.96	0.04	0.89	0.00	0.92
	8.8	2.27	0.94	0.06	0.92	0.00	0.98
	10.2	1.96	0.93	0.07	0.89	0.00	0.95
100	3.2	6.24	1.00	0.00	0.98	0.00	0.98
	4.8	4.16	1.00	0.00	0.95	0.00	0.95
	6.0	3.33	1.00	0.00	0.99	0.00	0.99
	7.6	2.63	1.00	0.00	0.93	0.00	0.93
	8.8	2.27	0.98	0.02	0.91	0.00	0.93
	10.2	1.96	0.96	0.04	0.95	0.00	0.99

Table D-9 Experimental data of catalytic compact sized reactor by SCWO technique, 400^{o}C, 25 MPa, $[HCHO]_0$ = 0.1 mol/L, $[CH_3OH]_0$ = 0.1 mol/L, $[C_2H_5OH]_0$ = 0.1 mol/L, $[CH_3COOH]_0$ = 0.1 mol/L at ambient condition, excess oxygen 100%

Flow rate of solution (mL/min)	**Contact time (sec)**	**TOC conversion**	**Yield**			**Carbon yield balance**
			TOC	CO_2	CO	
3.2	6.24	1.00	0.00	0.94	0.04	0.98
4.8	4.16	0.99	0.01	0.94	0.04	0.99
6.0	3.33	0.97	0.03	0.02	0.05	1.00
7.6	2.63	0.96	0.04	0.87	0.06	0.97
8.8	2.27	0.94	0.06	0.83	0.06	0.96
10.2	1.96	0.92	0.08	0.83	0.07	0.98

Table D-10 Experimental data of elimination hydrochloric acid before SCWO reactor by precipitation method, $[HCl]_0$ = 0.2 mol/L at ambient condition

Time on stream (min)	**$[HCl]_t$ (mol/L)**		**$[HCl]_t/[HCl]_0$**	
	0.1 MPa	25 MPa	0.1 MPa	25 MPa
0	0.00	0.00	0.00	0.00
10	0.03	0.03	0.16	0.13
20	0.04	0.03	0.19	0.17
30	0.07	0.07	0.33	0.33
40	0.07	0.05	0.32	0.26
50	0.07	0.09	0.35	0.46
60	0.08	0.09	0.39	0.44
70	0.07	0.12	0.32	0.56
80	0.07	0.10	0.36	0.49
90	0.08	0.10	0.36	0.48
100	0.08	0.10	0.39	0.49
110	0.07	0.11	0.35	0.55
120	0.07	0.11	0.36	0.52

Table D-11 Experimental data of elimination hydrochloric acid before SCWO reactor by ion exchange resin method, $[HCl]_0$ = 0.2 mol/L, 25°C, 0.1 MPa

Time on stream (min)	**$[HCl]_t$ (mol/L)**		**$[HCl]_t/[HCl]_0$**	
	Resin 3.14 g	Resin 6.25 g	Resin 3.14 g	Resin 6.25 g
0	0.00	0.00	0.00	0.00
10	0.00	0.00	0.00	0.00
20	0.00	0.00	0.00	0.00
30	0.02	0.00	0.02	0.00
40	0.20	0.00	0.99	0.00
50	0.21	0.00	0.99	0.01
60	0.20	0.21	0.99	1.00
70	0.20	0.21	0.99	1.00
80	0.21	0.21	1.00	1.00
90	0.21	0.20	0.99	0.99
100	0.21	0.21	1.00	1.00
110	0.20	0.20	0.99	0.99
120	0.21	0.21	0.99	1.00

Table D-12 Experimental data of elimination hydrochloric acid before SCWO reactor by ion exchange resin method, $[HCl]_0$ = 0.2 mol/L, $[HCHO]_0$ = 0.1 mol/L, 25°C, 0.1 MPa, resin 6.25 g

Time on stream (min)	**Hydrochloric acid**		**TOC concentration**	
	$[HCl]_t$ (mol/L)	$[HCl]_t/[HCl]_0$	$[TOC]_t$ (mol/L)	$[TOC]_t/[TOC]_0$
0	0.00	0.00	0.12	1.00
10	0.00	0.00	0.12	1.00
20	0.00	0.00	0.11	0.99
30	0.00	0.00	0.12	1.00
40	0.00	0.00	0.11	0.99
50	0.01	0.03	0.12	1.00
60	0.21	0.99	0.12	1.00
70	0.21	0.99	0.12	1.00
80	0.21	1.00	0.10	0.96
90	0.21	0.99	0.12	1.00
100	0.20	0.98	0.12	1.00
110	0.21	0.99	0.12	1.00
120	0.21	0.99	0.12	1.00

VITA

Miss Teerada Ruamchat was born on November 25, 1980 in Rayong, Thailand. She received her B.Sc. (Second class honors) degree in Chemical Engineering from Chulalongkorn University. Teerada joined the department of Chemical Technology at Chulalongkorn University as a doctoral student in 2003. She has received the Royal Golden Jubilee Scholarship from Thailand Research Fund for her Ph.D. study. Teerada also served as a teaching assistant for undergraduate courses “Material and Energy Balances” and “Applied Mathematic in Chemical Engineering”. While in graduate school, Teerada spent one year (2005) and two months (2007) doing research in “Oshima Laboratory” at The University of Tokyo, Tokyo, Japan. Her paper entitled “A Novel On-site System for the Treatment of Pharmaceutical Laboratory Wastewater by Supercritical Water Oxidation” has been published in “Environmental Sciences”. She also presented her work at 1 conference in Japan, 1 conference in Korea and 1 conference in Malaysia.